Oklahoma Department of Transportation
200 NE 21st Street, Oklahoma City, OK 73105-3204

FINAL REPORT ~ FHWA-OK-21-01

UTILIZING PAVEMENT FRICTION AND TEXTURE DATA FOR THE REDUCTION OF TRAFFIC CRASHES AND DELAYS

Joshua Q. Li, Ph.D., P.E.
Kelvin Wang, Ph.D., P.E.
Wenyao Liu, Graduate Student
Wenying Yu, Graduate Student

School of Civil and Environmental Engineering
Oklahoma State University
Stillwater, Oklahoma

March 2021

OKLAHOMA Transportation

The Oklahoma Department of Transportation (ODOT) ensures that no person or groups of persons shall, on the grounds of race, color, sex, religion, national origin, age, disability, retaliation or genetic information, be excluded from participation in, be denied the benefits of, or be otherwise subjected to discrimination under any and all programs, services, or activities administered by ODOT, its recipients, sub-recipients, and contractors. To request an accommodation please contact the ADA Coordinator at 405-521-4140 or the Oklahoma Relay Service at 1-800-722-0353. If you have any ADA or Title VI questions email ODOT-ada-titlevi@odot.org.

The contents of this report reflect the views of the author(s) who is responsible for the facts and the accuracy of the data presented herein. The contents do not necessarily reflect the views of the Oklahoma Department of Transportation or the Federal Highway Administration. This report does not constitute a standard, specification, or regulation. While trade names may be used in this report, it is not intended as an endorsement of any machine, contractor, process, or product.

UTILIZING PAVEMENT FRICTION AND TEXTURE DATA FOR THE REDUCTION OF TRAFFIC CRASHES AND DELAYS

FINAL REPORT ~ FHWA-OK-21-01

ODOT SP&R ITEM NUMBER 2309

Submitted to:
Office of Research and Implementation
Oklahoma Department of Transportation

Submitted by:
Joshua Q. Li, Ph.D., P.E.
Kelvin Wang, Ph.D., P.E.
Wenyao Liu & Wenying Yu (Graduate Students)

School of Civil and Environmental Engineering
Oklahoma State University

OKLAHOMA Transportation

March 2021

TECHNICAL REPORT DOCUMENTATION PAGE

1. REPORT NO. FHWA-OK-21-01	2. GOVERNMENT ACCESSION NO.	3. RECIPIENT'S CATALOG NO.
4. TITLE AND SUBTITLE Utilizing Pavement Friction and Texture Data for The Reduction of Traffic Crashes and Delays		5. REPORT DATE Mar 2020
		6. PERFORMING ORGANIZATION CODE
7. AUTHOR(S) Joshua Q. Li, Kelvin Wang, Wenyao Liu, and Wenying Yu		8. PERFORMING ORGANIZATION REPORT
9. PERFORMING ORGANIZATION NAME AND ADDRESS Oklahoma State University, Stillwater Oklahoma 74078,		10. WORK UNIT NO.
		11. CONTRACT OR GRANT NO. ODOT SPR Item Number 2309
12. SPONSORING AGENCY NAME AND ADDRESS Oklahoma Department of Transportation Office of Research and Implementation 200 N.E. 21st Street, Room G18 Oklahoma City, OK 73105		13. TYPE OF REPORT AND PERIOD COVERED Final Report Oct 2018 - Dec 2020
		14. SPONSORING AGENCY CODE
15. SUPPLEMENTARY NOTES N/A		

16. ABSTRACT

This project presented an integral process to include skid performance of different preventive treatments and their safety benefits into the life cycle cost analysis (LCCA) of pavements. Extensive data sets from several ODOT database systems were processed and analyzed. An enhanced safety performance function (SPF) was developed and the friction deterioration models were established for common treatments in Oklahoma. A spreadsheet VBA tool was programmed to combine the model results for the prediction of friction variations and their expected crash frequency. The safety costs were then integrated into the tool, and a case study was provided to demonstrate the proposed LCCA procedure. The outcomes of this study could result in significant benefits to reduce traffic fatalities, serious injuries, and traffic delays.

17. KEYWORDS Pavement friction, safety performance function, preventive treatments, life cycle cost analysis (LCCA)	18. DISTRIBUTION STATEMENT No restrictions. This publication is available from the Office of Research and Implementation, Oklahoma DOT.		
19. SECURITY CLASSIF. (OF THIS REPORT) Unclassified	20. SECURITY CLASSIF. (OF THIS PAGE) Unclassified	21. NO. OF PAGES 123	22. PRICE N/A

Form DOT F 1700.7 (08/72)

SI* (MODERN METRIC) CONVERSION FACTORS

APPROXIMATE CONVERSIONS TO SI UNITS

SYMBOL	WHEN YOU KNOW	MULTIPLY BY	TO FIND	SYMBOL
		LENGTH		
in	inches	25.4	millimeters	mm
ft	feet	0.305	meters	m
yd	yards	0.914	meters	m
mi	miles	1.61	kilometers	km
		AREA		
in^2	square inches	645.2	square millimeters	mm^2
ft^2	square feet	0.093	square meters	m^2
yd^2	square yard	0.836	square meters	m^2
ac	acres	0.405	hectares	ha
mi^2	square miles	2.59	square kilometers	km^2
		VOLUME		
fl oz	fluid ounces	29.57	milliliters	mL
gal	gallons	3.785	liters	L
ft^3	cubic feet	0.028	cubic meters	m^3
yd^3	cubic yards	0.765	cubic meters	m^3
		NOTE: volumes greater than 1000 L shall be shown in m^3		
		MASS		
oz	ounces	28.35	grams	g
lb	pounds	0.454	kilograms	kg
T	short tons (2000 lb)	0.907	megagrams (or "metric ton")	Mg (or "t")
		TEMPERATURE (exact degrees)		
°F	Fahrenheit	5 (F-32)/9 or (F-32)/1.8	Celsius	°C
		ILLUMINATION		
fc	foot-candles	10.76	lux	lx
fl	foot-Lamberts	3.426	candela/m^2	cd/m^2
		FORCE and PRESSURE or STRESS		
lbf	poundforce	4.45	newtons	N
lbf/in^2	poundforce per square inch	6.89	kilopascals	kPa

APPROXIMATE CONVERSIONS FROM SI UNITS

SYMBOL	WHEN YOU KNOW	MULTIPLY BY	TO FIND	SYMBOL
		LENGTH		
mm	millimeters	0.039	inches	in
m	meters	3.28	feet	ft
m	meters	1.09	yards	yd
km	kilometers	0.621	miles	mi
		AREA		
mm^2	square millimeters	0.0016	square inches	in^2
m^2	square meters	10.764	square feet	ft^2
m^2	square meters	1.195	square yards	yd^2
ha	hectares	2.47	acres	ac
km^2	square kilometers	0.386	square miles	mi^2
		VOLUME		
mL	milliliters	0.034	fluid ounces	fl oz
L	liters	0.264	gallons	gal
m^3	cubic meters	35.314	cubic feet	ft^3
m^3	cubic meters	1.307	cubic yards	yd^3
		MASS		
g	grams	0.035	ounces	oz
kg	kilograms	2.202	pounds	lb
Mg (or "t")	megagrams (or "metric ton")	1.103	short tons (2000 lb)	T
		TEMPERATURE (exact degrees)		
°C	Celsius	1.8C+32	Fahrenheit	°F
		ILLUMINATION		
lx	lux	0.0929	foot-candles	fc
cd/m^2	candela/m^2	0.2919	foot-Lamberts	fl
		FORCE and PRESSURE or STRESS		
N	newtons	0.225	poundforce	lbf
kPa	kilopascals	0.145	poundforce per square inch	lbf/in^2

*SI is the symbol for the International System of Units. Appropriate rounding should be made to comply with Section 4 of ASTM E380. (Revised March 2003)

Table of Contents

List of Figures

List of Tables

CHAPTER 1 INTRODUCTION

1.1 Background

It has been estimated in the United States that inferior highway pavement conditions could contribute to approximately 30% of the annual highway fatalities (FHWA, 2010). In particular, inadequate pavement friction or insufficient surface texture increases total crashes and also contributes to wet-weather crashes, resulting in increased fatalities, more serious personal injuries, and significant traffic delays. In Oklahoma, 73,267 crashes occurred in 2019, including 640 fatalities and 33,038 injuries.

Over the years, the Oklahoma Department of Transportation (ODOT) has been aggressively at the forefront in combating highway traffic safety problems and saving Oklahoman lives. As the most critical surface skid characteristics for safety, pavement texture and friction have been collected through the “Pavement Management Systems (PMS)” and the "Skid Studies Program". The statewide crash database, the SAFE-T: Statewide Analysis for Engineering & Technology, and the comprehensive construction management tool, the AASHTOWare SiteManager™, maintain abundant data sets that can be used to support highway safety management in Oklahoma. Meanwhile, ODOT is one of the national leaders in researching to better characterize friction and texture performance of pavements for improved roadway safety.

Better utilizing the available pavement friction, surface texture, roadway safety data, and relevant results, along with other necessary ODOT data sets, could result in significant benefits to reduce traffic fatalities, serious injuries, and traffic delays in Oklahoma. With a comprehensive statistical analysis using the integrated ODOT data sets, the critical influencing factors contributing to roadway crashes could be identified. Subsequently, the appropriate safety countermeasures can be applied to improve roadway safety and further reduce traffic delays.

1.2 Project Tasks

The main objective of this implementation study is to utilize pavement friction, surface texture, and other supporting data sets available at ODOT for the reduction of traffic crashes and delays in Oklahoma. Specifically, the research aims to address the following sub-objectives:

- to integrate relevant pavement condition, road geometry, traffic flow, and crash data in Oklahoma;
- to determine the statistical significance of these data items, especially friction and texture, to roadway crashes;
- to develop friction models based on ODOT data sets and pavement surface texture profile data from non-contact testing techniques;
- to demonstrate the role of friction and texture data in the selection of preventative maintenance strategies for safe roads;
- to develop enhanced safety performance function (SPF) for the Oklahoma roadway network using available data sets.

To accomplish the objectives of this study, the following six tasks, listed below, were performed.

- **Task 1 Literature Review**. This task involved a comprehensive literature review to develop an in-depth understanding of various aspects related to this project.
- **Task 2 Data Acquisition and Preprocessing**. The relevant data sources that could be used for the reduction of traffic crashes and delays in Oklahoma were investigated in this task, including pavement management system, SiteManger construction management system, skid studies program, statewide analysis for engineering & technology (SAFE-T) crash database, and additional data collected from previous ODOT projects.
- **Task 3 Statistical Analysis, Friction Models, and Demands**. Friction prediction models were developed based on available ODOT data or pavement surface texture data. Furthermore, the friction demands in terms of investigatory and intervention levels were established.
- **Task 4 Pavement Maintenance Strategies for Safety**. This task applied life-cycle cost analysis methodologies to determine the most cost-effective preservation maintenance strategies considering the corresponding traffic crashes and delays. Besides, a safety performance function (SPF) was developed to quantify the impacts of pavement skid performance on roadway crashes and thus to evaluate the safety effects of preservation maintenance.

- **Task 5 Analysis Tool**. An Excel analysis tool was developed to assist the data management and integrate roadway crashes into the life cycle analysis procedure for the selection of preventive treatments.
- **Task 6 Final Report and Training**. This task included the drafting and submission of the final report and delivering training for ODOT engineers.

1.3 Report Outline

This report consists of seven chapters. An overview of each chapter is given below:

- Chapter 1 provides the background and objectives of the project.
- Chapter 2 documents the summary of the literature review related to the project.
- Chapter 3 introduces the available data sets at ODOT and the procedure to integrate those data sets.
- Chapter 4 presents the development of safety performance function (SPF) and the establishment of pavement friction demands.
- Chapter 5 demonstrates the statistical analysis results and the pavement friction prediction models.
- Chapter 6 presents the procedure and results of the life cycle analysis considering roadway crashes and provides case studies and comparisons.
- Chapter 7 summarizes the conclusions and future recommendations of this study.

CHAPTER 2 LITERATURE REVIEW

Skid resistance of pavement plays a significant role in road safety and has been studied extensively in the last decade. The existing literature on the following five relevant research areas was summarized in this section: (1) pavement friction and texture; (2) pavement texture and measurement; (3) measurement of skid resistance of pavements; (4) preventive maintenance treatments for restoring skid resistance; and (5) relationships between aggregate characteristics and skid resistance.

2.1 Pavement Friction and Texture

2.1.1 Pavement Friction

Pavement friction is the force resisting the relative motion between vehicle tires and the pavement surface, and it is a critical factor influencing the crash rates on both wet and dry conditions for roads (Najafi et al., 2015; Flintsch et al., 2012; Hall et al., 2009). Pavement friction results from a complex interplay between two principal frictional force components: adhesion and hysteresis (Hall et al., 2009). Adhesion forces are most responsive to the micro-level asperities (microtexture) of the aggregate particles contained in the pavement surface, while the hysteresis forces developed within the tire are most responsive to the macro-level asperities (macrotexture) formed in the surface via mix design and/or construction techniques.

As a result, adhesion governs the overall friction of smooth-textured and dry pavements, while hysteresis is the dominant component of wet and rough-textured pavements.

Hall (2009) grouped the influencing factors of pavement friction forces into four categories: pavement surface characteristics, vehicle operational parameters, tire properties, and environmental factors. Considering various pavement surface conditions (including asphalt type, nominal aggregate size, and texture depth) and contact areas (considering tire loading, inflation pressure, and type of tire), Labbate (2001) investigated the skid resistance performance of pavements. The skid resistance showed an initial loss in the early life, followed by an increase in friction, and thereafter a reduction in the equilibrium condition. The rolling resistance increased with reduced contact areas.

The influence of asphalt mixture type and Portland cement concrete surface textures on friction performance of pavements has been widely studied (Asi, 2007; Ahammed and Tighe, 2008). Previous studies found that air temperature and pavement temperature could affect the friction performance of pavements, both in short-term and long-term cycles. At low testing speed, friction tended to decrease with increasing pavement temperature. An opposite trend was observed at high testing speed (Luo, 2003; Jahromi et al., 2011). Roe et al. (1998) noted that friction reduced with increasing testing speed and reached the minimum level at about 100km/h for smooth tires. The level of high-speed friction depended to a large extent on the low-speed friction. Friction on surfaces with low texture depth dropped more rapidly at high speed. Wilson (2006) identified up to 30% variations in friction performance over a short period of time. The seasonal variation of the friction coefficient was neither obvious nor predictable. Kotek and Florkova (2014) conducted long-term friction monitoring on various pavements and concluded that friction coefficients were affected by surface age, traffic intensity, and climatic conditions. Dan et al. (2017) measured friction coefficients of pavement specimens with different ages, contamination (water, snow, ice), and temperature conditions, and found that friction of new pavement exhibited the highest sensitivity to temperature variations.

2.1.2 Pavement Texture

Pavement texture is the commanding surface characteristic that affects tire-pavement friction, often categorized by various wavelengths into micro-texture (wavelength less than 0.5mm) and macro-texture (wavelength of 0.5mm to 50mm). Micro-texture is generally provided by the relative roughness of the aggregate particles in asphalt pavements and by the fine aggregates in concrete surfaces. Macro-texture is generally provided by proper aggregate gradation in asphalt pavements and by supplemental treatments such as tinning, broom, diamond grinding, or grooving in concrete surfaces (Flintsch et al., 2012).

Various parameters, such as traffic level, aggregate characteristics, and pavement texture, have been included to develop pavement friction prediction models (Ergun et al., 2005; Ahammed and Tighe, 2008; Ahammed and Tighe, 2012; Rezaei and Masad, 2013; and Ueckermann et al., 2015). Several research activities depended on pavement texture for friction performance evaluation using advanced data analysis methodologies (Rado and Kane, 2014; Kane et al., 2015; Kanafi et al., 2015; Kanafi and Tuononen, 2017; and Yang et al., 2017).

2.2 Relationship between Friction and Roadway Crash

Pavement friction and texture are among the most crucial surface factors that influence road safety. Insufficient pavement friction or surface texture can often be a determining factor for a collision, especially under wet conditions. Many studies have investigated the relationship between pavement friction/texture and road crashes and found that the probability of wet-skidding crashes could be reduced if friction between vehicle tire and pavement was enhanced. A recent study by Pulugurtha et al. (2008, 2012) found that crashes significantly decreased with the increase in pavement macro-texture. It recommended maintaining pavement macro-texture of at least 0.08 in. (2.0 mm) on tinned concrete pavements, and 0.04 in. (1.0 mm) on asphalt pavements to reduce crashes and enhance safety on Interstate highways.

Although it is believed that a direct relationship exists between pavement friction/texture and wet-crash rates, no specific threshold values have been established for pavement friction/texture to assure roadway safety (AASHTO, 2008). Pavement friction demands, which are specific to the characteristics of a particular roadway, must be considered when establishing such thresholds. Pavement friction demand is dictated by site conditions (such as longitudinal grade, superelevation, the radius of curvature, terrain, climatic conditions), traffic characteristics (volume and mix of vehicle types), and driver behaviors (prevailing speed, response to conditions, etc.). These conditions are continually changing over time and are different for every roadway, making it difficult to establish a “one size fits all” friction threshold (Merritt et al., 2015).

2.3 Safety Performance Functions

In the AASHTO Highway Safety Manual (HSM, 2010), highway safety is generally evaluated using safety performance functions (SPFs), which are detailed as statistical models to predict the expected average crash frequency for a certain roadway facility, mainly as a function of traffic exposure indicators. The HSM identifies three types of SPF applications:

- Network screening to identify locations that may benefit the most from a safety treatment.
- Determination of safety impacts of design alternatives. When SPFs are used in project-level decision-making, they are applied to estimate the average expected crash frequency for control conditions and the proposed alternatives.
- Determination of safety effects of engineering treatment. These are usually implemented in combination with statistical methods, such as Empirical Bayes (EB), to evaluate the effectiveness of before and after treatments.

Highway agencies are encouraged to develop state-specific SPFs for different roadway facilities and crash types (Merritt et al., 2015). The jurisdiction-specific SPFs are likely to enhance the reliability of the crash predictive method (HSM, 2010; Lu et al., 2012). For example, the SPF in Virginia was developed to include skid resistance and the radius of curvature in their SPFs for interstate and primary highway systems (De León Izeppi et al., 2016).

2.4 ODOT Efforts for Improved Highway Safety

To improve highway safety and save Oklahoman lives, the Oklahoma Department of Transportation (ODOT) operates several rigorous safety-related programs, including (1) the “Skid Studies Program” that schedules testing of pavement friction on an annual basis; (2) the Pavement Management Systems (PMS) program that administrates the data collection and management of pavements; (3) the Statewide Analysis for Engineering & Technology (SAFE-T) database that stores the statewide crash information available from 1998 to present; and (4) the SiteManager™ that provides for data entry, tracking, reporting, and analysis of contract data from award through finalization. It consists of various functionalities, such as contract records, contract administration, contractor payment, materials management, and laboratory inventory management system (LIMS).

Besides, ODOT continues supporting research work to better characterize pavement friction and texture performance for improved highway safety. ODOT has been actively participating in the Every Day Counts (EDC) initiatives to improve roadway safety, and closely collaborating with other agencies such as the Oklahoma Highway Safety Office (OHSO) in analyzing and improving highway safety in Oklahoma.

2.5 Summary

In this Chapter, a comprehensive literature review was conducted. The literature review focused on several relevant technical aspects, including pavement friction and texture, the relationship between friction and roadway crash, safety performance functions, and ODOT’s efforts for improving highway safety.

CHAPTER 3 DATA ACQUISITION AND INTEGRATION

This Chapter investigated relevant data sources at ODOT that could be used in this study. Several database systems managed by ODOT, including the Pavement Management System (PMS), Statewide Analysis for Engineering &Technology (SAFE-T) database, Skid Studies Program, and SiteManager® construction management system, were reviewed. In particular, the relevant data sets, such as pavement surface conditions, roadway geometry, traffic flow characteristics, pavement preventive maintenance treatments, materials testing and sampling results, crash type and severity, were extracted from these ODOT databases. Besides, the friction and texture data sets collected from the existing ODOT projects were also acquired. Since the extensive amount of data was obtained from different database platforms, the acquired data sets should then be linked and integrated for each pavement section under study, which would be used for SPF and friction model developments in Chapter 4 and Chapter 5.

3.1 Pavement Management System (PMS)

ODOT PMS maintains a computer database of pavement distresses and other roadway characteristics for the National Highway System (NHS) and State Highway System (SHS) routes. The PMS data is formatted with one record for every 0.01 miles of pavement, including the location information (highway name, control section number, mile point, control subsection, GPS, etc.), pavement surface characteristics (surface type, IRI, rutting, macro-texture, etc.), roadway geometry (grade, curvature, number of lanes, etc.), etc.

According to ODOT, the subsections of a control section are generated based on multiple criteria in the ODOT Road Inventory Manual, such as state highway junction, political jurisdiction, urban area boundary, surface width, or type change. The subsection breaks are subject to change among different years if pavement type or the number of lanes alters. More details on the breaking rules of the control subsection can be found in ODOT Road Inventory Manual (ODOT, 2010).

Each subsection of a control section can be considered as a uniform roadway segment. Therefore, the roadway subsection was selected as the basic unit for further analysis in this study, and the corresponding data from the various ODOT database was aggregated for each subsection. Table 3-1 presented the summary of the available subsections in the ODOT PMS database from 2012 to 2016.

Table 3-1 Subsections in the ODOT PMS Database (2012-2016)

Highway Classification	Year	# of Subsection	Avg Length of Subsection	Lane Miles
Interstate Highway	2012	0.00	0.00	0.00
Interstate Highway	2014	1316.00	1.02	1346.00
Interstate Highway	2016	1338.00	1.01	1346.00
United Highway	2012	771.00	0.91	702.00
United Highway	2014	1328.00	1.05	1397.00
United Highway	2016	491.00	0.86	421.00
State Highway	2012	198.00	1.11	221.00
State Highway	2014	184.00	1.14	211.00
State Highway	2016	0.00	0.00	0.00
Total	/	5626.00	1.00	5643.00

3.2 Statewide Analysis for Engineering &Technology (SAFE-T)

SAFE-T is a statewide crash database garnered from collision report forms submitted by law enforcement officers (Adams and Warren, 2017). Detailed Oklahoma crash data is available since 1998. The SAFE-T database can generate reports in several formats based upon multiple criteria, such as date ranges, highway filters, control section, division, etc. Crash data is recorded as a point location event with a wide variety of relevant information, including the location information (highway name, control section number, mile point, subsection ID, GPS, etc.), collision type (rear-end, head-on, etc.), collision severity levels (fatality, injured, property damage, etc.), traffic volume in terms of annual average daily traffic (AADT), and roadway characteristics (shoulder, median, etc.).

3.3 SiteManager™ Construction Management System

The ODOT SiteManager™ data system is a comprehensive client/server-based construction management tool, which provides features for data entry, tracking, reporting and analysis of contract data from award through finalization. SiteManager™ construction data consists of various functionality, such as contract records, contract administration, contractor payment, materials management, the sampling test results of pavement mixture.

The locations of the construction sites are descriptive in SiteManager ™, but not linked to the GPS coordinates or the subsections of the control sections as used in the other ODOT database. In order to integrate with other data sets, a manual location matching procedure was implemented for each construction site by examining and comparing the ODOT control section maps and the corresponding location descriptions.

3.4 Skid Studies Program

Historically, the Skid Studies Program at ODOT was managed through the Strategic Asset & Performance Management (SAPM) Division. ODOT used to perform systematic skid studies for the entire highway system before 2010, while in recent years the scope had been downsized to the annual testing of US-69, all the Interstate Highways, as well as the Strategic Highway Research Program (SHRP) sites (ODOT, 2018). Currently, ODOT is transitioning to special skid resistance testing based on an on-demand basis, rather than running through the Skid Studies Program in SAMP.

ODOT collected friction data using a locked-wheel skid tester, a common friction measurement equipment, operating at 50mph during testing. The friction data was recorded at an interval of approximately 0.5 miles, reported by control sections as individual files. A significant amount of data pre-processing efforts was devoted to combining those files in various years into a unified database with universal data formats, since the scope of friction testing sites had been changed during the past years, and the reporting items and data formats were slightly different from year to year.

Friction data collected at ODOT from 2012 to 2016 were gathered and summarized in Table 3-2. Friction data was collected in the outer lane for both directions for divided roads, while one direction for undivided roads. The total lane miles of the yearly skid testing ranged from 0 to 8172 kilometers (0 to 5,078 miles) during the study periods, yielding a total of 29,517 kilometers (18,341 miles) of field friction data collection. No friction data was received in 2016, while only a handful of control sections on US-69 were tested in 2013.

Table 3-2 Data Summary of ODOT Skid Program (2012 – 2016)

Year	Location	# of Control Section	Testing Lane-miles
2012	I-35, US, SH	474	5,078
2013	US-69	14	213
2014	IS, US, SH	664	7,148
2015	IS, US, SH	553	5,903
2016	/	0	0
Total	IS, US, SH	1705	18,341

3.5 Other Data Sources

In addition to the database systems managed by ODOT, ODOT has been sponsoring research projects with extensive pavement field condition data collection. During the past three years, field performance data, including 1mm 3D pavement image data, pavement cracking, rutting, roughness, macro-texture, and friction data, had been collected multiple times on the selected testing sites. These data sets can be used as additional data sources for this project.

3.6 Linking the Various Data Sets for Each Subsection

A significant challenge in the data compilation is the coordination of the various data sets using a uniform referencing system for efficient and consistent data processing. For example, SAFE-T crash data is referenced by control subsections with GPS coordinates; friction data is referenced by control section and milepost; the PMS data contains both information; while the SiteManager™

construction data only includes descriptive information on project locations, which must be manually collected by comparing with the ODOT Contract Section Maps. Data inconsistency is another challenge during the data process and integration. For example, the coding of the traveling directions within the various databases is inconsistent. The PMS database uses “5” for the primary directions while “6” for the secondary directions of a roadway segment, while the crash and friction data use letters to define the directions.

After manually modifying the inconsistent data items into the same formats, all the relevant data sets were linked and summarized for each subsection of a highway control section for further statistical analysis. The data items obtained from each subsection are listed in Table 3-3.

Table 3-3 Data Items Provided in the ODOT Datasets

Data Source	**Data Item**
SAFE-T	Crash data (frequency, type, severity)
SAFE-T	Average annual daily traffic (AADT)
SAFE-T	Presence of medians and shoulders
Skid Studies Program	Friction
PMS	Segment identification: location, length
PMS	Pavement surface conditions: surface type, texture, IRI (rutting)
PMS	Roadway geometry (grade, curve, number of lanes)
SiteManager®	Maintenance rehabilitation & reconstruction (MR&R) Works

CHAPTER 4 SAFETY PERFORMANCE FUNCTION AND FRICTION DEMANDS

The safety performance functions (SPFs) are detailed as statistical models to predict the expected average crash frequency for a specific roadway facility, mainly as a function of traffic exposure indicators. Although skid resistance is commonly agreed as an essential factor in highway safety, it has not been considered in the current SPFs in the Highway Safety Manual (HSM) to estimate crash rates of various roadway categories.

Friction demand, on the other hand, is a critical aspect of pavement friction management. An appropriate level of pavement friction must be maintained across all pavement sections within a given highway network. The level of friction considered appropriate must be determined based on each section's friction demand. Several factors are generally used for the establishment of friction demand, such as the traffic levels, highway function class, climate zone, crash history, and age of surfacing, while the number of crashes or crash rates is the most widely used indicators for the determination of the investigatory and intervention friction threshold levels.

The various data items processed from Chapter 3 enable in-depth statistical modeling for the development of SPF and friction demand levels. In this Chapter, an enhanced SPF was developed based on count data models using ODOT safety-related data sets. Meanwhile, the friction demand levels were determined using the methodologies recommended in the AASHTO *Guide for Pavement Friction*.

4.1 Data Processing

4.1.1 Identify Highway Segment

The acquired data described in Chapter 3 were divided into uniform roadway segments per the subsections of a control section. First, a complete list of highway segments was generated for all the unique subsections in the ODOT PMS database, along with the starting and ending mileposts to define each segment. Subsequently, the initial list of segments was filtered by two criteria. Segments with missing roadway characteristics were eliminated, especially for those without friction data. Meanwhile, the segments with MR&R works during the analysis period were excluded to minimize the impacts of site conditions changes on roadway crashes.

The ability to associate all data for a given roadway segment is critical to the accuracy and continued using them for model development. A major challenge is the coordination of the various data sets using a common referencing system for efficient data processing. As discussed in Chapter 3, SAFE-T crash data are referenced by control subsections with GPS coordinates, friction data are referenced by control section and milepost, PMS data contain both information, while the site construction data only provide descriptive location information manually collected from the ODOT Contract Section Maps. In addition, the coding conventions of some data items are inconsistent among the database, such as the definitions of roadway directions.

After manually modifying the inconsistent data to the same format, all required data were linked to each highway segment by subsection ID and direction of travel. As a result, the sample size was reduced to 1835 roadway segments.

Furthermore, 24 segments were excluded as they were found to have MR&R works from 2012 to 2016, resulting in a final data size of 1811 segments. The basic information of the selected final list of segments is summarized in Table 4-1.

Table 4-1 Lane Miles Analyzed (2012-2016) by Highway Class

Highway Classification	IS Hwy	US Hwy	State Hwy	Total
# of Segment	1103	587	121	1811
Average Segment Length	1.14	1.24	1.26	1.18
Lane Miles	1254	726.62	152.3	2132.93

Table 4-2 Crash Data (2012-2016) by Highway Class

Highway Class	IS Hwy	US Hwy	State Hwy	Total	Percent
Total Crash	25,941	3,644	454	30,039	100.0%
Crash Severity	/	/	/	/	/
Fatal	135	52	7	194	0.65%
Personal Injury	7,369	1,126	172	8,667	28.85%
Property Damage	18,437	2,466	275	21,178	70.50%
Pavement Condition	/	/	/	/	/
Dry	21,652	3,131	413	25,196	83.88%
Wet	4,289	513	41	4,843	16.12%
Type of Crash	/	/	/	/	/
Fixed-Objects	5,600	638	99	6,337	21.10%
Sideswipe	4,779	434	34	5,247	17.47%
Angle-Related	2,532	1,125	146	3,803	12.66%
Rollover	893	137	29	1,059	3.53%
Head-On	49	35	4	88	0.29%
Rear End	12,088	1,275	142	13,505	44.96%

4.1.2 Crash Data

Roadway crashes are classified into a wide range of types. However, only vehicle crashes that are mainly caused by roadway characteristics should be included in this study. This task turned out to be challenging since most crashes were possibly caused by multiple factors. After close consultation with ODOT engineers, Several types of crashes were determined not to be primarily due to inadequate infrastructure conditions and therefore excluded for further analysis. These types included vehicle-train, vehicle-pedestrian, vehicle-animal crashes, and crashes that involved alcohol, drugs, work zones. Furthermore, crashes that occurred on contaminated pavement conditions (snow, ice, oil, et al.) were eliminated from the analysis considering that full contact between tire and pavement surfaces could not be guaranteed. After filtering and aggregating the crash data for the subsections, 34.5 % of the segments had no crash during the analysis period. The detailed crash information is displayed in Table 4-2. The 5-year crash data of analysis show that 29.50% of the crashes led to fatalities or injuries, while 70.50% were property damage crashes. On average, 83.88% of crashes occurred on dry conditions and 16.12% on wet surfaces.

4.1.3 Safety-Related Data Sets

Several factors appear to influence roadway safety performance in previous studies (HSM 2010; Arhin et al. 2015; Fwa et al. 2016; Aram 2010; Miller and Zoloshnja 2009), including traffic volume (AADT), roadway surface conditions (friction, texture, surface type, roughness), and geometry factors (longitudinal grade, horizontal curvature, number of lanes, presence of shoulder and median). These factors, available in the ODOT databases, were acquired and linked to each corresponding segment.

The surface type under this study included asphalt (AC), jointed concrete (JCP), and continuously reinforced concrete pavement (CRCP). For each segment, friction performance was measured in terms of two indices: the average friction number and the interquartile range (IQR) of friction. IQR is the difference between the 75th and 25th percentiles of data, which is a statistical measurement of variability within a segment. Besides, the average of the lowest quartile of mean profile depth (MPD) was used to indicate the worst conditions of surface texture.

International roughness index (IRI), generally expressed in inch per mile, is a standard roadway roughness measure reflecting the reaction of a vehicle to roadway profiles. FHWA (1990) recommended a threshold of 2.7 m/km (170 in/mile) for acceptable ride quality and a threshold of 1.5m/km (95 in/mile) for good ride quality. Accordingly, IRI was ranked as “Good”, “Acceptable”, or “Poor” for each of the 16.1-meter (0.01-mile) ODOT PMS data, and the lowest ranking level within the subsection was assigned to the segment.

Rutting is common distress along the two pavement wheel paths and presents a safety risk to vehicles during wet weather with reduced skid resistance, which could lead to loss of control or hydroplaning accidents (Fwa et al., 2016). In this study, a rut depth of 12.7mm (0.5 in) was selected as the threshold between high and medium rut severity, and 6.4mm (0.25 in.) was chosen in between medium and low rut severity (AASHTO 1989; Lister and Addis 19770; Sousa et al. 1991). Similar to that for IRI, the most severe level was assigned to each corresponding segment.

Table 4-3 Potential Contributing Factors for Crash Analysis

Class	Factors	Description	Statistical Distribution
Crash Exposure	Segment Length	Segment Length (mile)	Min.: 0.05; Max.: 10.2; Mean: 1.178
Crash Exposure	AADT	AADT (vehicle/day)	Min.: 1600; Max.:158,561; Mean: 28,653
Crash Exposure	Rural or Urban	1-Rural; 2-Urban	Rural: 55.5%; Urban: 44.5%
Skid Resistance	Average Friction	The average friction value	Min.: 16.9; Max.: 62.0; Mean: 40.13
Skid Resistance	IQR of Friction	Interquartile of friction	Min.: 0; Max.: 26.95; Mean: 2.85
Skid Resistance	MPD	The average of lowest quartile MPDs	Min.: 0.336; Max.: 2.524; Mean: 0.766
Surface Conditions	Avg. IRI Ranking	1-Good; 2-Acceptable; 3-Poor	Good: 4.8%; Acceptable: 19.8%; Poor: 75.4%
Surface Conditions	Max. Rut Ranking	1-Good; 2-Acceptable; 3-Poor	Good: 6.4%; Acceptable: 23.3%; Poor: 70.3%
Surface Conditions	Pavement Type	1-AC; 2-JCP; 3-CRCP	AC: 57.8%; JCP: 30.6%; CRCP: 11.7%
Roadway Geometry	Avg. Grade	Average grade value	Min.: 0.033; Max.: 4.516; Mean: 1.013
Roadway Geometry	Avg. degree of curvature	Average degree of curvature	Min.: 0; Max.:17.293; Mean: 0.266
Roadway Geometry	Maximal degree of curvature	The largest degree of curve	Min.: 0; Max.: 66.62; Mean: 1.188
Roadway Geometry	Length of curves	Total length of curves with radius < 1000 (m)	Min.: 0; Max.: 2.95; Mean: 0.103
Roadway Geometry	Number of Lanes	# of lanes	2, 3, 4, 6, 8, 10
Roadway Geometry	Presence of Shoulder	0-No; 1-Yes	No: 4.1%; Yes: 95.9%
Roadway Geometry	Presence of Median	0-No; 1-Yes	No: 10.7%; Yes: 89.3%

Many research efforts revealed the radius of the horizontal curve was significant to roadway crashes (Krammes et al. 1993; Aram 2010). Studies also showed the differences between straight sections and curves, which became pronounced at a radius of about 1000 meters (3281 ft) or less (USDOT 1984). Therefore, in this study, curves with a radius below 1000 meters (3281 ft), or a degree of curvature greater than 1.75°, were considered to have negative effects on roadway safety. The total length of such curves within each segment was calculated for further crash analysis.

The influencing factors and their descriptive statistics are shown in Table 4-3.

4.2 Safety Performance Function (SPF)

4.2.1 Overview of Crash Modeling Methods

The crash prediction modeling (i.e. SPF) requires statistical analysis to map the relationship between crash data and roadway characteristics. Before the analysis, it is critical to understand the distribution of crash data. Crash occurrences are discrete and non-negative integers, as well as random and rare events. Therefore, roadway safety in terms of the frequency of crashes is often studied, which involves the number of crashes occurring in some geographical space (usually a homogeneous roadway segment or intersection) over a specified period.

Because crash-frequency data are non-negative integers, Poisson regression models have been used for analysis for several decades (Lord and Mannering 2010). In a Poisson regression model, the probability of roadway segment i having y_i accidents per period (5 years in this study) is given by:

$$P(y_i) = \exp(-\lambda_i)\lambda_i^{y_i}/y_i! \tag{4-1}$$

Where λ_i is the Poisson parameter for segment i, which equals the expected number of accidents per period in segment i. The Poisson regression model is estimated by specifying the Poisson parameter λ_i as a function of explanatory variables, where the most common functional form being $\lambda_i = \exp(\beta X_i)$.

However, Poisson models restrict its distribution with equal mean and variance. Thus, it is not able to handle over-dispersion or under-dispersion problems, where the mean of the crash counts does not take the same value of the variance.

The Poisson-Gamma (Negative Binomial) regression model is an extension of the Poisson model to overcome such possible dispersion problems in the crash data. The Negative Binomial model introduces an error term ϵ into the Poisson parameter:

$$\lambda_i = \exp(\beta X_i + \epsilon) \tag{4-2}$$

When ε approaches zero, the Negative Binomial model becomes a Poisson model. The addition term ε allows the variance of data to differ from the mean, as defined below with k as the over-dispersion parameter:

$$\mathrm{VAR}(y_i) = \mathrm{E}(y_i) + kE(y_i)^2 \tag{4-3}$$

In this project, the enhanced SPF was developed using negative binomial regression models with a log-linear relationship between crash frequency and roadway characteristics.

4.2.2 SPF and Empirical Bayes Method

SPFs are regression equations that estimate the average crash frequency for a specific site type. In the HSM (2010), the SPFs were developed for three facility types (rural two-lane roads, rural multilane highways, and urban and suburban arterials). An example of SPF for roadway segments on rural two-lane highways is:

$$N_{SPFs} = (AADT) \times (L) \times 365 \times 10^{-6} \times exp(-0.312) \tag{4-4}$$

where AADT is the average annual daily traffic volume (vehicles per day), and L is the length of the roadway segment (miles). Both are crash exposure-related factors, while roadway conditions and characteristics have not been considered.

The SPFs in the HSM must be calibrated to local conditions since exiting SPFs are only directly representative of the sites used to develop them (HSM 2010). Two parameters should be determined in the calibration process: the calibration factor and the calibrated dispersion parameter. The calibration factor (C) is determined by:

$$C = \sum_{all\ sites} observed\ crashes / \sum_{all\ sites} predicted\ crashes \tag{4-5}$$

where predicted crashes for each site are calculated using the SPF predictive model. Subsequently, the calibration factor works as a multiplier to the SPF prediction:

$$SPF_{Calibrated} = C * SPF_{existing} \tag{4-6}$$

Furthermore, the statistical reliability of average crash estimation can be improved by combining observed crash frequency and estimates of the average crash frequency, using the Empirical Bayes predictive method (EB Method) to compensate for the potential bias resulting from regression-to-the-mean (RTM) errors. The RTM is the tendency of crash fluctuations where a comparatively high crash frequency is followed by a low crash frequency (Hauer 1996). Failure to account for the RTM bias may result in an over-estimation or under-estimation of long-term crash frequency. The EB method uses a weighted adjustment factor, w, which is a function of the SPF's over-dispersion parameter, k, in the negative binomial distribution:

$$w = 1/(1 + k \times (\textstyle\sum_{all\ study\ years} N_{predicted})) \tag{4-7}$$

Therefore, the expected average crash frequency for the analyzed period is calculated:

$$N_{expected} = w \times N_{predicted} + (1 - w) \times N_{observed} \tag{4-8}$$

4.2.3 Selection of Influencing Variables

Variable selection is a process to determine a set of independent variables for the final regression model from a pool of candidate variables. The subset of the independent variables needs to be as complete and realistic as possible. On the other hand, the independent variables included should be as few as possible to eliminate irrelevant variables, which will decrease the precision of the model and increase the complexity of data collection. To balance the goodness-of-fit and model simplicity, the backward stepwise method was implemented for the model selection and development.

The backward stepwise method is often used in variable selection for regression models. It starts with a model including all candidate variables. At each step, the variable with the least significance is removed until all the remaining variables are significant. To determine the best final model in this process, the

Akaike Information Criterion (AIC) and the log-likelihood ratio test are performed. The AIC, proposed by Akaike (1973), has been routinely used during the past decades:

$$\text{AIC} = -2log\left(L(\hat{\theta})\right) + 2K \tag{4-9}$$

Where log is the maximized log-likelihood value and K is the number of estimable parameters in the approximating model. It is desired to rescale the AIC values so that the minimum AIC (AIC_{min}) has a value of zero. The AIC value can be rescaled as the simple difference:

$$\Delta_i = AIC_i - AIC_{min} \tag{4-10}$$

To better interpret the relative likelihood of a model, the Akaike weight is calculated as below (Burnham and Anderson 2002):

$$w_i = \exp\left(-\frac{1}{2}\Delta_i\right) / \sum_{r=1}^{R} \exp\left(-\frac{1}{2}\Delta_i\right) \tag{4-11}$$

Subsequently, the model with the highest Akaike value is selected as the best model. Furthermore, the best model can be compared to other models in terms of the evidence ratios:

$$ER_i = w_{best}/w_i \tag{4-12}$$

The evidence ratios help strengthen the evidence for or against the various alternative hypotheses. A large evidence ratio suggests strong support that one model is better than the other.

Another technique to determine the best model is the log-likelihood ratio (LLR) test, which is generally used to compare two nested models where one model is obtained from the other by setting some of the parameters to be zero. The null hypothesis of this technique assumes the reduced model (L_r) is true. While the alternative hypothesis supposes the current model (L_c) is true. To test the null hypothesis, the likelihood-ratio is calculated using Equation 4-13 and compared with the critical Chi-Square value (χ_k^2). LLR is distributed as χ^2 statistic with k degree of freedom, where k is the difference in the number of parameters estimated between the two models including the intercepts (Lord et al., 2013). A larger LLR leads to small p-values, which indicates that the null hypothesis can be rejected. In other words, the reduced model is not preferred in comparison to the current model.

$$LLR = 2 \times \left(\log(L_r) - \log(L_c) \right) \tag{4-13}$$

4.2.4 Safety Performance Function Modeling Results

The negative binomial regression model was developed using 5 years of statewide crash data in Oklahoma. The function form, as shown in Equation 4-4, was adopted to develop the enhanced SPF incorporating roadway characteristics. It should be noted that the natural log transformation of segment length (L) and AADT were used herein, the same form as that used in the AASHTO HSM (2010):

$$N_{SPF} = \beta_1 L \times \beta_2 (AADT) \times exp\left(\alpha + \sum_{3}^{i} \beta_i \times X_i \right) \tag{4-14}$$

where: β_1 = coefficient of the influencing variable X_i; α = intercept.

The initial model was built with all of the listed parameters in Table 4-3 and then eliminated the least significant parameter step by step. The corresponding AIC was computed for each model and summarized in Table 4-4.

Table 4-4 Akaike Information Criterion for Model Selection

Model	AIC	Δ_i	w_i	ER_i	Variable Removed
1	10769.96	6.97	0.010	32.62	/
2	10767.96	4.97	0.028	12.00	Max. Rut Level
3	10766.10	3.11	0.072	4.74	Smallest Quartile MPD
4	10764.38	1.39	0.170	2.00	Avg. Degree of Curve
5	10762.99	0.00	0.341	1.00	Length of Curve
6	10763.43	0.44	0.274	1.25	Rural or Urban
7	10766.10	3.11	0.072	4.74	Pavement Type
8	10767.99	5.00	0.028	12.18	Avg IRI Level
9	10772.47	9.48	0.003	114.43	Max. Degree of Curve
10	10779.20	16.21	0.000	3310.98	Avg Grade

Table 4-5 Log-Likelihood Ratio Test Results

Model	#Df	Chisq	Pr(>Chisq)
6	13	/	/
5	14	2.44	0.12

The Akaike weights (w_i) in Table 4-4 indicate that Model 5 has a 34.1% chance of being the best model, followed by Model 6, which eliminates an additional variable. The evidence ratio (ER_i) of Model 6 over Model 5 is 1.25, suggesting that Model 5 is 1.25 times more likely to be the best fit. Since the chances of being the best model are close for Model 5 and 6, the LLR test was performed to determine the final model. As shown in Table 4-5, the p-value is greater than 0.05, failing to reject the null hypothesis. In other words, including the extra variable does not provide a significant improvement on the goodness-of-fit of the model. In conclusion, Model 6 was selected as the final SPF model in this study. The estimated coefficients and over-dispersion parameters are displayed in Table 4-6. The enhanced SPF is obtained by inserting the coefficients into the model, as shown in Equation 4-14.

Table 4-6 SPF Model Regression Analysis Results

Parameters	Coefficients	Std. Error	z value	Pr(>|z|)	Sig.Code
(Intercept)	-8.28	0.688	-12.037	< 2e-16	***
Ln of Segment Length	0.60	0.046	12.902	< 2e-16	***
Ln of AADT	1.24	0.066	18.767	< 2e-16	***
Avg Friction	-0.02	0.006	-2.455	0.0141	*
IQR Friction	-0.06	0.013	-4.667	3.1E-06	***
Avg IRI Level	0.16	0.072	2.259	0.0239	*
Pavement Type	-0.14	0.063	-2.159	0.0308	*
Avg Grade	0.20	0.066	3.051	0.0023	**
Max. Degree of Curve	0.03	0.011	2.410	0.0160	*
# of Lanes	0.19	0.051	3.733	0.0002	***
Presence of Shoulder	-1.37	0.196	-7.000	2.6E-12	***
Presence of Median	-0.93	0.164	-5.627	1.8E-08	***

Note: 1). Significance codes: 0 '***' 0.001 '**' 0.01 '*' 0.05 '.' 0.1 ' ' 1
2). Dispersion parameter for Negative Binomial=0.4166
3). AIC: 10763.43

In addition to segment length and AADT considered in the AASHTO HSM SPF model, nine pavement surface condition parameters and roadway geometry factors are significant contributors to roadway vehicle crashes. The positive regression coefficients for some factors, such as segment length, AADT, number of lanes, IRI level, degree of curvature of horizontal curves, and longitudinal grade, imply that the average risk of crashes is expected to increase with the increase of those factors. These findings are consistent with several previous studies (HSM 2010; Arhin et al. 2015; Fwa et al. 2016; De León Izeppi et al. 2016). On the other hand, the risk of crashes decreases with the increases in the other factors which have negative coefficients. It is desirable that higher surface friction can significantly reduce vehicle crashes, especially under wet conditions (FHWA 2016). As proved in

Table 9, both the average friction and the variance of friction (IQR) have negative effects on vehicle crashes. Besides, the presence of shoulder and/or median helps to reduce the risk of crashes, which is consistent with that illustrated in the HSM (2010). For pavement type, which is a categorical variable, it suggests that certain pavement types generate fewer crashes as compared to others. Such findings should be further explored and verified in future research due to the unbalanced data sets in terms of pavement types.

4.2.5 Crash Estimation with Empirical Bayes Method

Because a traffic crash is generally a rare event, one shortcoming of safety estimates based on accident counts is that they may be too imprecise to be useful. They are subject to a common, long recognized, regression-to-mean (RTM) bias in the safety analysis. For practical reasons, one is often interested in the safety of entities that either requires attention because they seem to have too many accidents or merit attention because they have fewer accidents than expected. The Empirical Bayes (EB) method is commonly known to address two problems of safety estimation; it increases the precision of estimates beyond what is possible when one is limited to the use of two-three years of history accidents, and it corrects for the RTM bias.

With the enhanced SPF, the expected crash number in the five years was estimated by combing with the EB method. An example is provided on US-69 and displayed in Figure 4-1. The figure displays the data by the segments on US-69. The observed crash within each segment is marked with a triangle symbol, and the predicted crash from the SPF predictive model is plotted with circular circle symbols.

In general, the estimation from the SPF model is found to be higher on those segments with zero observed crashes and lower than those segments with observed high crash rates. To reduce the RTM bias and produce more reliable crash estimations, the SPF predicted crash rate is further improved with the EB Method, as shown in Equations 4-7 and 4-8. After employing the EB method, the expected crash rate is plotted with a dotted line in Figure 4-1.

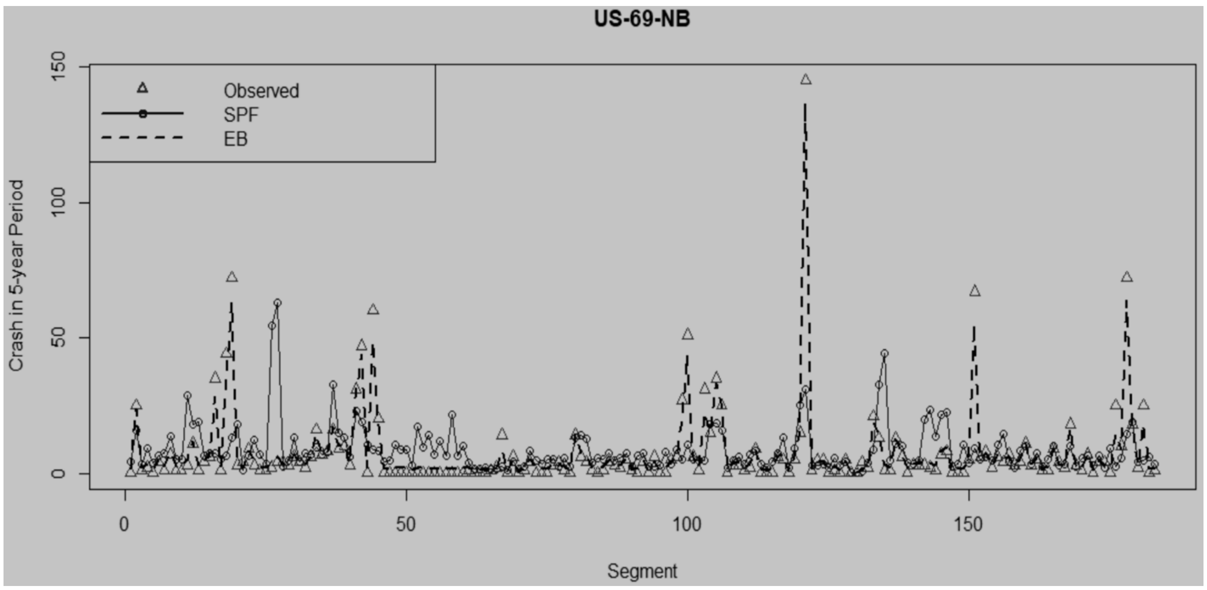

Figure 4-1 Observed, SPF Prediction, and Expected Crashes on US-69 NB

4.3 Friction Demands

4.3.1 Pavement Friction Management Program

Highway safety management in the U.S. began in 1966 with the passage of the Highway Safety Act to improve and expand the nation's highway safety activities. The Act established the State and Community Highway Safety Grant Program (U.S.C. Title 23, Section 402), commonly known as the "402" program. The aspects of a safety management program of interest to pavement engineers are the design and maintenance of roadway surfaces that enhance highway safety by reducing skid-related crashes (i.e., ensuring there is adequate friction at the pavement–tire interface throughout a pavement service life). As a result, highway agencies have been increasingly interested in setting up or improving pavement friction management (PFM) programs that help ensure adequate levels of surface friction and texture to minimize the risk of skid-related crashes (FHWA, 1980). Figure 4-2 shows a typical example of PFM programs. The procedure of successful strategies for managing pavement friction includes the following key steps:

- Network definition - subdivide the highway network into distinct pavement sections and group the sections according to levels of friction need.
- Network-level data collection - gather all the necessary information, including pavement friction and texture, and crash data.
- Network-level data analysis - Analyze friction and/or crash data to assess overall network condition and identify friction deficiencies. Herein, investigatory and intervention levels for friction are established, based on which a detailed site investigation or the application of a friction restoration treatment is developed.
- Detailed site investigation - Evaluate and test deficient pavement sections. Subsequently, causes and remedies are determined for restoration design over the project length in terms of non-friction-related items, such as alignment, the layout of lanes, intersections, and traffic control devices, the presence, amount, and severity of pavement distresses, and longitudinal

and transverse pavement profiles; and the current pavement friction characteristics including both micro-texture and macro-texture.

- Selection and prioritization of short- and long-term Restoration treatments - Plan and schedule friction restoration activities as part of the overall pavement management process by comparing costs and benefits of the different restoration alternatives over a defined analysis period.

This project followed the framework in Figure 4-2 and made the most use of the available ODOT datasets described in Chapter 3. The pavement sections were consistent with the current control sections and subsections in the PMS dataset. The crash data were recorded in the SAFE-T dataset, and the friction data were processed from the Skid Studies Program. The establishment of the investigatory and intervention levels is introduced herein, and the selection of treatments through a life cycle cost analysis will be investigated in the following chapters.

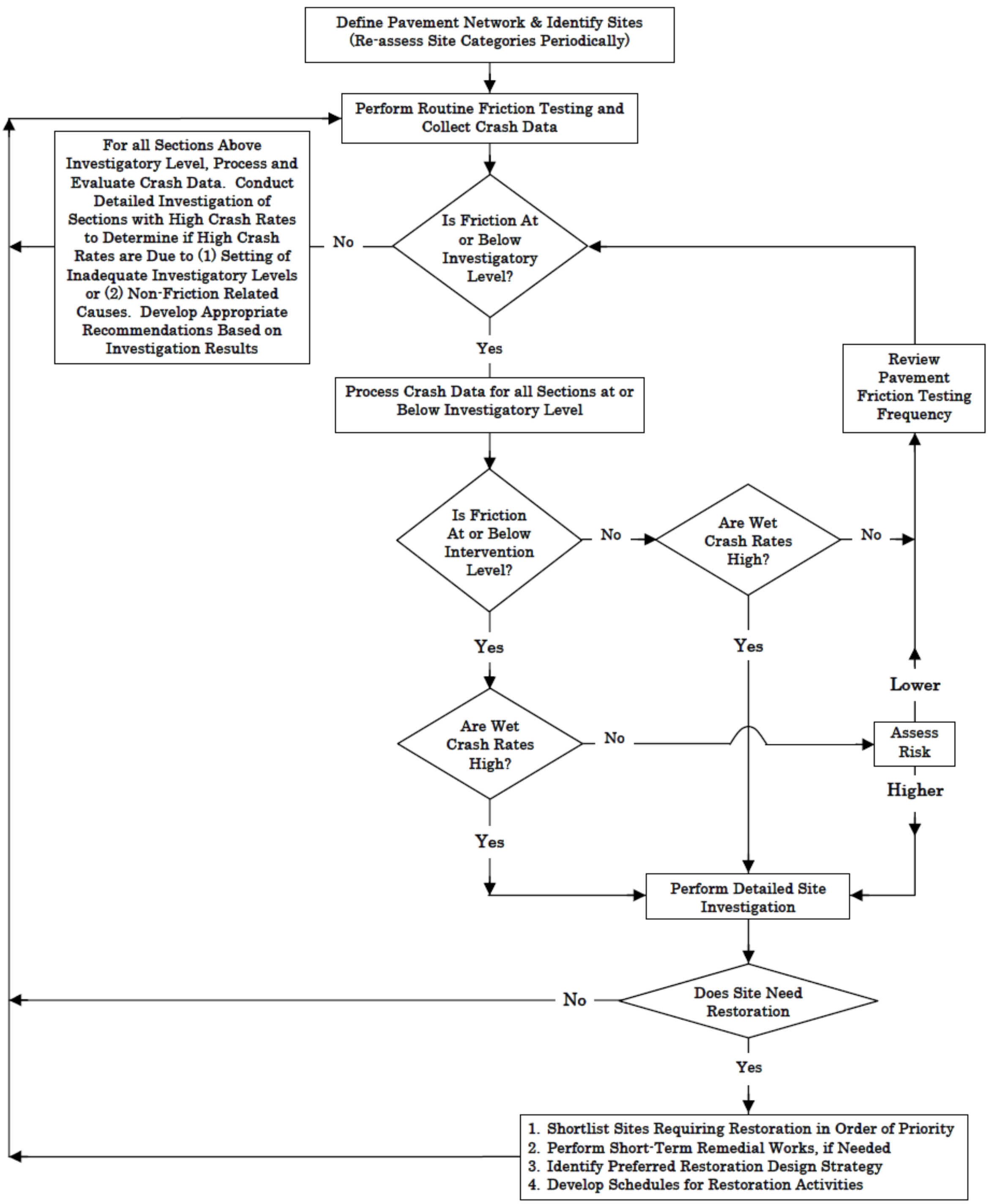

Figure 4-2 Flowchart of An Example PFM Program (AASHTO, 2009)

4.3.2 Methods for Determining Friction Demand

Because conditions and circumstances change along a highway, it is challenging to define one single friction threshold between “safe” and “potentially unsafe.” Although the ideal situation is to have friction supply meet or exceed friction demand over the entire system, such a practice would be prohibitively expensive (as well as largely unnecessary) and would not generate the cost-benefits associated with a better-targeted strategy. A more practical approach, therefore, is to maintain an appropriate level of pavement friction within the highway network, based on each section’s friction demand. This approach ensures the provision of adequate friction levels for a variety of roadways (intersections, approaches to traffic signals, tight curves) and traffic conditions.

In a PFM program, the adequacy of friction is assessed using the two distinct threshold levels defined earlier in this Chapter - investigatory and intervention levels. Pavement sections with measured friction values at or below an assigned investigatory level are subject to a detailed site investigation to determine the need for a warning or remedial action, such as erecting warning signs, performing more frequent testing and analysis of friction data and crash data, or applying a short-term restoration treatment. For pavement sections with friction values at or below the intervention level, remedial action may consist of either immediately applying a restoration treatment or programming a treatment into the maintenance or construction work plan and erecting temporary warning signs at the site of interest.

Presented in the sections below are three feasible methods to establish the investigatory or intervention friction levels, either in terms of friction number (FN) or international friction index (IFI), as recommended in the *AASHTO Guide of Pavement Friction* for use in identifying deficient or potentially deficient PFM sections.

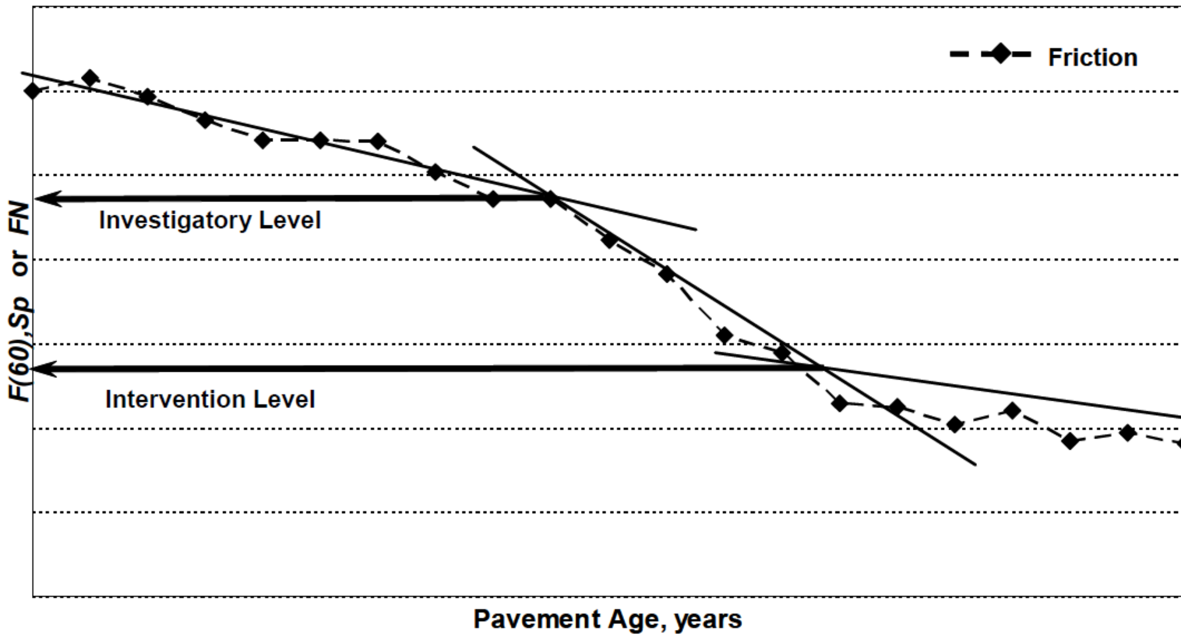

Figure 4-3 Setting Investigatory and Intervention Levels Using Time History of Pavement Friction (AASHTO, 2009)

Method 1 establishes thresholds only using historical pavement friction data. An example graphical-based Method 1 is presented in Figure 4-3. This method uses historical trends of friction loss determined by plotting friction loss against pavement age or time for a specific friction demand category. The investigatory level is set at the pavement friction value where friction loss begins to increase at a significantly faster rate. The intervention level is then set at a certain amount (e.g., five FN points) or percentage (e.g., 10 percent) below the investigatory level. The friction value at which friction loss begins to increase rapidly can be determined graphically or through analytical/statistical methods.

Method 2 establishes thresholds using both historical pavement friction data and crash data. This method compares historical pavement friction and crashes data for the given friction demand category for which levels are being set. Figure 4-4 shows a plot of friction and wet-to-dry crash trends for a specific friction demand category. The investigatory level is set corresponding to a large change in friction loss rate, while the intervention level is set where there is a significant increase in crashes.

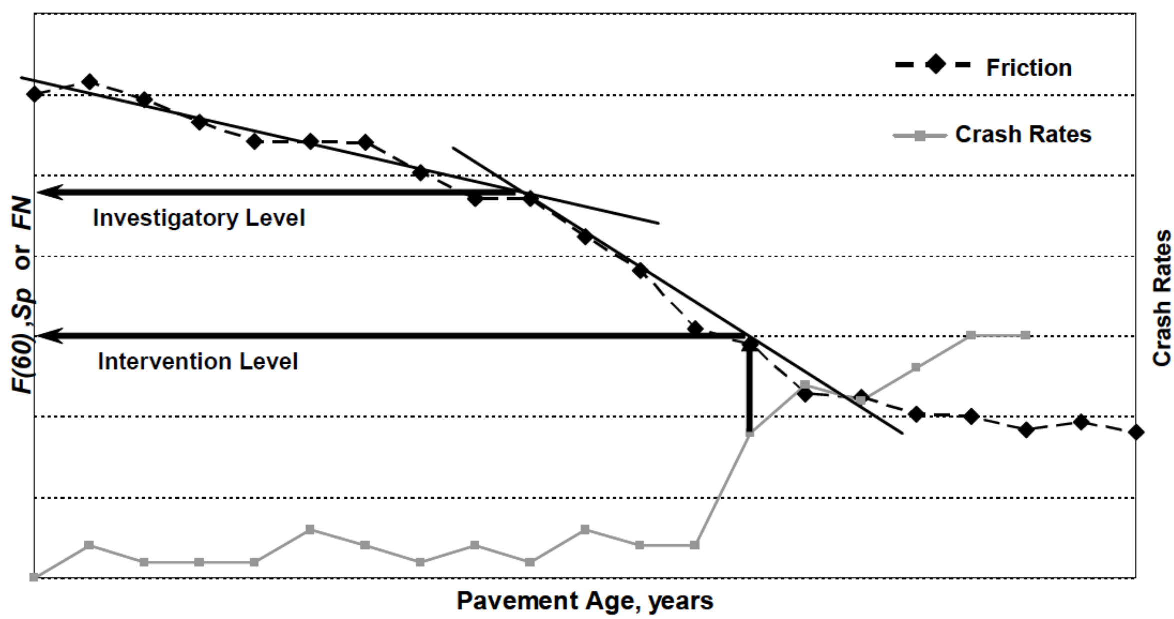

Figure 4-4 Setting Investigatory and Intervention Levels Using Time History of Friction and Crash Rate History (AASHTO, 2009)

Method 3 establishes thresholds using pavement friction distribution and crash rate - friction trend. This method uses the distribution of friction data versus the crash rates that correspond with the friction for the category of the roadway for which the levels are being set. As the most robust approach, Method 3 has the advantage of allowing one to discern the number of roadway sections below a certain level and to adjust the level to accommodate a highway agency's needs and budget.

4.3.3 Determining Friction Demand with Crash Frequency

The data used to determine the friction demands were preprocessed from the available data items at ODOT as described in Chapter 3. 1, 812 subsections were filtered out with friction values compiled from the Skid Studies Program and crash numbers from the SAFE-T database. The recorded friction values of each year from 2010 through 2018 were compiled together with the numbers of crashes on these pavement subsections. The paired friction values and numbers of crashes were compiled and summarized in Table 4-7.

Table 4-7 Subsection Counts and No. of Crashes by Friction Range

Friction Range	Subsection NO.	Mean of Crash Number
<20	28	14.9
[20,25)	115	17.5
[25,30)	366	12.0
[30,35)	1116	5.6
[35,40)	1670	3.3
[40,45)	1709	2.5
[45,50)	1164	1.8
[50,55)	511	1.2
[55,60)	128	0.9
[60,65)	19	1.2
≥65	4	1.0

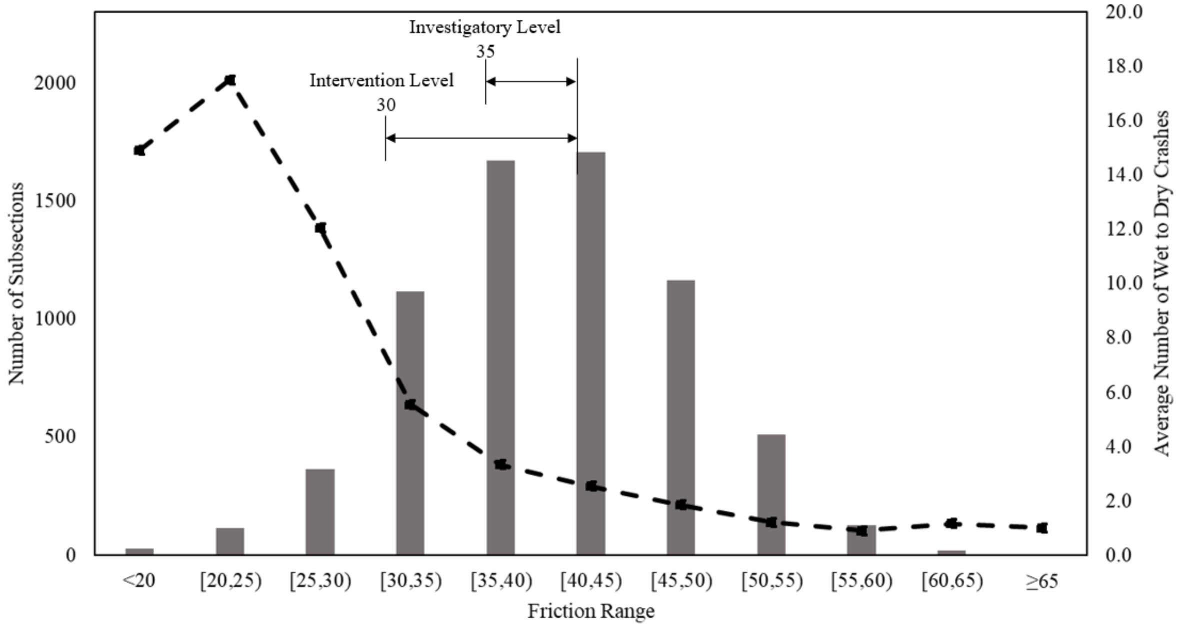

Figure 4-5 Setting Investigatory and Intervention Levels Using Oklahoma Friction and Crash Data

Method 3 was applied in this project to establish the friction demand thresholds using pavement friction distribution and crash rate–friction trend, with the following four steps:

- Step 1 - plotted a histogram of counting pavement subsections with friction value at several ranges. On the same graph, plotted the average mean number of the wet-to-dry crash for the friction value at the same range (Figure 4-5).
- Step 2 - calculated the mean pavement friction (mean= 40.3) and standard deviation (sd = 7.4) for all the studied subsections.
- Step 3 - set the investigatory level as the mean friction value minus “X” times of standard deviations of friction. The factor “X” was adjusted in consideration of the wet-to-dry crashes curve. According to Figure 4-5, “X”

was set to 0.7, and the investigatory level was set to 35, where the wet-dry crashes began to increase considerably.

- Step 4 - set intervention level as the mean friction value minus “Y” times of standard deviations of friction. The factor “Y” was more significant than “X” and was adjusted so that the intervention level to a minimum satisfactory wet-to-dry crash rate or by the point where the amount of money was available to repair that many roadway sections. Herein, “Y” was recommended to be 1.4, and the intervention level was set as 30. However, the friction levels could be further adjusted based on the cost and benefit analysis.

4.4 Summary

This Chapter described the detailed procedures of processing the ODOT datasets for the development of enhanced Safety Performance Function (SPF) and the establishment of friction demand levels. The developed SPF can be used to predict the expected number of crashes under different pavement conditions. On the other hand, the friction demands are a crucial component for the Pavement Friction Management program. An in-depth analysis of friction and crash data suggested that the investigatory level could be set to 35 and the intervention level be 30. The findings from this Chapter would be integrated into Chapter 6 to quantify the safety costs for various pavement preventive treatments.

CHAPTER 5 PAVEMENT FRICTION PREDICTION MODELS

Predicting pavement friction is an important step in a Pavement Friction Management program for the selection and prioritization of restoration treatments. The various data sources from Chapter 3 enable the use of in-depth statistical modeling techniques to develop friction prediction models for different pavement maintenance treatments. In this Chapter, the friction performance after each treatment was analyzed, and conventional regressional friction models were developed using the ODOT datasets. Meanwhile, advanced deep learning (DL) based algorithms were also implemented for friction prediction directly using pavement surface texture profiling data, which could provide an additional alternative for evaluating skid resistance on roadway segments without filed friction data.

5.1 Conventional Regression Models

Figure 5-1 shows the compiling process of friction numbers for the subsections before and after maintenance treatments based on the data sets from the ODOT database. Pavement subsections received preventive treatments were identified from the SiteManager™ database, and their construction material properties were also acquired. The descriptive location information in SiteManager™ for each subsection was then linked to the corresponding control section ID and the GPS coordinates in the PMS database. Subsequently, the traffic volumes on the subsections were obtained from the ODOT traffic maps. The friction numbers before and after each treatment were compiled from the Skid Program.

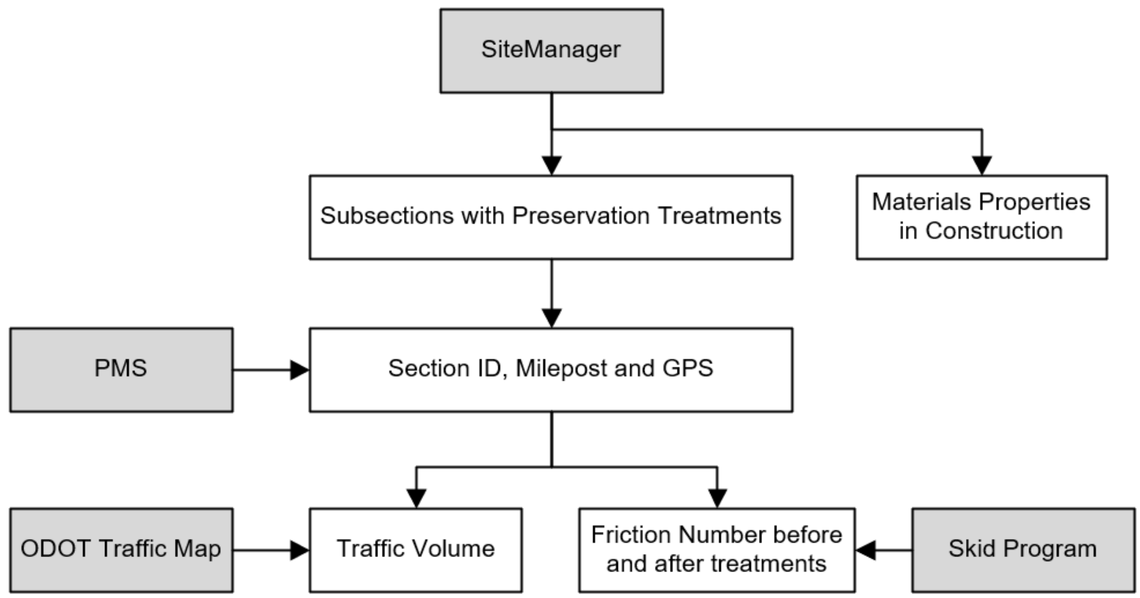

Figure 5-1 Flowchart for Conventional Friction Model Development

After a comprehensive data compiling process, 770 subsections with complete data sets were identified for further analysis, who received three primary types of maintenance treatments. Table 5-1 summarized the number of subsections for each treatment type. A thin overlay is the most widely used treatment type, while UTBWC has the least number of subsections. The following analyses were conducted on three aspects: the friction performance for each treatment, the influencing factors of friction performance, and the development of regressional friction prediction models.

Table 5-1 Summary of Subsections with Preventive Treatments

Treatment Type	Subsection Number	SiteManager Definitions
Thin Overlay	/	Superpave Mix
AC TypeS4	526	Asphalt Concrete Type S4
AC TypeS5	89	Asphalt Concrete Type S5
AC TypeS6	12	Asphalt Concrete Type S6
UTBWC	34	Ultra-Thin Bonded Wearing Couse
Diamond Griding	109	P.C. Concrete for Pavement

5.1.1 Friction Performance of Preservation Treatments

The identified subsections were further filtered where friction numbers were available shortly after the construction (within 1 year), in order to investigate the friction performance immediately after each treatment, as summarized in Table 5-2. Figure 5-2 visualized the distribution of friction numbers for each treatment type. Pavements with diamond grinding treatments demonstrated the highest average friction numbers, possibly resulted from the enhanced macrotexture after grinding. The friction numbers of pavements with UTBWC treatments were slightly higher than those with thin overlays. Thin overlays paved with AC S6 mixes had a higher average friction number than S4, S5 mixes, and UTBWC. However, it should be noted that the sample sizes for S6 mixes and UTBWC were relatively small, whose results may not be accurate.

Table 5-2 Summary of Pavement Friction Immediately After Maintenance

Maintenance Type	Section Count	Min.	Max.	Mean	Standard deviation
Thin Overlay	122	28.8	58.4	41.7	6.1
AC TypeS4	83	28.8	58.4	40.8	6.5
AC TypeS5	31	33.2	49.9	42.9	4.7
AC TypeS6	8	43.0	53.3	46.4	3.6
UTBWC	7	37.0	54.5	43.6	7.0
Diamond Grinding	32	35.5	52.4	45.6	5.2

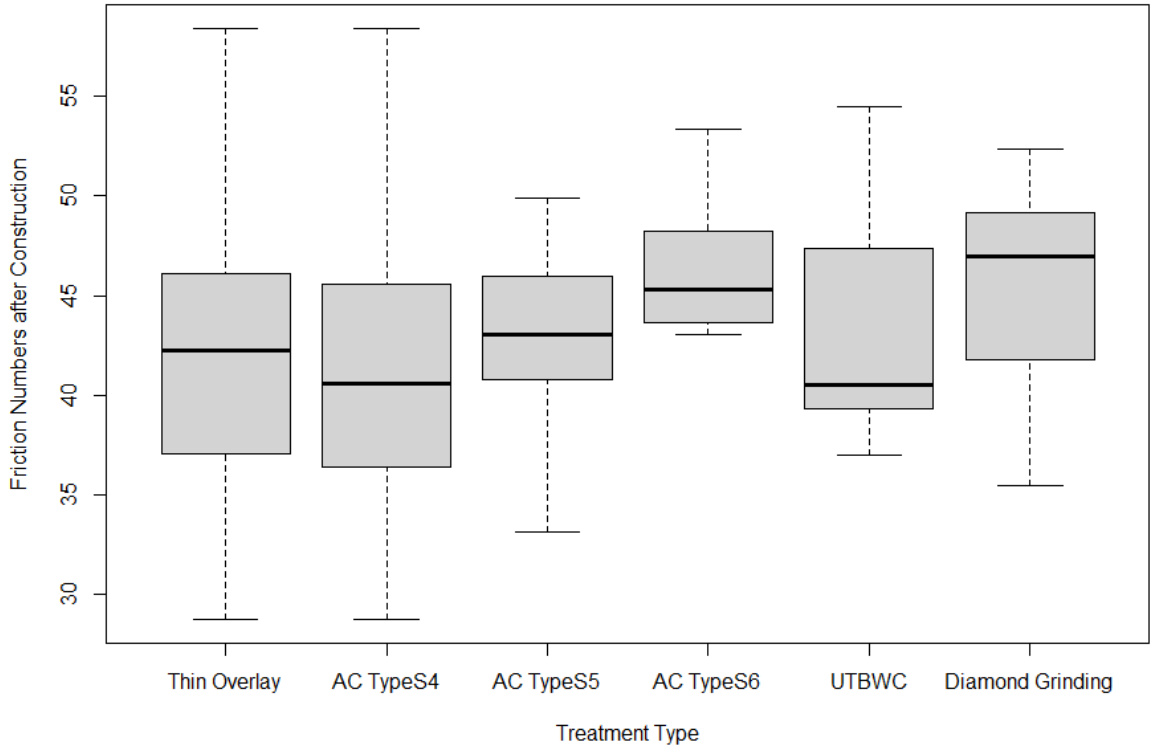

Figure 5-2 Boxplot of Pavement Friction for Each Treatment Type

5.1.2 Influencing Factors on Friction Performance

The multivariance linear analysis was conducted to investigate the influencing factors on the friction performance for the preventive treatments. The friction number was the dependent variable while treatment age, treatment type, traffic volume (AADT), binder type, and aggregate type and properties (Los Angeles LA Abrasion, Micro Deval, and rock type) were adopted as the independent variables. The three categorical factors: the treatment type, binder type, and aggregates type were coded into nominal scales. For example, the thin overlay S4 was set as the default nominal type while the other treatment types (S4 and S5) were compared to S4 as an indicator variable.

Table 5-3 Pavement Friction Multivariant Analysis Results

Variable	Estimate	Std. Error	t value	Pr(>|t|)	Significance
Intercept	47.46	2.82	16.85	<0.001	***
Treatment Age (Year)	-0.44	0.20	-2.23	0.027	*
AADT (1000 vehicles / day)	-0.10	0.03	-3.84	0.000	***
Treatment Type (AC TypeS4 as comparison)	/	/	/	/	/
AC TypeS5	3.35	0.79	4.26	<0.001	***
AC TypeS6	3.41	2.30	1.48	0.140	
UTBWC	6.15	1.27	4.84	<0.001	***
Diamond Grinding	2.53	1.55	1.63	0.105	
Binder Grade (PG 64-22 as comparison)	/	/	/	/	/
PG 70-28	3.61	2.59	1.39	0.165	
PG 76-28	-0.74	1.31	-0.56	0.575	
LA Abrasion	-1.23	0.45	-2.77	0.006	**
Micro Deval	1.17	0.29	4.10	<0.001	***
Aggregate Type (Rhyolite as comparison)	/	/	/	/	/
Limestone	4.84	3.26	1.48	0.140	
Sandstone	11.24	5.34	2.11	0.037	*
Granite	13.41	4.69	2.86	0.005	**

Note: 1. Significance Codes: 0 ‘***’ 0.001 ‘**’ 0.01 ‘*’ 0.05 ‘.’ 0.1 ‘ ’ 1
2. Residuals: Min -11.02, 1Q -2.81, Median 0.18, 3Q 2.86, Max 14.16
3. Residual standard error: 4.09 on 167 degrees of freedom
4. Multiple R-squared: 0.53, Adjusted R-squared: 0.50
5. F-statistic: 14.6 on 13 and 167 DF, p-value: <2e-16

The multivariant analysis results were summarized in Table 5-3. The regression model had an adjusted R squared value of 0.50, indicating roughly 50% of the variance in friction numbers could be explained by the influencing factors. The friction values declined at the rate of 0.44 units per year. An addition of 1000 AADTs in traffic volume would cause 0.1 units to decrease in pavement friction.

As compared to the S4 treatment, the S5 and S6 treatments could improve the pavement frictions by 3.35 and 3.41 units, while the diamond grinding and

UTBWC lifted the friction by 2.53 and 6.15 units, respectively. In other words, UTBWC performed the best in improving pavement friction. For binder grade, PG 64-22 was used as the baseline type, but the statistical results indicated pavement friction was not sensitive to the change of binder grade.

The aggregate properties had significant influences on pavement friction based on the statistical analysis results. LA abrasion and Micro-Deval are two essential properties for aggregates. The LA abrasion test subjects coarse aggregate samples (retained on the No. 12 (1.70 mm) sieve) to abrasion, impact, and grinding in a rotating steel drum containing a specified number of steel spheres. The LA abrasion test tends to break aggregates while the Micro-Deval test tends to polish them. As a result, a lower LA abrasion loss value indicates that the aggregates are tougher and more resistant to abrasion. On the contrary, aggregates with a higher Micro-Deval value tend to result in higher pavement friction. The statistical results in Table 5-3 confirmed these assumptions.

For the aggregate type, rhyolite was set as the comparison group, and the analysis showed that sandstone and granite aggregates could significantly increase pavement frictions, while the results for treatments with limestone were not statistically significant.

5.1.3 Regressional Friction Prediction Models

The statistical regressional model derived from Table 5 3 was comprehensive by considering all the statistically important variables. However, on many occasions, the values for serval variables are unknown on existing pavement surfaces. Besides, the major objective of this study was to select the appropriate preventive treatment for a maintenance project with optimal skid performance and thus safety benefits. For this specific application, the traffic volume, aggregate type and properties, binder type can be assumed to be identical. Therefore, in this section, a simplified linear friction prediction model for each treatment type was developed considering the treatment type as the only independent variable. The friction deterioration before and after each treatment was examined.

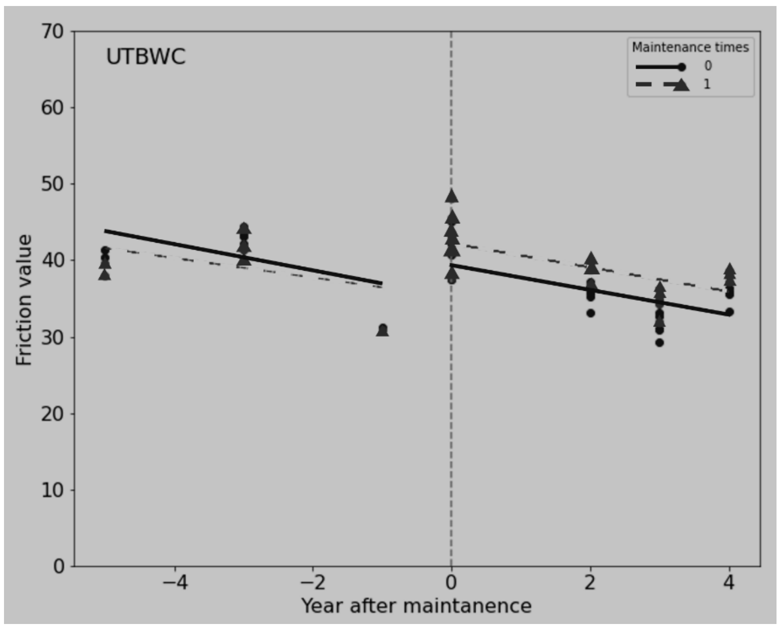

Figure 5-3 Friction Variations of Pavement Sections After UTBWC Treatment

Taking UTBWC as the example, the friction variations on the pavement sections before and after UTBWC treatments were plotted in Figure 5-3. On the left half of the figure, both the sections in red and in blue had not received any treatment yet. It is observed that those sections ("before treatment") showed very similar determination trends in terms of the friction numbers. On the right half of the figure, the sections in red from the left half received their first UTBWC treatment ("after treatment") while those in blue remained untreated ("before treatment"). A performance jump was observed when comparing surface friction values for the "before treatment" and "after treatment" sections. A linear friction model was thus built with the intercept of 42.5 (initial friction after treatment) and a deterioration rate of -0.8 units per year.

Similarly, the linear deterioration models for thin overlay and diamond grinding were also built, whose results were summarized in Table 5 4. In recent years, ODOT has installed dozens of high friction surface treatments (HFST) to address safety needs at high demanding locations. The research team used the OSU Grip Tester and collected seven rounds of friction data (November 2015, March 2016, June 2016, September 2016, January 2017, July 2017, and December 2017) on 6 HFST sites (3 sites on SH-20 in Salina, 2 sites on I-40 and 1 site on I-44 in Oklahoma City. The friction data were plotted in Figures 5-4. The average friction values of the six HFST sites from the seven collection events were 0.97, 0.89, 0.79, 0.73, 0.66, 0.69, and 0.61. The friction numbers measured from the Grip Tester were transformed to the skid numbers measured with the ODOT locked wheel tester (referred to as SN) using the conversion equation developed from in the ODOT SP&R 2306 research project. Subsequently, the linear regression model for HFST was also developed, whose results were added to Table 5-4.

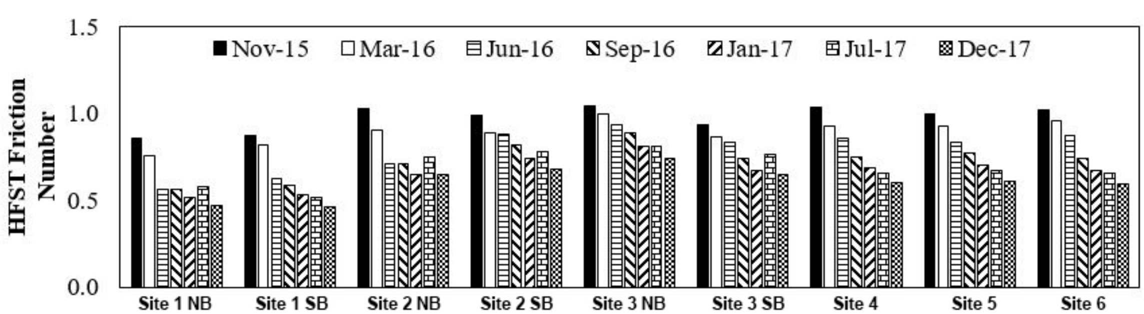

Figure 5-4 Friction Deterioration of HFST Sites in Oklahoma

Table 5-4 Linear Friction Deterioration Models

Maintenance Type	Intercept	Deterioration Rate	Subsection No.	R^2
Thin Overlay	41.4	-0.5	98	0.42
UTBWC	42.5	-0.8	29	0.45
Diamond Grinding	44.5	-0.6	10	0.43
HFST	95.0	-5.9	6	0.93

HFST had the highest intercept in the friction model, followed by the diamond grinding, UTBWC, and thin overlay. Slight differences were observed between the intercepts in Table 5 4 and the average value shown in Table 5 2. The reason was that the data used in this section did not include sites with more than one treatment during the analysis period. For deterioration rates, HFST deteriorated at the highest rate, followed by UTBWC, diamond grinding, and thin overlay. The R^2 of HFST reached over 0.93, while those for the other three treatment types were around 0.44, indicating only about 44% of the variances in friction numbers could be explained by the regression models. More robust models are therefore expected for reliable analysis results.

5.2 Deep Convolutional Neural Network (CNN) Friction Model

It is widely accepted that surface macro-texture is a predominant contributor to pavement friction and wet-pavement safety. In a friction model, most state highway agencies characterize macro-texture data using traditional indicators. However, such methods depend on simple averaging of the profile peaks, which abandon the rich detailed information of the texture profiles. It is expected that friction models developed directly using high-resolution raw surface texture data could generate more accurate results than those based on the traditional texture indicators.

In this section, deep learning (DL) based friction prediction model was developed using the most recent development in artificial intelligence. The DL model development process includes two critical steps: (1) obtain the raw pavement surface texture profile data at the top critical portion where the tire-road contact occurs; (2) utilize the convolutional neural network (CNN), one of the commonly used DL architectures, for the development of DL friction model named as FrictionNet.

5.2.1 Data Acquisition and Processing

The data used herein were acquired from 49 high friction surface treatment (HFST) sites in 12 states in the U.S., including Oklahoma, through a research project sponsored by the Federal Highway Administration (FHWA). The locations of the data collection sites are shown in Figure 5-5. Pavement macrotexture data and friction data were collected in parallel at traffic speed using the AMES™ high-speed profiler and the OSU Grip Tester, respectively.

The AMES Model 8300 Survey Pro High-Speed Profiler is used to collect surface macro-texture data at 0.5 mm (0.020 in) sampling intervals at speeds between 40 km/h (25 mph) and 112 km/h (70 mph). The system is certified by the FHWA Long-Term Pavement Performance program and other state testing agencies (AMES 2017). The Grip Tester, designed following the ASTM E2340/E2340M-11R15 standard (ASTM E2340/E2340M-11R15 2015), can continuously measure pavement longitudinal friction operating around the critical slip of an anti-lock braking system (ABS). The device can operate at the highway speed of 80 km/h (50 mph) as well as the low speed of 32 km/h (20 mph) using the desired water film thickness sprayed in front of the testing tire during data collection.

Figure 5-5 Friction Data Collection Site Locations

In addition to the HFST sections, the adjacent untreated lead-in and lead-out pavement sections 300 ft before and after the HFST treatments were also tested in the data collection. These sections included those on flexible pavements, rigid pavements, and bridge decks with or without grooving (Figure 5-6). The surface macrotexture data was collected at 0.020-in (0.5-mm) sampling interval at speeds between 25 mi/h (40 km/h) and 70 mi/h (112 km/h). The friction data from the Grip Tester was continuously measured at 3-ft (1-m) interval.

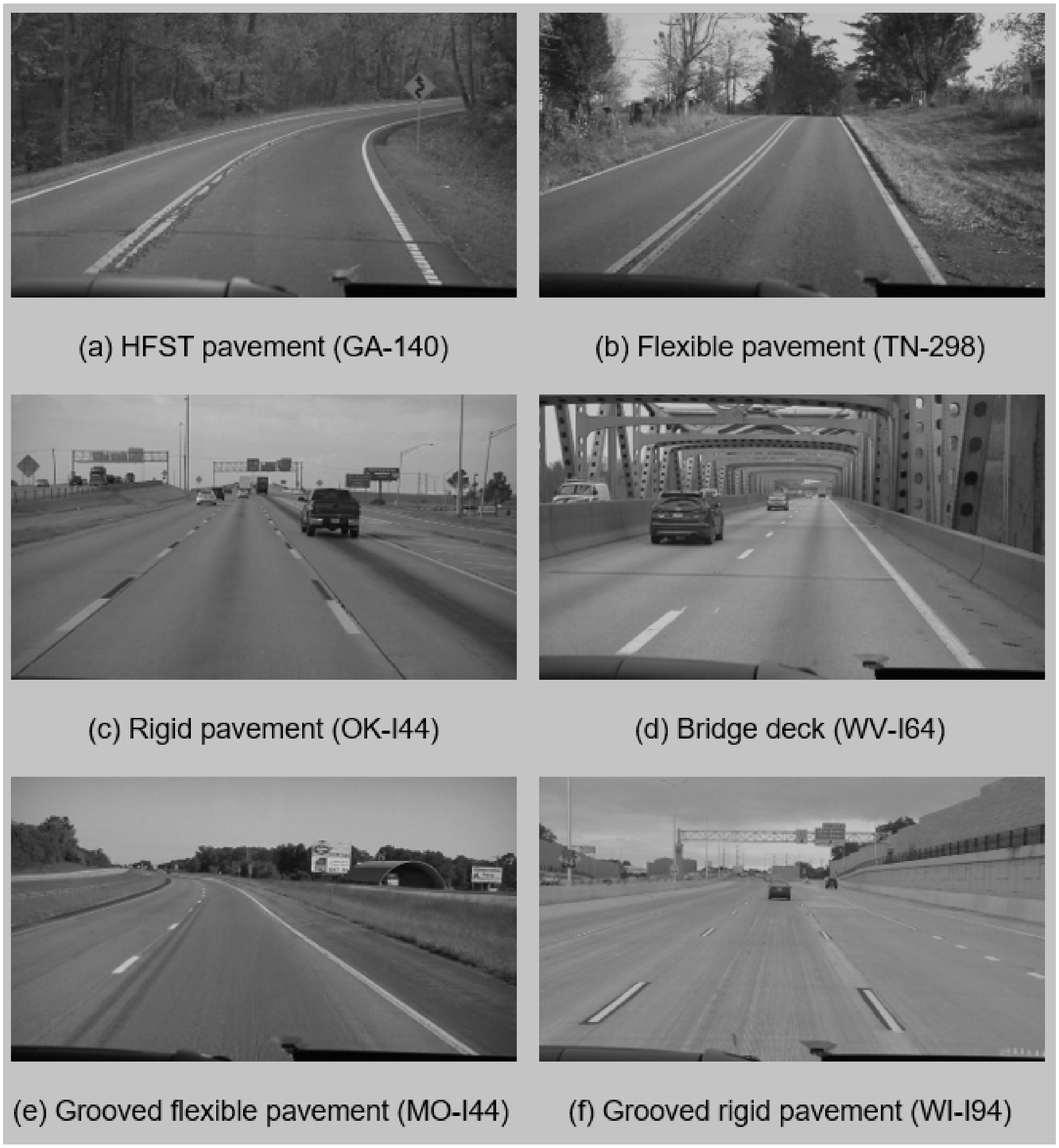

(a) HFST pavement (GA-140)
(b) Flexible pavement (TN-298)
(c) Rigid pavement (OK-I44)
(d) Bridge deck (WV-I64)
(e) Grooved flexible pavement (MO-I44)
(f) Grooved rigid pavement (WI-I94)

Figure 5-6 Examples Pavement Categories

After collecting pavement macro-texture and friction data, the measured macro-texture profile and friction number are paired for every 1-meter segment for the DL model development. Instead of using the raw macro-texture profiles, the spectrogram of the macro-texture profile was obtained and fed to the CNN network as the training input. Every 1-meter raw macro-texture profile contained 2,000 texture points, while its corresponding spectrogram had a dimension of 50 × 38. The transformation of raw texture profile into spectrogram has been successfully implemented in many one-dimensional (1D) audio signal processing studies for CNN network training and information retrieval (Dieleman and Schrauwen 2014 and Huang et al. 2015). Figure 5-7 shows an example spectrogram with time and frequency decompositions of a macro-texture profile. The collected friction numbers are rounded to the nearest 0.1 ranging from 0.2 to 1.0 to represent skid performance of diversified pavement surface categories.

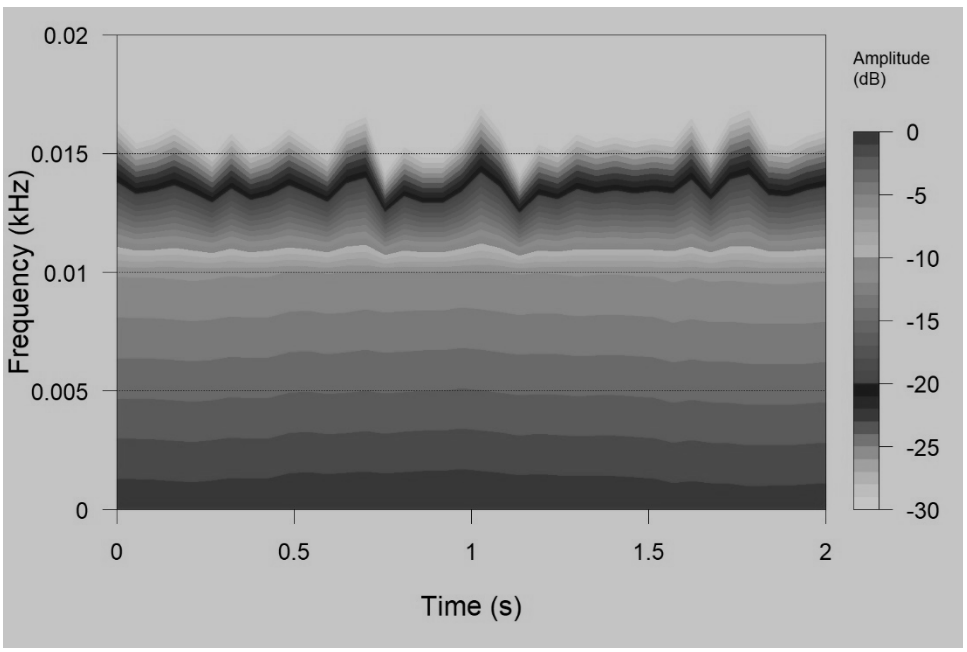

Figure 5-7 Example Spectrogram of Texture Profile

Data collection accomplished on the field sites had a total length of 63,648 m (208,818.9 ft). The obtained texture and friction data had an imbalanced distribution between the different classes. For example, there were 15,319 friction values equal to 0.8 whereas only 2,328 of them were 1.0. The data imbalance feature could underperform the CNN model since CNN architecture assumes a balanced distribution of classes in the training data. Therefore, the sampling method, as introduced in other studies (Chen et al. 2004 and He and Garcia 2009), was adopted herein to generate a balanced distribution of classes in the prepared dataset and to improve the performance of the proposed model. Finally, the 63,000 pairs of macro-texture and friction data with a balanced distribution of classes were prepared for the development of FrictionNet. 80%, 10%, and 10% of the prepared data were randomly selected for training, validation, and testing, respectively.

5.2.2 Deep CNN Modeling and Training

As depicted in Figure 5-8, the proposed deep-learning CNN model FrictionNet was constituted of six layers: two convolution layers, three fully-connected layers, and one output layer. The convolution layers extracted feature maps of the input, while the fully connected layers connected neurons between layers and classify the input. The input of the proposed FrictionNet was the spectrogram of raw texture profile with the size of 50 × 38. The output layer produced the probability distribution of predicted 9 friction levels based on the result of the softmax function. There were 64 and 96 kernels with size 3 × 3 for the first and second convolutional layers. 64, 96, and 32 neurons were contained in each fully-connected layer from the left to the right as shown in Figure 5-8. After each convolutional layer, average pooling was added with the size of 2 × 2 without overlapping. The activation function employed hyperbolic tangent function for the convolutional and fully connected layers, which has been commonly used in artificial neural networks (Cireşan et al. 2012).

The tuned parameters of FrictionNet, in a total of 606,409, were summarized in Table 5-6. The network was trained using the 50,400 pairs of pavement texture spectrogram and friction data sets. With one NVIDIA GeForce GTX TITAN Black graphics processing unit (GPU) card, the training process took 2.73 hours and reached maximum training and validation accuracy. The MXNet library (https://mxnet.incubator.apache.org/) was implemented as the platform herein for the development of FrictionNet.

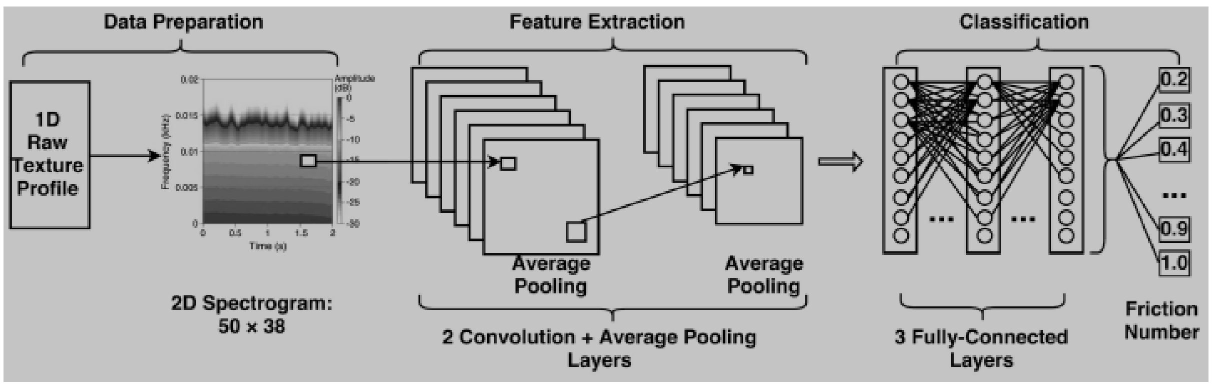

Figure 5-8 Deep Learning-based FrictionNet Architecture

Table 5-5 Parameters for FrictionNet

Layer	Number of parameters
Layer 1: convolution	640
Layer 2: convolution	55,392
Layer 3: fully connected	540,736
Layer 4: fully connected	6,240
Layer 5: fully connected	3,104
Layer 6: output	297
Total	606,409

Selecting the appropriate combination of various training techniques was influential in the training process for FrictionNet to achieve high prediction accuracy and reduce training time. Stochastic gradient descent and Xavier initialization were related to the weight information during the training of the model; L2 regularization and dropout layers were applied to combat overfitting for the network; Cross-Entropy and softmax function were adopted concerning the classification of the predicted friction numbers. The brief introductions to the techniques with the best performance for the proposed model were described in the following.

Learning method. The weighting parameters can be updated during the learning process via several approaches: AdaGrad optimizer (Duchi et al. 2011), RMSprop optimizer (Hinton et al. 2012), and stochastic gradient descent (Krizhevsky et al. 2012). Stochastic gradient descent demonstrated the best performance and was adopted in this CNN model as the learning method with a batch size of 30 examples, the momentum of 0.9, and weight decay of 0.0005. A small weight decay was essential to tune the CNN model, and the update of weight was defined as

$$\begin{cases} v_{i+1} = 0.9 * v_i - 0.0005 * \varepsilon * w_i - \varepsilon * \left\langle \frac{\partial L}{\partial w} \middle| w_i \right\rangle_{D_i} \\ w_{i+1} = w_i + v_{i+1} \end{cases} \tag{5-1}$$

where i is the iteration index, v is the momentum variable, ε is the learning rate, and the component inside of the open angle bracket is the average over the i^{th} batch D_i of the deviation of the objective with respect to w, evaluated at w_i (Krizhevsky et al. 2012).

Weight initialization. Right weight initialization is important to ensure the network converging with reasonable training time and controllable loss function. Three methods: uniform, normal, and Xavier initialization had been tested to initialize the weights in each layer of the proposed network. The Xavier initialization, which is designed to keep the scales of gradients at roughly the same level within all layers, worked best in practice among them. This initializer filled the weights with random numbers in the range of [-c, c], where c equals to the square root of 2.34 divided by n_i in this model and n_i is the number of neurons feeding into weights (Glorot and Bengio 2010).

Combat overfitting. Overfitting refers to a model that approximates the training data too well that the noise or random fluctuations in the training data is picked up and learned as concepts by the model (Brownlee 2016). Overfitting could occur during the tuning of the 606,409 parameters in the FrictionNet model. Regularization methods, including L2 regularization and dropout layers, were applied to combat the overfitting of the network. L2 regularization, also known as weight decay, modified the cost function by adding an extra term which was the sum of the squares of all the weights in the network. The extra term was expressed as

$$L2RegularizationTerm = \frac{\lambda}{2n}\sum_{w} w^2 \tag{5-2}$$

Where λ>0 is known as the regularization parameter, and *n* is the size of the training set (Nielsen 2017).

The dropout layer is another efficient technique to reduce overfitting with significant improvements over other regularization methods (Krizhevsky et al. 2012 and Srivastava et al. 2014). Two dropout layers were utilized after the first and the second fully-connected layers with the probability of 0.25. With this dropout layer, 25% of the hidden neurons in the two fully-connected layers would be randomly excluded during training. This significantly increased the robustness of the model with different random subsets of the neurons, and therefore reduced test errors and overfitting (Krizhevsky et al. 2012).

***Cost Function*.** The cost will be high if the proposed model cannot accurately classify friction numbers. Cross-Entropy was employed in FrictionNet as the cost function of the softmax classifier to address the learning slowdown issue and measure how close the actual output to the desired output (Nielsen 2017). Since the prediction of friction number via FrictionNet was a discrete multi-class classification problem, the Cross-Entropy was defined as:

$$H(p,q) = -\sum_x p(x) log q(x) \tag{5-3}$$

where p and q are the actual and predicted friction number at x^{th} training individually. Cross-Entropy could improve the learning speed and learn at a rate controlled by the similarity between the actual and predicted friction number (Zhang et al. 2017).

***SoftMax Function*.** The SoftMax function is popular as the final layer of a neural network that yields the predicted probability scores for multi-classification problems (Glorot and Bengio 2010, Krizhevsky et al. 2012, Abdel-Hamid et al. 2014, and Nielsen 2017). The calculated probabilities ranged from 0.0 to 1.0 for each class, while the sum of all probabilities should be 1.0. The target class would have the highest probability score among all the possible classes. The SoftMax function was explained as

$$P\left(y = j \middle| z^{(i)}\right) = \emptyset_{softmax}\left(z^{(i)}\right) = \frac{e^{z^{(i)}}}{\sum_{j=0}^{k} e^{z_k^{(i)}}} \tag{5-4}$$

where the net input z is defined as $z = w_0x_0+w_1x_1+\ldots+w_mx_m$ (w is the weighted vector, x is the feature vector of a training sample, and w_0 is the bias unit) (Raschka

2015). It computed the probability that the training sample *x(i)* belonged to class j was given the weight and net input *z(i)*. Accordingly, the softmax function was applied to the output layer so that the FrictionNet could be used to predict friction level among the 9 classes ranging from 0.2 to 1.0 at 0.1 intervals.

5.2.3 Prediction Results

The performance of FrictionNet was evaluated based on the classification accuracy score, which was defined as the number of correct predictions divided by the total number of model predictions multiplied by 100 to turn it into a percentage. The classification accuracy score was expressed as below:

$$\text{accuracy}\ (y, \hat{y}) = \frac{1}{n}\sum_{i=0}^{n-1} 1(\hat{y}_i == y_i) * 100 \tag{5-5}$$

Where y^ and *y* are the predicted and actual friction levels.

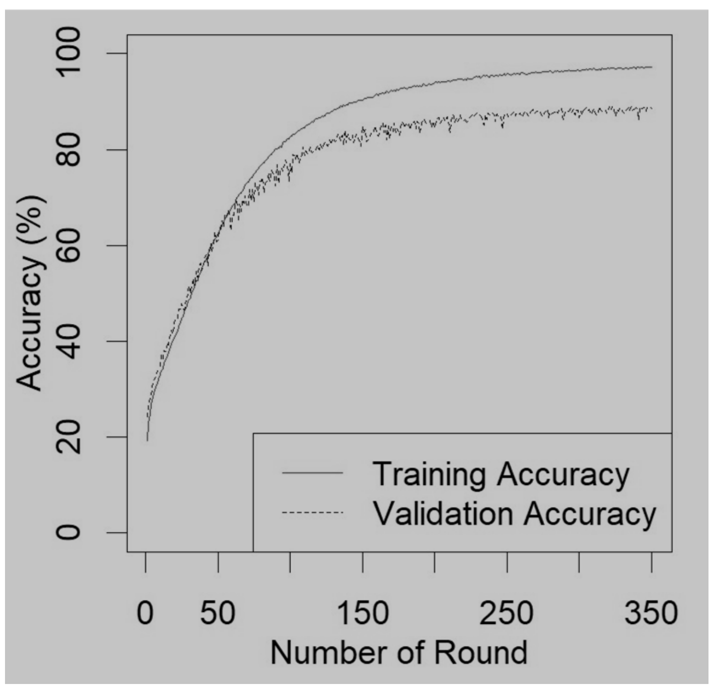

Figure 5-9 Accuracy of FrictionNet

50,400 and 6,300 pairs of pavement texture spectrogram and friction data sets were randomly selected for the training and validation of FrictionNet. The classification accuracies for training and validation were displayed in Figure 5-9. As observed, the accuracy was improved as the training round increases. The highest classification accuracy of FrictionNet was 96.85% observed at the 314th iteration. Therefore, the parameters derived at the 314th iteration were considered as the "optimal" for the FrictionNet architecture. The accuracy of training data achieved at 96.85% while 88.92% for validation data. With the L2 regularization and dropout layers, the validation classification accuracy remained approximately to that of the training data, indicating no overfitting problem in this model.

The testing data was selected from one of the testing sites. It was approximately 6,300-meter or 3.9-mile in length, which contained 6,300 texture profiles. The optimal parameters obtained from training and validation data training were applied in prediction on testing data. The predicted and actual friction levels were summarized in Table 5-6. The numbers located along the diagonal line in the confusion matrix represented the correct predictions for each friction level. 5,573 correct predictions and 727 false predictions were obtained from the model for the testing data sets, resulting in a classification accuracy of 88.37%. There were two potential reasons for the incorrect predictions. First was the location wondering of GPS from two data collection devices. In detail, pavement texture and friction data were collected via two separate vehicles and then paired based on their GPS coordinates, which may produce slightly different readings. Also, the wandering of the two vehicles during field data collection may vary. Second, the noises in the input of FrictionNet, though addressed by the spectrogram technique, may still have impacts on the friction prediction accuracy. Nevertheless, the results in Table 5-6 show that FrictionNet could predict correct friction levels with high accuracy.

Table 5-6 Summary of FrictionNet Prediction Accuracy

Actual/predicted friction	**0.2**	**0.3**	**0.4**	**0.5**	**0.6**	**0.7**	**0.8**	**0.9**	**1**
0.2	**687**	17	12	12	8	5	4	0	4
0.3	20	**577**	34	12	12	3	10	5	2
0.4	24	54	**557**	18	16	6	9	7	6
0.5	16	28	16	**618**	12	3	8	3	2
0.6	9	18	5	4	**638**	7	8	3	3
0.7	4	11	5	2	2	**659**	9	2	3
0.8	10	34	11	11	18	28	**562**	39	13
0.9	9	8	7	6	4	11	28	**616**	7
1	0	1	2	0	0	1	2	0	**653**

The total processing time for the entire testing section was 1.78 minutes. On average, it takes 16.95 milliseconds per processing of one texture profile. The processing time was much shorter than the time took to collect the responding 3.9-mile field data at 60 mph (approximately 3.90 minutes). In addition, the FrictionNet was implemented on a single middle-class GPU. With more advanced algorithms and powerful GPU, the processing time could be reduced further. Therefore, the current FrictionNet can predict friction numbers from the collected texture data in real-time.

To better visualize the performance of FrictionNet, the actual and predicted friction levels of 50 randomly selected samples from the testing data were plotted in Figure 5-10. Only 3 false predictions appeared in the 50 selected samples. The prediction accuracy on validation and testing data sets was 88.92% and 88.37%

which excelled the accuracy of the regression model using traditional texture indicators.

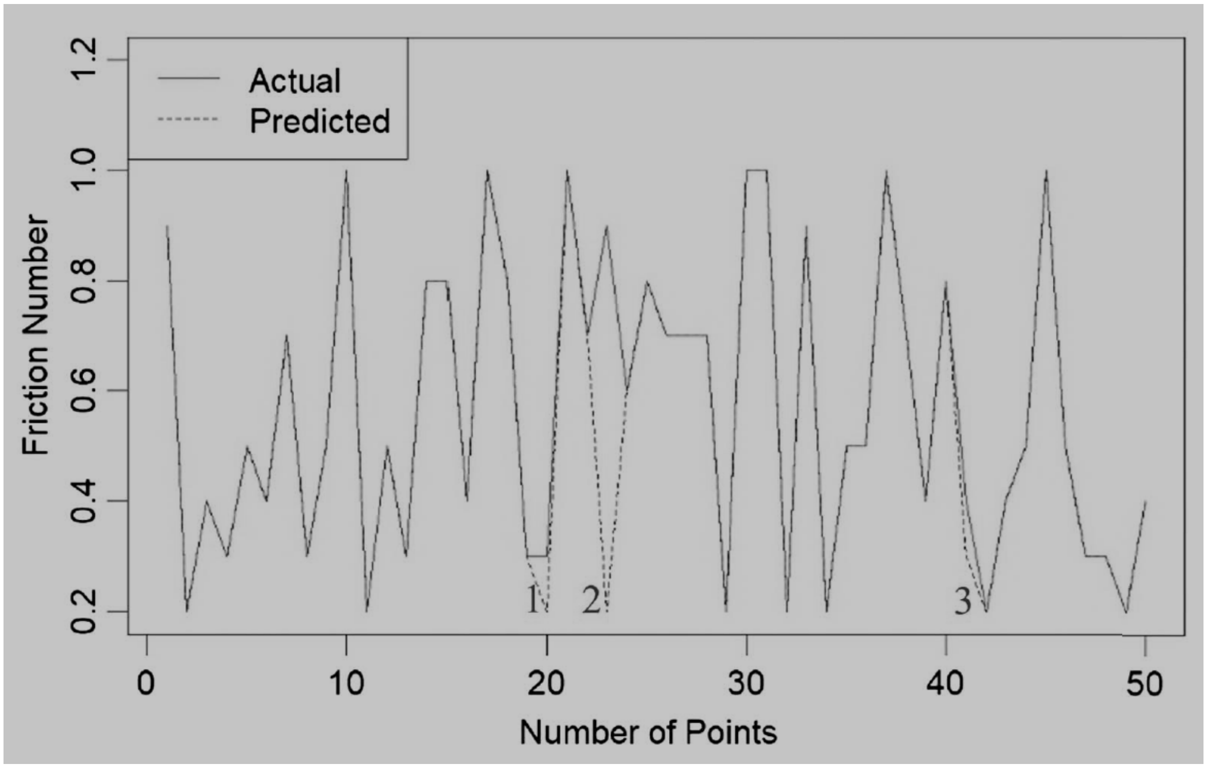

Figure 5-10 FrictionNet Validation Results

5.3 Summary

This Chapter analyzed the friction performance of the commonly used treatment types in Oklahoma. The influencing factors on friction were identified based on multivariate analysis methods, and the deterioration models were developed using ODOT data sets. The deterioration models can be combined with the SPF model developed in Chapter 4 to predict the friction variations and the expected crash numbers of the pavements with various preventive treatment options during the entire life cycle period, which will be discussed and applied in Chapter 6 for the selection and prioritization of restoration treatments.

Meanwhile, deep-learning techniques were applied in this Chapter for the development of the FrictionNet model directly using pavement surface texture profiles. The FrictionNet results demonstrated promising accuracy in classifying pavement friction levels, which could enable transportation agencies to predict friction performance from texture profiles in real-time.

CHAPTER 6 LIFE CYCLE COST ANALYSIS FOR COMPARING MAINTENANCE STRATEGIES

With the enhanced SPF and the friction prediction models developed in Chapter 4 and Chapter 5, the different maintenance strategies can be prioritized based on agency, user, but also safety-related costs during the life cycle analysis period. The RealCost software developed by FHWA has been widely used by state highway agencies to predict agency and user costs. A VBA spreadsheet tool was developed to supplement RealCost by including the calculation of safety costs in the life cycle cost analysis procedure.

6.1 Life Cycle Cost Analysis

6.1.1 The LCCA Procedure

Transportation agencies advocate for effective measures evaluating the costs, benefits, timing, longevity, and decision-making process to determine an effective pavement program (MnDOT, 2014). As an increasingly challenging issue, preservation is especially critical in Oklahoma due to its relatively small transportation budget and correspondingly fragile maintenance budget (Riemer et al., 2010). Instead of conducting costly, time-consuming rehabilitation and reconstruction projects, proactive preservation is more cost-effective to provide the traveling public with improved safety and mobility, reduced congestion, smoother and longer-lasting pavements (Geiger, 2005).

Life cycle cost analysis (LCCA) is an engineering economic analysis tool that many state agencies require for pavement construction and rehabilitation decision making (MnDOT, 2017; Gransberg et al., 2010; Bilal et al., 2009; J. Hall et al., 2009; Monsere et al., 2009; Cambridge et al., 2005). The basic steps involved in an LCCA, as shown in Figure 6-1, were summarized from the FHWA *Life Cycle Cost Analysis Primer* (FHWA 2002) and the *Interim Technical Bulletin* (FHWA 1998):

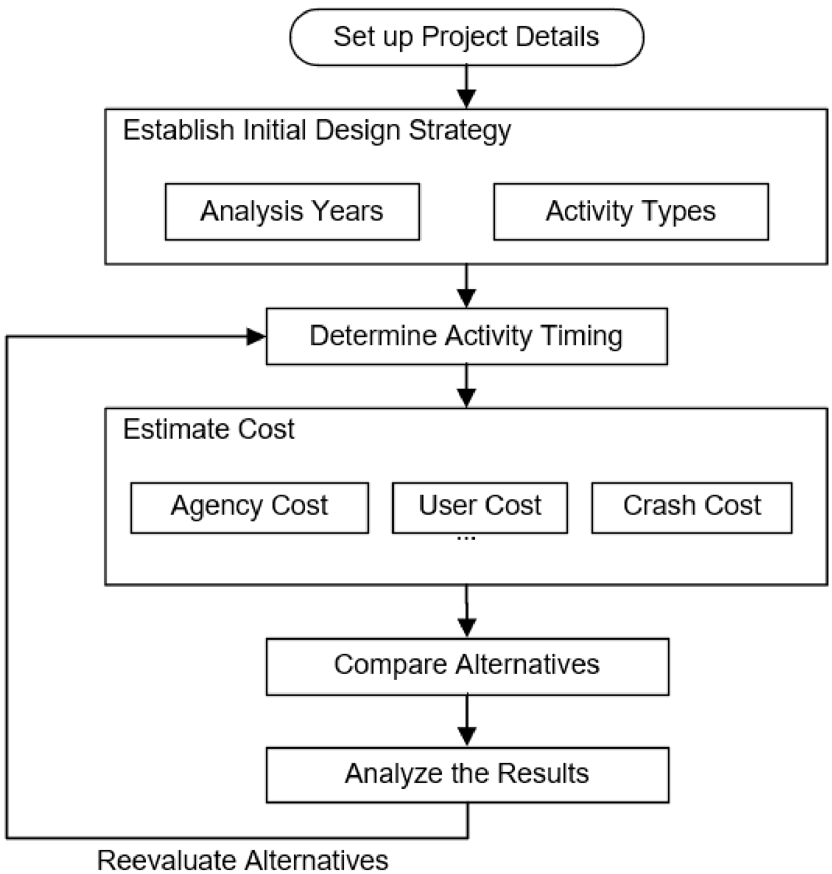

Figure 6-1 Flowchart of Life Cycle Cost Analysis

- Make initial strategy and analysis decisions (strategies and analysis period). The strategies involve rehabilitation and maintenance activities of each alternative expected over the analysis period. The analysis period should be sufficiently long to reflect long-term cost differences between alternatives. The activity timing is generally determined by the analyst's judgment based on experience and historical data.

- Estimate costs. Costs associated with the owning agency and users are calculated for each alternative. Agency costs included costs for project supervision and administration, materials, labor, and traffic control for the initial installation, as well as any rehabilitation and maintenance costs required over the life cycle of the alternative. User costs incurred by the traveling public include those in both work-zone and non-work-zone phases. Generally, the user costs incurred during non-work-zone phases are excluded in LCCA due to a lower likelihood of difference among alternatives (FHWA, 2002).
- Compare alternatives. Comparison usually involves expressing each alternative using a common metric such as the net present value (NPV) or a benefit-cost ratio (B/C).
- Analyze the results and reevaluate alternatives. Results should be scrutinized for the most influential costs, factors, and assumptions. LCCA has two possible computational approaches: *deterministic* and *probabilistic* (FHWA, 1998). The deterministic approach uses discrete input values and a single output value and has been the traditional LCCA type used in transportation decision making (FHWA, 2002). A *probabilistic* approach generally involves sensitivity analysis and risk analysis. Original design strategy alternatives should be reevaluated base on these results analysis in order to improve the cost-effectiveness of each alternative. The

deterministic LCCA is less complex than a probabilistic type and can be appropriate when uncertainty is not expected to have a material effect on the outcome of the economic analysis (FHWA, 2003).

6.1.2 Available Tools

Currently, several software programs are available on the market for the LCCA of pavements. The two most well-known tools are the RealCost software developed by the Federal Highway Administration (FHWA) and the LCCAExpress by the Asphalt Pavement Alliance (APA). Both RealCost and LCCAExpress use the LCCA principles recommended by the FHWA to compare the economics of alternative designs for a given road project. LCCAExpress is an executable program and outputs an Excel file with only one worksheet, which is less friendly for secondary development as compared to RealCost. The RealCost software is a VBA program building on a 32-bit version of Microsoft Excel, and it exhibits its inputs and results in multiple worksheets. Agency and user costs can be calculated from both tools during the life cycle period. However, neither RealCost nor LCCAExpress have considered safety costs resulting from roadway crashes in the prioritization of alternative maintenance strategies.

6.2 Calculation of Cost Components

6.2.1 RealCost Software Outputs

RealCost allows pavement designers to investigate the effects of cost, service life, and economic inputs for life-cycle pavement investment decisions, whose graphical user interface (GUI) is shown in Figure 6-2.

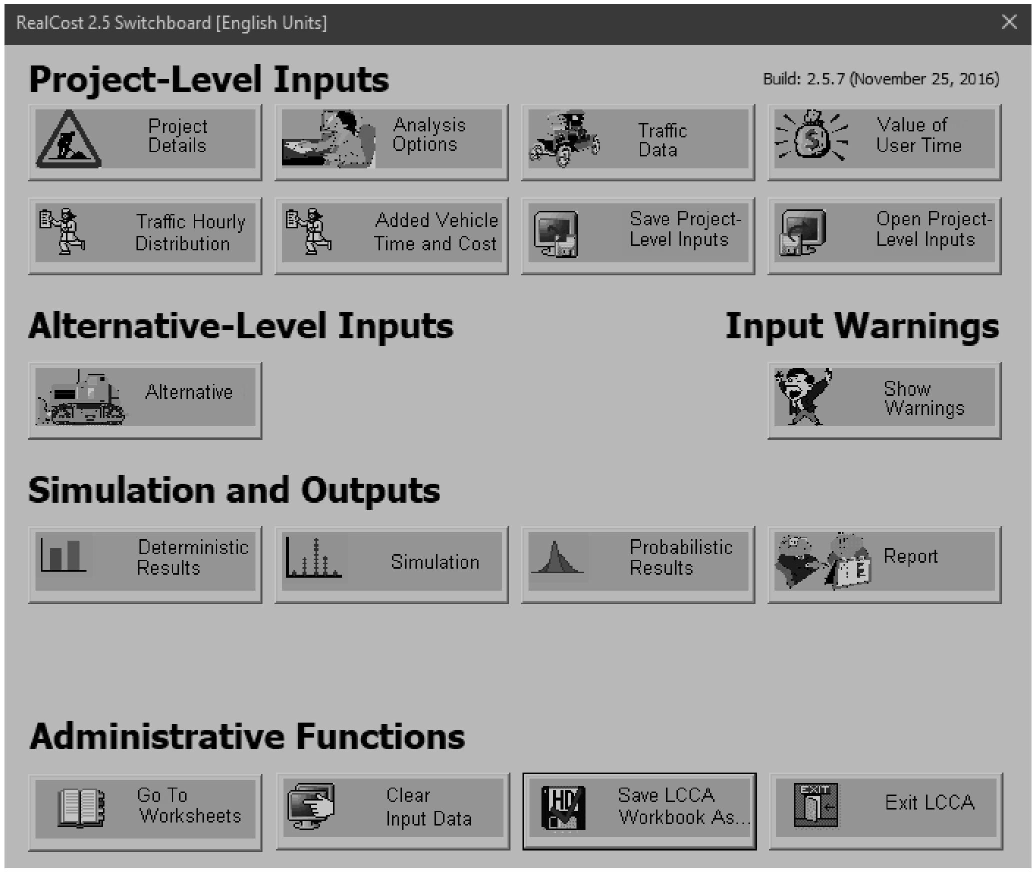

Figure 6-2 User Interface of RealCost

Figure 6-3 shows the interface to define activity information including time, type, construction cost, and work zone inputs for each alternative, and to save the input files of all alternatives being considered. After specifying project and alternative details, the software calculates life-cycle values for both agency and user costs associated with construction and rehabilitation using the FHWA’s work zone user cost calculation method. The user costs are calculated by comparing the traffic demand to roadway capacity on an hour-by-hour basis. The RealCost software can perform both deterministic and probabilistic LCCA modeling of pavements, and also supports deterministic sensitivity analyses and probabilistic risk analyses.

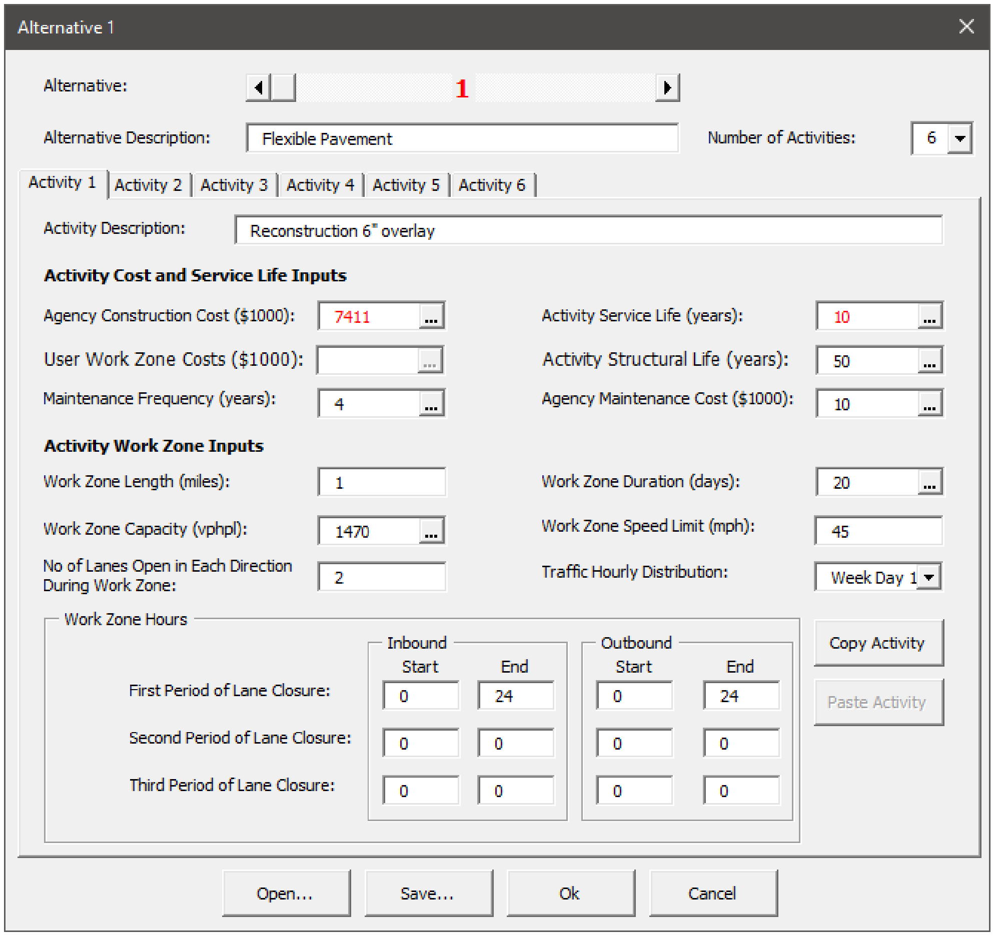

Figure 6-3 Alternative Details in RealCost

RealCost provides both tabular and graphic comparisons of agency and user costs. Example figures produced from RealCost are shown in Figure 6-4. The users can not only compare the total costs of alternatives but also estimate the expenditure of agency and users during the analysis period. Similar to any economic tool, LCCA provides critical information to the overall decision-making process, but the analyst should make the final decision after combining other considerations such as risk, available budgets, and political and environmental concerns.

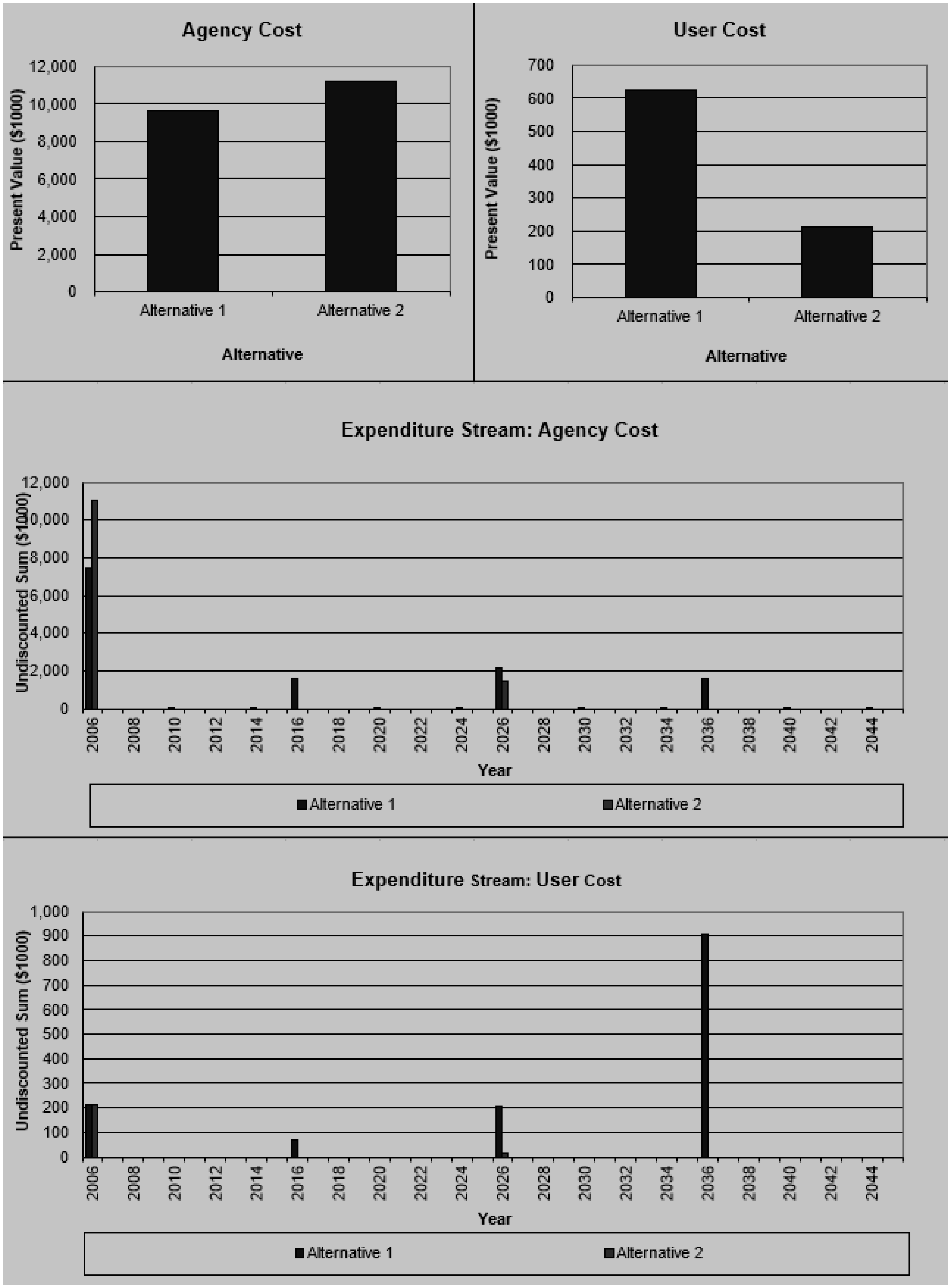

Figure 6-4 Example Output Figures in RealCost

Despite its friendly user-interface and streamlined LCCA procedure, the RealCost software has its limitation and disadvantages. For example, the software does not calculate agency costs or service lives for individual construction or rehabilitation activities. These values must be input by the analyst and should reflect the construction and rehabilitation practices of the agency. Besides, the crash-related safety costs are not considered in the software calculation. Neglecting the difference in pavement safety performance may results in incorrect calculation of the overall costs of preservation treatments, especially for those targeted to improve roadway safety such as the high friction surface treatments (HFST).

6.2.2 Safety Cost

The findings in the former chapters have pathed the way to estimate and integrate safety costs into the LCCA procedure. The friction prediction models can predict the surface skid variations during its life cycle after a preservation treatment is installed. Subsequently, the expected number of crashes for the segment under study is estimated using the enhanced SPF, in which pavement friction and several other indicators (in Chapter 4) are its influencing factors. Finally, the safety cost of each alternative can be obtained by multiplying the number of expected crashes with the unit crash cost.

The FHWA's *Crash Costs for Highway Safety Analysis guideline* documented a comprehensive review on the calculation of the unit crash costs considering various crash severities and types and their applications. Two types of injury scales are included in the guideline: the KABCO scale and the maximum abbreviated injury scale (MAIS). KABCO, as defined in the Model Minimum Uniform Crash Criteria

(MMUCC), is a standardized set of data elements and attributes for crash reporting, where K stands for Fatal Injury, A stands for Suspected Serious Injury, B for Suspected Minor Injury, C for Possible Injury and O for No Apparent Injury.

On the other hand, the Abbreviated injury scale (AIS) is an integer scale developed by the Association for the Advancement of Automotive Medicine to rate the severity of individual injuries. AIS classifies individual injuries per their relative severity on a six-point scale, as shown in Table 6-1, with 1 meaning very minor and 6 meaning currently untreatable injuries. Based on AIS, the MAIS is applied in the roadway crash classification using the score of the most severe injury suffered by an injured person in a crash.

These two types of injury scales are transformable in some states. As presented in Table 6-2, ODOT sets various MAIS severity levels that directly equal to KABCO severities and uses the MAIS person-injury unit costs for the KABCO crash unit cost.

Table 6-1 AIS Injury Codes

AIS Code	Injury	Example	Probability of Death (%)
0	None	No injury	0
1	Minor	Superficial laceration	0
2	Moderate	Fractured sternum	1-2
3	Serious	Open humerus fracture	8-10
4	Severe	Perforated trachea	5-50
5	Critical	Ruptured liver with tissue loss	5-50
6	Maximum	Total severance of aorta	100
9	Not further specified	N/A	N/A

Table 6-2 ODOT MAIS to KABCO Direct Conversion

MAIS	KABCO	Description	Comprehensive Crash Unit Cost
MAIS 6	K	Fatal Injury	$9,600,000
MAIS 4	A	Suspected Serious Injury	$2,553,600
MAIS 2	B	Suspected Minor Injury	$451,200
MAIS 1	C	Possible Injury	$28,800
MAIS 0	O	No Apparent Injury	$4,200

As the enhanced SPF developed in Chapter 4 only predicts the expected crash frequency without crash severity and types, it is important to study the probability of crashes in each level. The distribution of the crashes in the MAIS scale was surveyed in the national report *The Economic and Societal Impact of Motor Vehicle Crashes* published by the National Highway Traffic Safety Administration (NHTSA). Besides, the Oklahoma Highway Safety Office (OHSO) provides an online Interactive Crash Maps in Oklahoma. Table 6-3 summarized the crashes of different severity levels in Oklahoma from 2017 to 2019. The weighted unit crash cost is therefore estimated to be 205 thousand dollars as shown in Table 6-3.

Table 6-3 Weighted Crash Unit Cost Estimation in Oklahoma (2017~2019)

Severity Level	2017	2018	2019	Total	Percent	Comprehensive Crash Unit Cost ($1000)
K	613	603	584	1800	0.83%	$9,600.0
A	2,146	2,054	1,809	6,009	2.78%	$2,553.6
B	7,326	7,471	7,370	22,167	10.26%	$451.2
C	13,024	12,721	13,343	39,088	18.10%	$28.8
O	48,306	48,431	5,0161	146,898	68.02%	$4.2

6.2.3 Developed VBA Spreadsheet Tool

A VBA spreadsheet tool was developed in this project to combining the outputs from the RealCost software (agency and user costs) with the safety costs estimated for each preventive maintenance strategy. Figure 6-5 illustrates the flowchart for the development of the VBA tool.

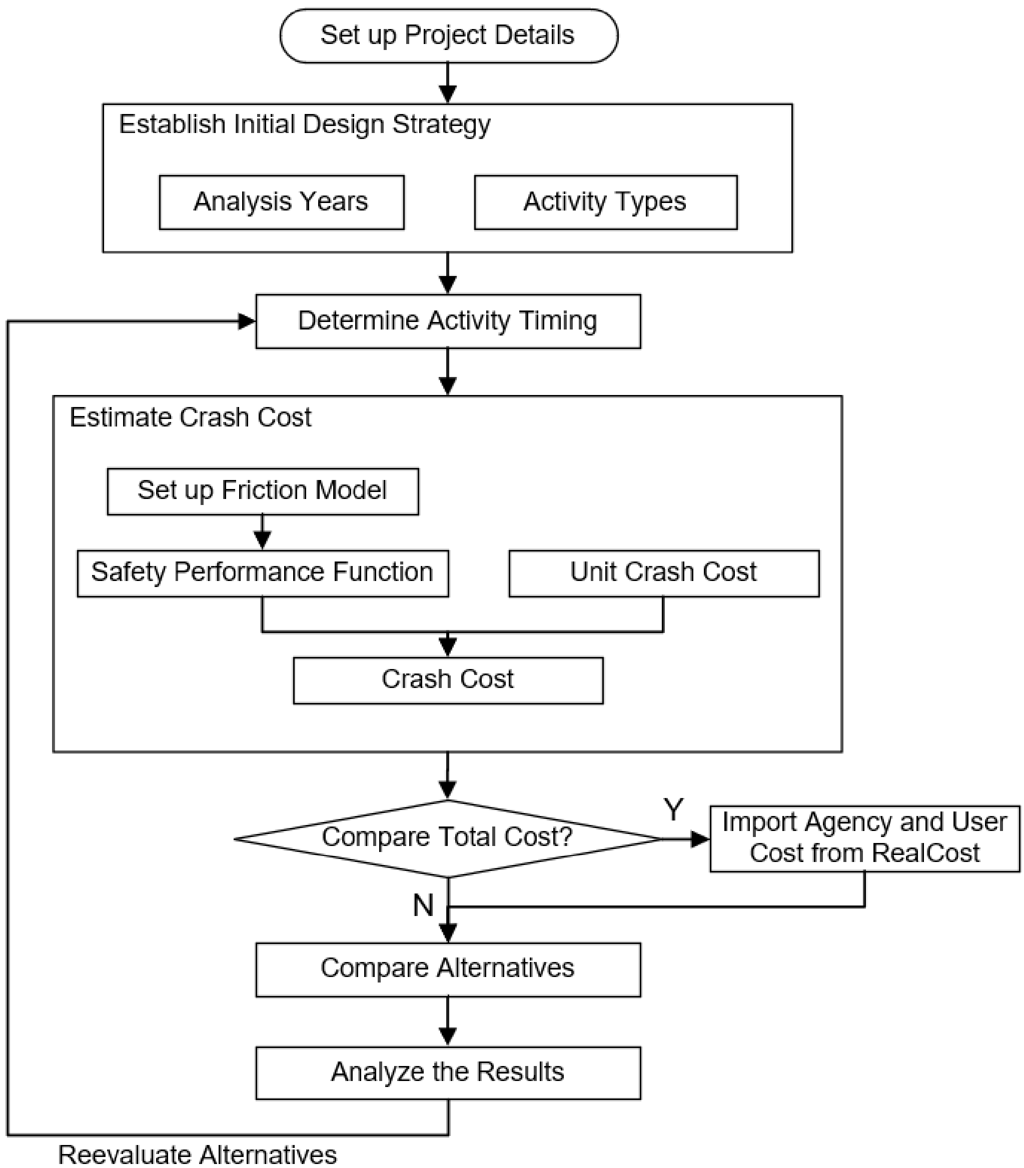

Figure 6-5 Flowchart of Developed Software

The spreadsheet tool provides a graphical interface to make the software easy to use (Figure 6-6). The developed spreadsheet allows users to input project details for various maintenance strategies, update the friction prediction models and the SPFs for crash estimation, and finally calculate and visualize the safety cost of each strategy. The tool imports the agency and user costs calculated in the RealCost software (version 2.5) and thus enable the comparisons of the total costs of each alternative. All the user inputs, calculation results, and visualization charts are stored in multiple worksheets in one Excel file. A step-by-step user's guide is provided in Appendix A.

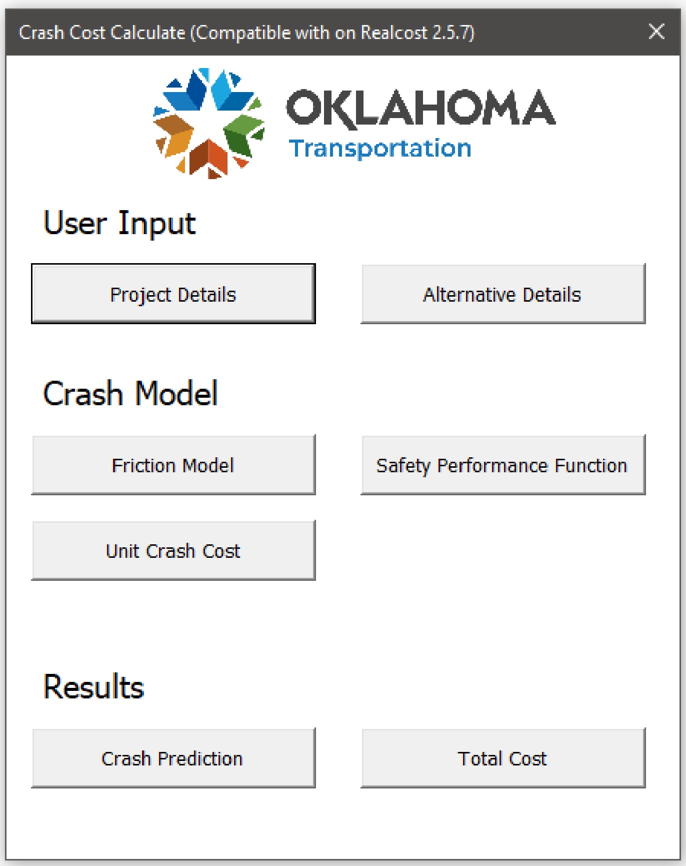

Figure 6-6 User Interface of Safety Cost Calculator

6.3 Case Study and Results

6.3.1 Preventive Treatments

A variety of preservation treatments have the capabilities to improve surface texture and enhance pavement friction performance. Table 6-4 summarized the construction cost, expected service life, and friction performance for each of the common preservation treatments in Oklahoma. The average cost and service life data were adopted from the ODOT SP&R 2275 project final report, while the initial friction numbers and the deterioration rates were obtained from the regression models as described in Chapter 5. It is observed that High Friction Surfacing Treatments (HFST) provides superior friction performance, while the average installation cost is more expensive than the other types of treatments.

Table 6-4 Unit Cost, Expected Life and Friction Performance of Treatments

Treatment Type	Average Cost per Square Yard (US dollars)	Expected Service Life (Year)	Initial SN	Deterioration Rate
Thin Overlay	3.25	8 – 12	41.4	-0.5
Chip Seal	1.77	3 – 5	NA	NA
UTBWC	4.00	8 – 10	42.5	-0.8
HFST	19.00	7 – 12	95	-5.9
Microsurfacing	2.5	7 – 10	NA	NA

6.3.2 Example Project and Alternative Details

In this case study, three typical preventive treatments: HFST, UTBWC, and thin overlay, were chosen to demonstrate the life cycle cost analysis considering their safety costs in the decision-making process. As shown in Figure 6-7, the example project has a length of 0.5 miles, two 12-ft lanes in each direction with the presence of both median and shoulders. The analysis period is 30 years beginning from 2021. The discount rate is set to 4%. There are 20,000 average annual daily traffic (AADT) with a yearly growth rate of 4%. The average longitudinal grade is 2 degrees, and the maximum degree of horizontal curvature is 8 degrees (716.7 ft of curve radius) within the roadway segment. For each activity, the preservation treatment work is conducted on one lane while leaving the other lane open and then switch to the open lane.

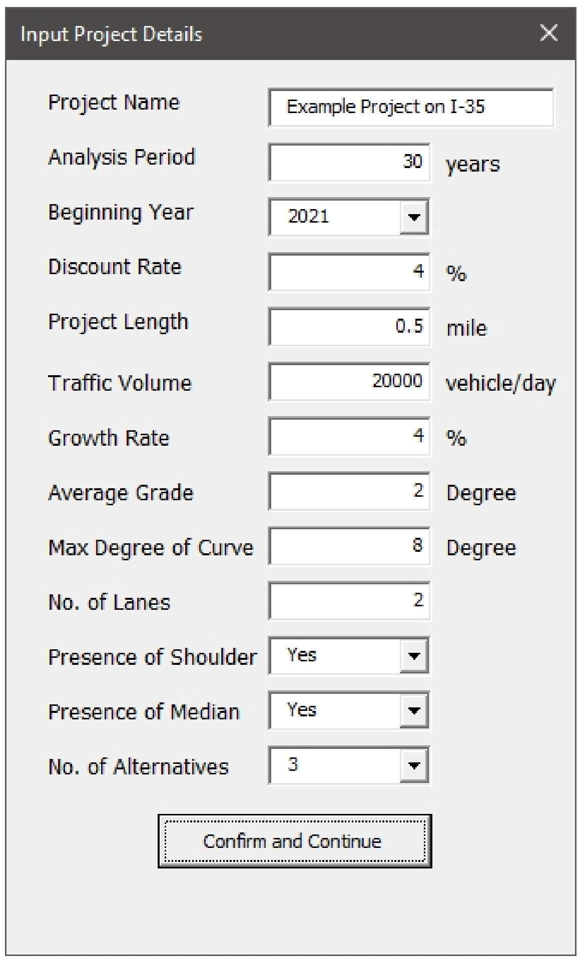

Figure 6-7 Project Details for the Example Project

The intercepts and the deterioration rates of the linear friction prediction models for the analysis were set based on results in Table 5-4 and Table 6-4. The SPF model used the default coefficients developed in Chapter 4. The unit crash cost was weighted by the probabilities of crashes at different severity levels based on the ODOT crash data from 2017 to 2019, as shown in Table 6.3. The service lives of the three alternatives were set as the average of the expected range (Table 6.4): HFST 8 years, UTBWC 9 years, and thin overlay 10 years. After specifying these parameters, the VBA spreadsheet tool automates the predictions of friction variations during the life cycle and their expected crash numbers and safety costs of each alternative.

The agency and user costs were estimated using the RealCost Software. The project details used in the safety cost calculator were inconsistent with the inputs for RealCost. Additional details in RealCost included: speed limit 75 mph, percentage of single-unit trucks 5%, percentage of combination unit trucks 10%, free flow capacity 2047 pc/ln/hr, and the rural model for the hourly traffic distribution. The values of user time were set to software default values: 11.5 $/hour for passenger cars, 18.5 $/hour for single unit trucks, and 21.5 $/hour combination unit trucks. The traffic hourly distribution and added vehicle time and cost were also set to default value as they are not the focus of this project and thus kept the same for all three alternatives.

The agency cost was calculated by multiplying the average construction cost with the surface treatment area (6,400 square yards for 2 lanes). The activity inputs for work zones were kept the same as the differences in their construction processes among the three treatments could be neglected. After setting these parameters, the

RealCost software can automate the deterministic analysis process and output the agency and user costs of each alternative. Table 6-5 summarized the alternative treatment results from the RealCost software for the example project.

Table 6-5 Alternative Details in RealCost for the Example Project

RealCost Alternative Items	HFST	UTBWC	Thin Overlay
Number of Activities	4	4	3
Agency Construction Cost ($1000)	121.6	25.6	20.8
Activity Service Life (Years)	8	9	10
Maintenance Frequency (Years)	8	9	10
Agency Maintenance Cost ($1000)	10	10	10
Activity Work Zone Inputs	/	/	/
Work Zone Length (miles)	1	1	1
Work Zone Duration (days)	20	20	20
Work Zone Capacity (vphpl)	1500	1500	1500
Work Zone Speed Limit (mph)	40	40	40

6.3.3 Results and Comparison

Figure 6-8 illustrates the agency and user costs of each alternative discounted to the present values. The undiscounted agency and user costs by analysis year, also named as expenditure stream, are presented in Figure 6-9. It is observed that the agency cost of HFST is much higher than those of UTBWC and Thin Overlay. Although the user cost of HSFT is slightly lower, the total costs (sum of agency and user costs) of HFST show that it is the most expensive treatment option if safety costs are not considered in the life cycle cost analysis.

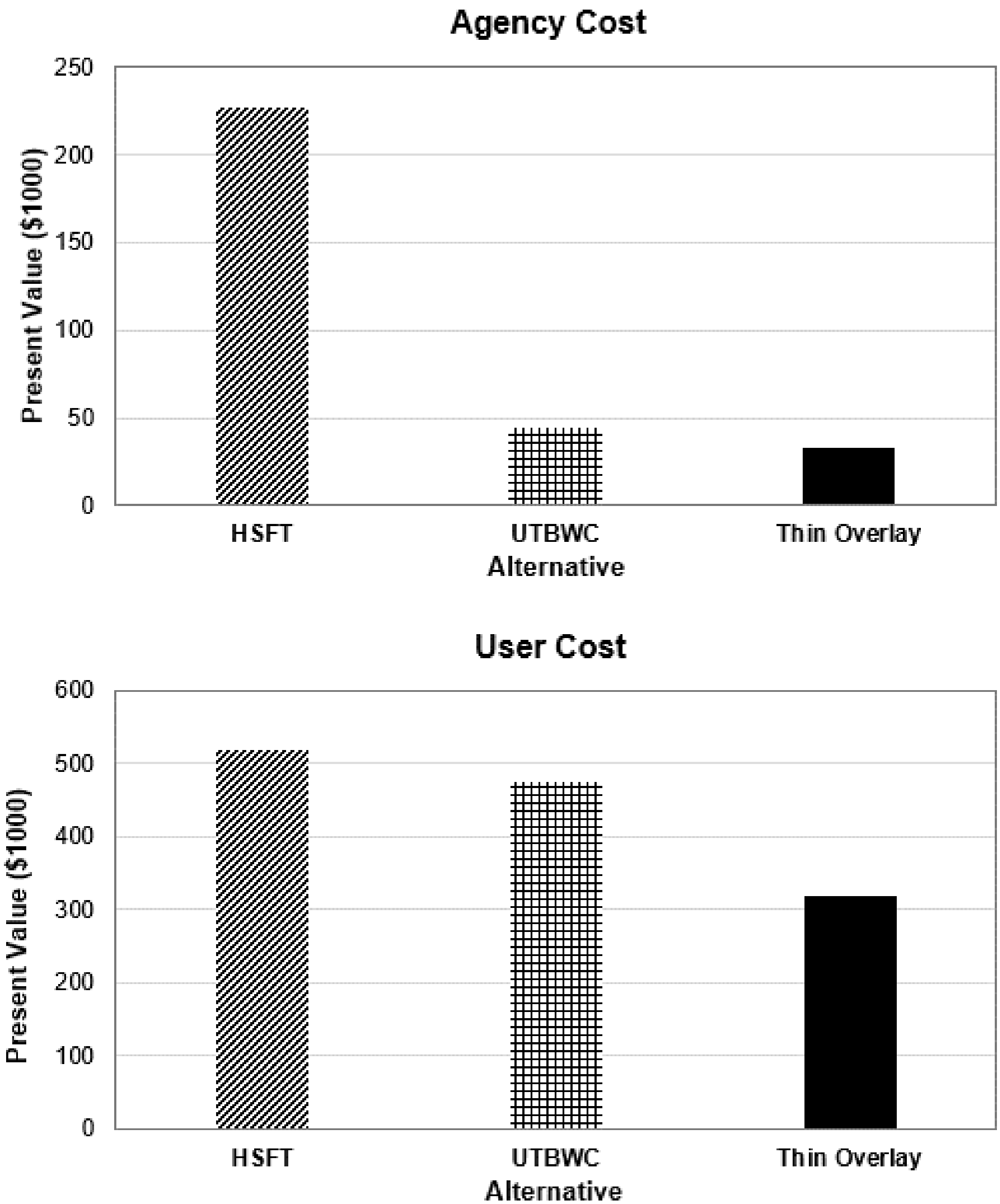

Figure 6-8 Agency and User Costs for the Case Study

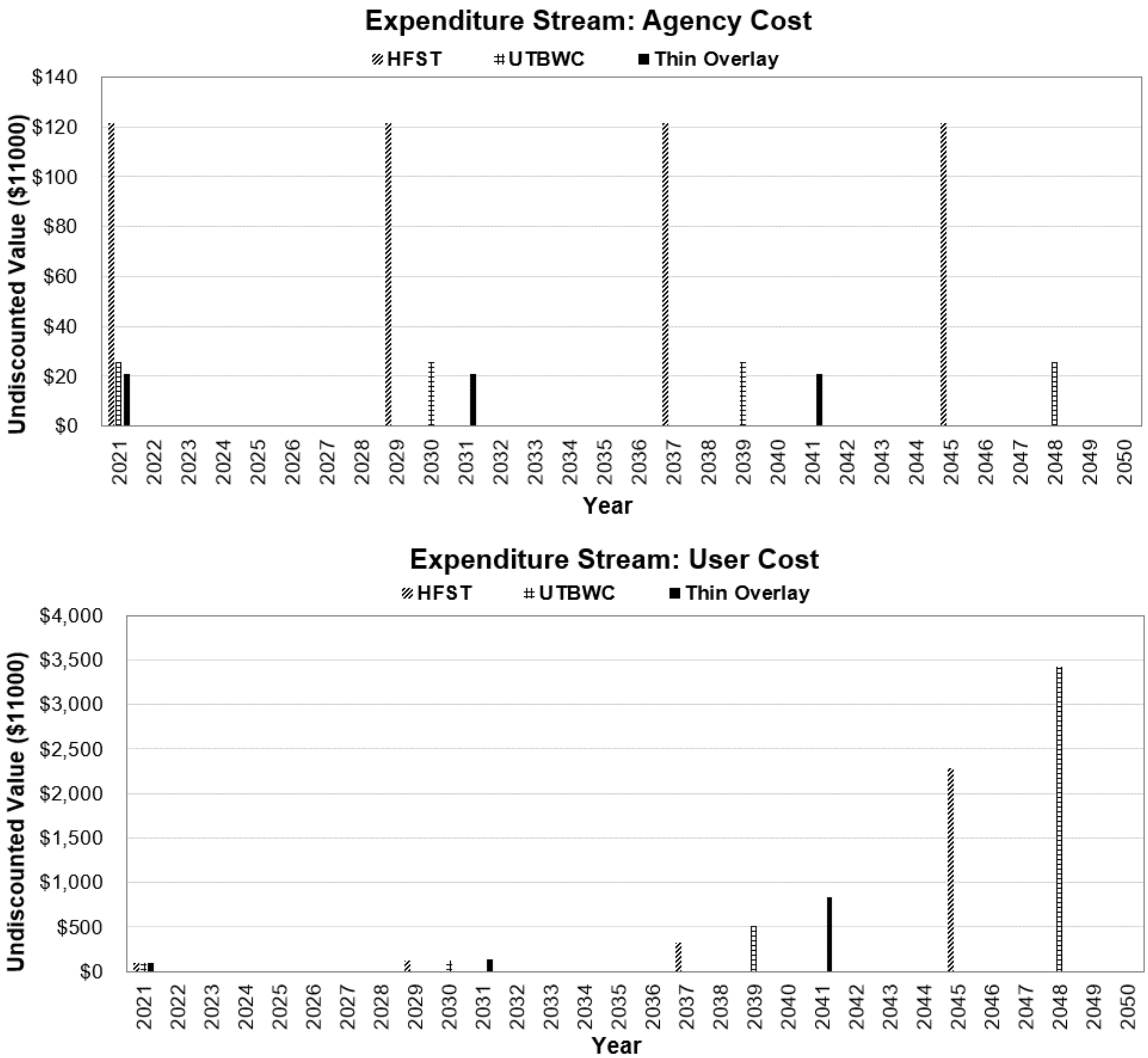

Figure 6-9 Agency and User Costs Expenditure Stream for the Case Study

The influences of the safety costs were analyzed using the developed VBA spreadsheet tool. Figure 6-10 plots the predicted friction variations of the three investigated alternatives. The friction demands established in Chapter 4, including the investigatory and intervention level, are also presented in the figure with red dash lines. As observed, all the investigated alternatives meet the friction demands over the life cycle analysis period. HFST owns the highest predicted friction numbers, while the UTBWC and thin overlay behave slightly differently in friction performance.

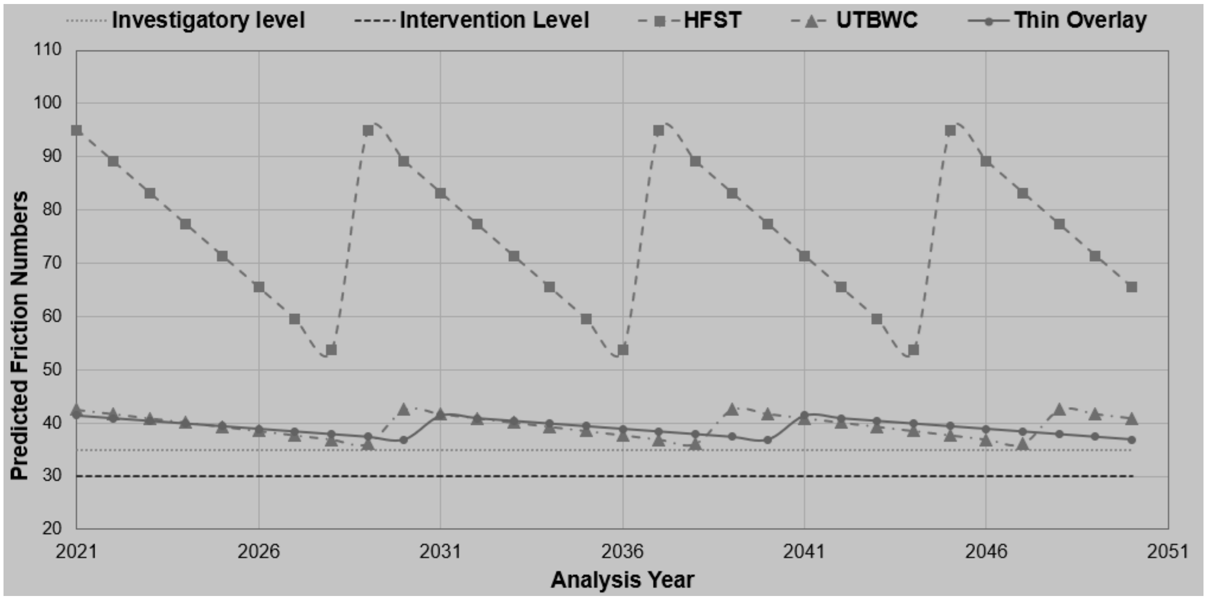

Figure 6-10 Friction Variations of HFST, UTBWC, and Thin Overlay

Subsequently, the predicted friction numbers were fed into the enhanced SPF, which was integrated into the Spreadsheet tool, to estimate the expected crash numbers during the life cycle analysis period, as shown in Figure 6-11. It is observed that higher friction numbers of HFST make the pavement safer with much less predicted crash numbers. By multiplying the number of estimated crashes with the unit crash cost, the total safety costs during the life cycle period of HFST, UTBWC, and thin overlay were calculated and summed (Figure 6-12). The crash costs over the analysis years are presented in Figure 6-13. The HFST decreases the crash costs dramatically due to its improvement in pavement Friction and the reduction in the number of crashes.

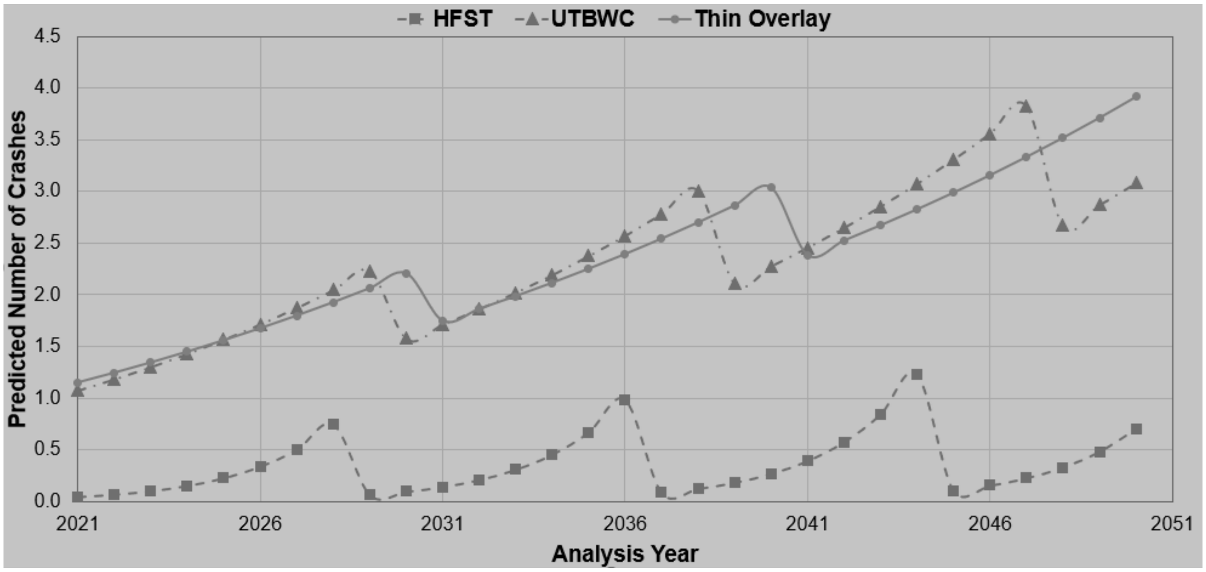

Figure 6-11 Predicted Friction Numbers for the Case Study

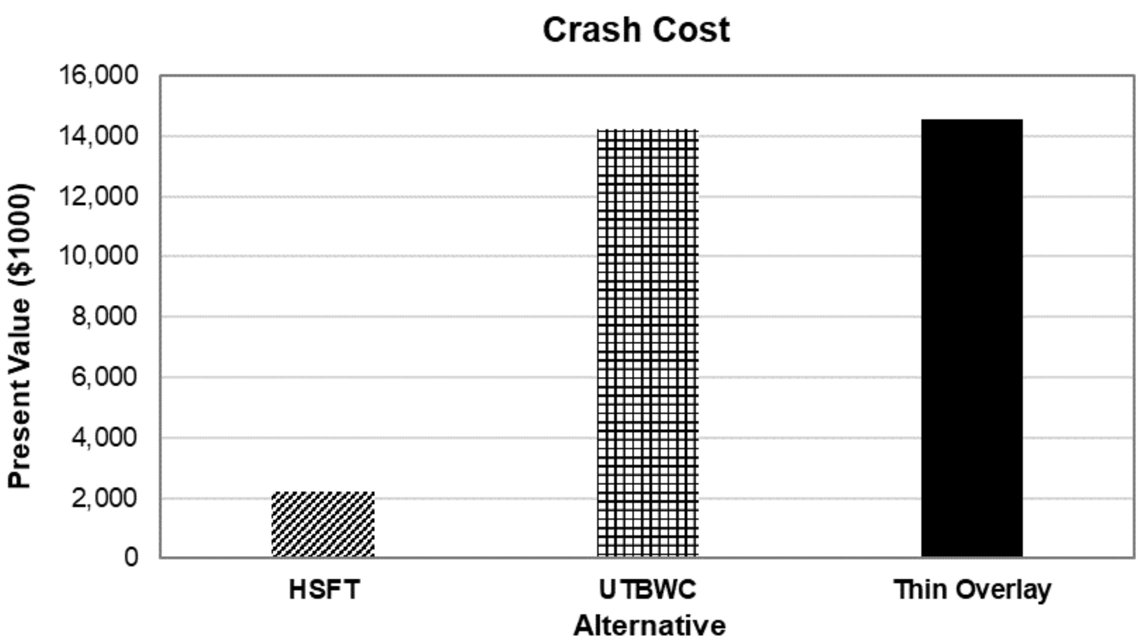

Figure 6-12 Crash Costs of HFST, UTBWC, and Thin Overlay

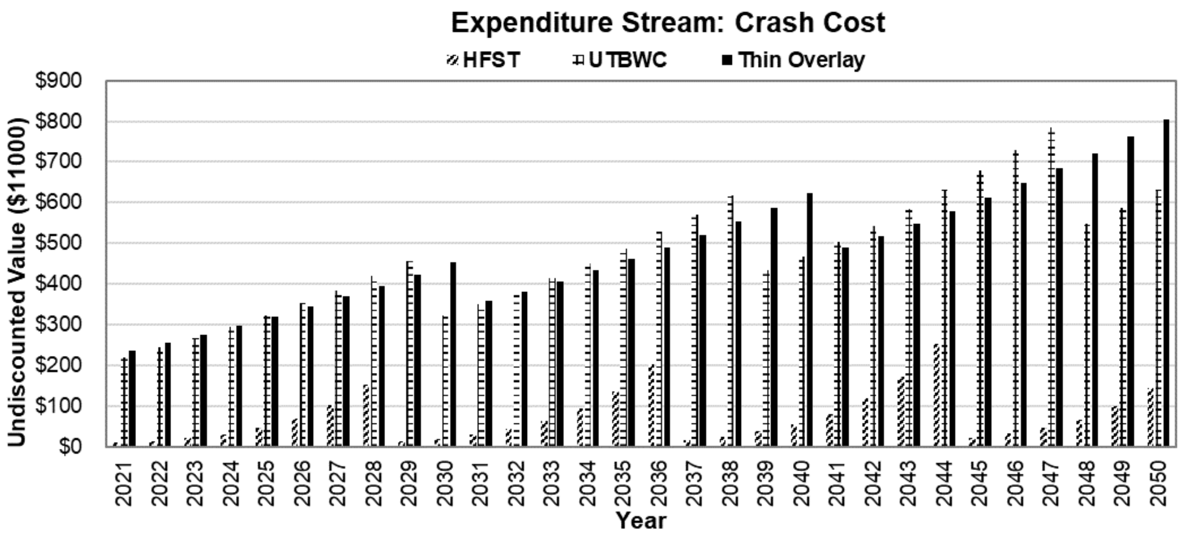

Figure 6-13 Crash Cost Expenditure Stream for the Case Study

Table 6-6 Total Costs for HFST, UTBWC, and Thin Overlay

Cost ($1000)	Agency Cost - HFST	User Cost - HFST	Agency Cost - UTBWC	User Cost - UTBWC	Agency Cost – Thin OL	User Cost – Thin OL
RealCost Results	$226.84	$519.45	$43.95	$473.53	$32.80	$317.48
Subtotal	/	$746.29	/	$517.48	/	$350.28
Crash Cost	/	$2,224.01	/	$14,210.14	/	$14,553.01
Total	/	$2,970.30	/	$14,727.14	/	$14,903.29

Adding the predicted safety costs to the agency and user costs estimated in RealCost, the total costs of the three alternatives were calculated and summarized in Table 6-6. It is observed that the total cost of HSFT is the lowest when taking crash cost into account. On the other hand, if only the agency and user costs are compared for prioritization, HFST would not be selected. However, HFST is an effective treatment for projects with high historical or potential crash frequency and high friction demands, such as those located at intersections with high volume traffic, segments with sharp curves, interchange ramps, and slippery bridge decks.

6.4 Summary

This chapter reviewed the concepts, procedures, and available software tools for life cycle cost analysis. RealCost has been widely used by state highway agencies to predict agency and user costs. However, RealCost does not include safety costs in its calculation. The developed VBA spreadsheet supplements such needs using the friction models and the enhanced SPF developed in this project to predict the expected crash numbers and the corresponding safety costs.

A case study was presented to compare the life cycle cost of three common preservation treatments: HFST, UTBWC, and thin overlay. The results show that the agency cost of HFST is the highest among the three alternatives, the user cost of HFST is also slightly higher due to the additional traffic delay in work zones with shorter service life. However, the total life cost of HFST is the lowest when safety costs are considered. Although the high agency costs could limit the application of HFST, it would be a cost-effective alternative in expected roadway crash reduction, especially for sites with high demands of surface skid resistance.

CHAPTER 7 CONCLUSIONS

Better utilizing the available pavement friction, surface texture, roadway safety data, and relevant results, along with other necessary data sets, could result in significant benefits to reduce traffic fatalities, serious injuries, and traffic delays. The Oklahoma Department of Transportation (ODOT) has been leading research in characterizing friction and texture performance of pavements for improved roadway safety.

In this project, several database systems managed by ODOT, including the Pavement Management System (PMS), Statewide Analysis for Engineering &Technology (SAFE-T) database, Skid Studies Program, and the SiteManager® construction management system, were investigated and the relevant data sets were linked and acquired for safety analysis. Those data sets include roadway geometry, traffic flow characteristics, pavement preventive maintenance treatments, materials testing and sampling results, crash type and severity, pavement surface conditions, friction and texture. In total, 1,811 subsections were identified with complete data sets that were required for the development of enhanced safety performance functions (SPFs) and the establishment of the friction demand levels.

The developed SPF was used to predict the expected number of crashes under different pavement conditions. In addition to segment length and AADT that are currently considered in the AASHTO HSM SPF model, nine pavement surface condition parameters and roadway geometry factors were identified to be statistically significant to roadway vehicle crashes. The positive regression coefficients include the segment length, AADT, number of lanes, IRI level, degree of curvature of horizontal curves, and longitudinal grade, implying that the average risk of crashes is expected to increase with the increase of those factors. On the other hand, the risk of crashes decreases with the increases of the other factors with negative coefficients, such as the average friction, the variance of friction (IQR), the presence of shoulder and/or median.

Establishing the friction demands is a key component for the Pavement Friction Management program. An in-depth analysis of friction and crash data was conducted following methodologies recommended in the AASHTO Guide for Pavement Friction. The investigatory level and the intervention level were set to 35 and be 30 for Oklahoma roadways.

Besides, the friction performance of the commonly used treatment types in Oklahoma was analyzed. The influencing factors on friction were identified based on multivariate analysis methods, and the deterioration models were developed using ODOT data sets. The deterioration models were then combined with the developed SPF model to predict the friction variations and the expected crash numbers of the pavements with various preventive treatment options, whose results were further used in the life cycle cost analysis for the selection and prioritization of restoration treatments.

Meanwhile, deep-learning techniques were applied for the development of the FrictionNet model directly using pavement surface texture profiles. The FrictionNet results demonstrated its capability in classifying pavement friction levels based on real-time texture profiles.

Finally, a VBA-based spreadsheet tool was developed to integrate the findings of this study and implement them in the life cycle cost analysis for project selection with optimized skid performance and maximized safety benefits. This tool depends on the RealCost software for the calculations of agency and user costs, while includes the life cycle safety costs by combing results from the friction models and the enhanced SPF. A case study was presented to compare the life cycle cost of three common preservation treatments: HFST, UTBWC, and thin overlay. The results showed that the agency cost of HFST was the highest among the three alternatives, but the total life cycle cost of HFST was ranked the lowest when safety costs were considered.

This project presented an integral process to include pavement skid performance of different preventive treatments and their safety benefits in the life cycle cost analysis. The outcomes of this project could bring significant benefits to reduce traffic fatalities, serious injuries, and traffic delays in Oklahoma.

It should also be acknowledged that various data limitations have limited the development of rigorous and accurate friction models. The location referencing information of the pavement sections was inconsistent among the various ODOT database systems. Pavement friction data were collected only for Oklahoma's interstate highways through the ODOT's Skid Program, but on many occasions the measurements were incomplete. As a result, the friction models for some preventive treatments were developed based on a small number of data samples. It is anticipated that more special on-demand skid data could be collected for sites with various treatment types.

REFERENCES

Abdel-Hamid O., et al. 2014. Convolutional Neural Networks for Speech Recognition. IEEE/ACM Transactions on Audio, Speech, and Language Processing, 22(10), pp. 1533-1545.

Adams, A., and Warren, M. 2017. ODOT 2017 SAFE-T User Manual. ODOT Traffic Engineering Collison Analysis & Safety Branch.

Ahammed, M. A. and Tighe, S. L. 2008. Pavement Surface Mixture, Texture and Skid Resistance: A Factorial Analysis. Airfield and Highway Pavements, DOI: 10.1061/41005(329)32.

Ahammed, M.A. and Tighe, S.L. 2012. Asphalt Pavements Surface Texture and Skid Resistance - Exploring the Reality. Canadian Journal of Civil Engineering, Vol. 39,1-9.

Akaike, H. 1973. Information Theory and An Extension of The Maximum Likelihood Principle. Second international symposium on information theory. pp. 267-281.

American Association of State Highway and Transportation Officials (AASHTO). 2009. Guide for Pavement Friction. AASHTO. Washington D.C.

Arhin, S. A., Noel, E. C., and Ribbiso, A. 2015. Acceptable International Roughness Index Thresholds based on Present Serviceability Rating. Journal of Civil Engineering Research, Vol. 5(4), 90-96. DOI: 10.5923/j.jce.20150504.03

Asi, I.M., 2007. Evaluating skid resistance of different asphalt concrete mixes. Building and Environment, 42(1), pp.325-329.

ASTM Standard E2340/E2340M-11R15, 2015. Standard Test Method for Measuring the Skid Resistance of Pavements and Other Trafficked Surfaces Using a Continuous Reading, Fixed-Slip Technique. ASTM International, West Conshohocken, PA, DOI: 10.1520/ E2340_E2340M-11R15.

Burnham, K. P., and Anderson, D. R. 2002. Model Selection and Multimodel Inference: A Practical Information-Theoretic Approach, Second Edition. New York: Springer.

Chen C., A. Liaw, and L. Breiman. 2004. Using Random Forest to Learn Imbalanced Data. University of California, Berkeley, vol. 110.

Cireşan D., U. Meier, and J. Schmidhuber. 2012. Multi-column Deep Neural Networks for Image Classification. 2012 IEEE Conference on Computer Vision and Pattern Recognition, Providence, RI, pp. 3642-3649.

Dan, H.C., He, L.H. and Xu, B., 2017. Experimental Investigation on Skid Resistance of Asphalt Pavement Under Various Slippery Conditions. International Journal of Pavement Engineering, 18(6), pp.485-499.

De León Izeppi, E., Katicha, S. W., Flintsch, G. W., Mccarthy, R., and Mcghee, K. K. 2016. Continuous Friction Measurement Equipment as a Tool for Improving Crash Rate Prediction: A Pilot Study. VTRC 16-R8, 2016. <http://www.virginiadot.org/vtrc/main/online_reports/pdf/16-r8.pdf> (May 17 2019)

De León Izeppi, E., Katicha, S. W., Flintsch, G. W., McCarthy, R., and McGhee, K. 2016. Continuous Friction Measurement Equipment as A Tool for Improving Crash Rate Prediction: A Pilot Study. Virginia Transportation Research Council, Charlottesville, VA.

Department of Transportation. 1984. Highway Link Design Advice Note TA43/84. HMSO, London.

Dieleman S. and B. Schrauwen, 2014. End-to-End Learning for Music Audio. 2014 IEEE International Conference on Acoustics, Speech and Signal Processing (ICASSP), pp. 6964-6968.

Ergun, M., lyinam, S. and lyinam, A.F. 2005. Prediction of Road Surface Friction Coefficient Using Only Macro and Microtexture Measurements. Journal of Transportation Engineering, Vol. 131,311-319$.

Federal Highway Administration (FHWA). 1998. Life Cycle Cost Analysis in Pavement Design: Interim Technical Bulletin. Washington D.C. U.S.

Federal Highway Administration (FHWA). 2002. Life Cycle Cost Analysis Primer.

Federal Highway Administration (FHWA). 2002. Pavement Life Cycle Assessment Framework. Washington, D.C. United States.

Flintsch, G.W., McGhee, K.K., Izeppi, E. L., and Najafi, S. 2012. The Little Book of Tire Pavement Friction.

Fwa, T. F., Chu, L., and Tan, K. H. 2016. Rational Procedure for Determination of Rut Depth Intervention Level in Network-Level Pavement Management. Transportation Research Record: Journal of the Transportation Research Board, 2589(1), 59-67. DOI:10.3141/2589-07

Glorot X. and Y. Bengio. 2010. Understanding the Difficulty of Training Deep Feedforward Neural Networks. Proceedings of the Thirteenth International Conference on Artificial Intelligence and Statistics, in PMLR 9, pp. 249-256.

Harmon, T., Bahar, G.B. and Gross, F.B., 2018. Crash Costs for Highway Safety Analysis. Federal Highway Administration, U.S. DOT. Washington, D.C.

Hauer, E. 1996. "Statistical Test of Difference between Expected Accident Frequencies." Transportation Research Record. Journal of the Transportation Research Board, 1542(1), 24-29.

He H. and E.A. Garcia. 2009. Learning from Imbalanced Data. IEEE Transactions on Knowledge and Data Engineering, 21(9), pp.1263–1284.

Highway Safety Manual. 2010. American Association of State Highway and Transportation Officials. Washington, D.C.

Hinton et al. 2012. Lecture 6a Overview of Mini-batch Gradient Descent. http://www.cs.toronto.edu/~tijmen/csc321/slides/lecture_slides_lec6.pdf. Accessed 5 February. 2018.

Huang J.T., J. Li, and Y. Gong. 2015. An Analysis of Convolutional Neural Networks for Speech Recognition. 2015 IEEE International Conference on Acoustics, Speech and Signal Processing (ICASSP), pp. 4989-4993.

Jahromi, S.G., Mortazavi, S.M.R., Voussough, S. and Yingjian, L., 2011. Evaluation of pavement temperature on skid frictional of asphalt concrete surface. International Journal of Pavement Engineering, 12(1), pp.47-58.

Kanafi, M.M. and Tuononene, A.J. 2017. Top Topography Surface Roughness Power Spectrum for Pavement Friction Evaluation. Tribology International, 107,240-249.

Kanafi, M.M. et al. 2015. Macro- and Micro-Texture Evolution of Road Pavements and Correlation with Friction. International Journal of Pavement Engineering, 16: 2,168-179, DOI:10.1080 / 10298436.2014 .937715.

Kane, M., Rado, Z., Timmons, A. 2015. Exploring the Texture-Friction Relationship: from Texture Empirical Decomposition to Pavement Friction. International Journal of Pavement Engineering, Vol. 16, No. 10, pp. 919-918, DOI: 10.1080/10298436.2014.972956.

Kotek, P. and Florková, Z., 2014. Comparison of The Skid Resistance at Different Asphalt Pavement Surfaces Over Time. Procedia Engineering, 91,459-463.

Krizhevsky A., I. Sutskever, and G. E. Hinton. 2012. Imagenet Classification with Deep Convolutional Neural Networks. Advances in Neural Information Processing Systems 25, pp.1106–1114.

Labbate, Alessandro. 2001. A Classification of Asphalt Surfacing Textures Based On 3D Imagery. Ph.D. Dissertation.

Lord, D., and Mannering, F. 2010. The Statistical Analysis of Crash-Frequency Data: A Review and Assessment of Methodological Alternatives. Transportation Research Part A: Policy and Practice, 44(5), 291-305.

Lord, D., Park, B.J. and Levine, N. 2013. Chapter 16: Poisson Regression Modeling. CrimeStat IV: A Spatial Statistics Program for the Analysis of Crime Incident Locations, Version 4.0. Ned Levine and Associates, Houston, TX, and Washington, D. C.

Lu, J., A. Gan, K. Haleem, P. Alluri, and K. Liu. 2012. Comparing Locally-Calibrated and Safety-Analyst Default Safety Performance Functions for Florida's Urban Freeways. Presented at the 91st Annual Meeting of the Transportation Research Board, Washington, D.C.

Luo, Y., 2003. The Effect of Pavement Temperature on Frictional Properties of Pavement Surfaces at the Virginia Smart Road (Doctoral dissertation, Virginia Tech).

Merritt, D.K., Lyon, C.A., and Persaud, B. N. 2015. Evaluation of Pavement Safety Performance. FHWA-HRT-14-065.

MMES Engineering. 2017. AMES 8300 Portable High-Speed Profiler. Accessed 29 January. 2018, from http://floridaridesonus.org/wp-content/uploads/2017/08/Ames-Eng-Brochure.pdf.

Najafi, S. et al. 2015. Linking Roadway Crashes and Tire-Pavement Friction: A Case Study. International Journal of Pavement Engineering. DOI: 10.1080/10298436.2015.1039005.

Nielsen M., 2017. Neural Networks and Deep Learning. Online Book. Accessed 19 August. 2017, from http://neuralnetworksanddeeplearning.com/index.html.

ODOT. 2010. Road Inventory Manual, 7th Ed. Oklahoma Department of Transportation.

ODOT. 2018. ODOT State Planning and Research Work Program FFY2019. Oklahoma Department of Transportation. p. 18, p. 25.

Pulugurtha, S. S. 2012. Assessment of the Effect of Pavement Macrotexture on Interstate Crashes. Journal of Transportation Engineering, DOI: 10.1061/(ASCE)TE.1943-5436.0000357.

Pulugurtha, S. S., Kusam, P. R. and Patel, K. 2008. Relationship between Pavement Macrotexture and Crash Incidences on North Carolina Roads. Final Report 2007-12. North Carolina Department of Transportation, Raleigh, NC.

Rado, Z. and Kane, M. 2014. An Initial Attempt to Develop an Empirical Relation between Texture and Pavement Friction Using the HHT Approach. Wear, Vol. 309,233-236.

Raschka S. 2015. Python Machine Learning. Birmingham, UK: Packt Publishing.

Rezaei, A. and Masad, E. 2013. Experimental-based Model for Predicting the Skid Resistance of Asphalt Pavements. International Journal of Pavement Engineering, Vol. 14, No. 1, 24-35.

Roe, P.G., Parry, A.R. and Viner, H.E., 1998. High and Low Speed Skidding Resistance: The Influence of Texture Depth.

Srinivasan, R., Carter, D., and Bauer, K. 2013. Safety Performance Function Decision Guide: SPF Calibration vs SPF Development. Report No. FHWA-SA-14-004.

Srivastava N., G. Hinton, A. Krizhevsky, I. Sutskever, and R. Salakhutdinov. 2014. Dropout: A Simple Way to Prevent Neural Networks from Overfitting. Journal of Machine Learning Research, 15, pp. 1929–1958.

Ueckermann et al. 2015. A Contribution to Non-contact Skid Resistance Measurement. International Journal of Pavement Engineering, Vol. 16, No. 7,646-659.

Wang, H., and Wang, Z. 2013. Evaluation of Pavement Surface Friction Subject to Various Pavement Preservation Treatments. Construction and Building Materials, 48, 194-202

Wilson, D.J., 2006. An Analysis of The Seasonal and Short-Term Variation of Road Pavement Skid Resistance, Doctoral dissertation.

Yang, G., Li, Q.J., Zhan, Y.J., Wang, K.C. and Wang, C., 2018. Wavelet Based Macrotexture Analysis for Pavement Friction Prediction. KSCE Journal of Civil Engineering, 22(1), pp.117-124.

Zhang A. et al. 2017. Automated Pixel-Level Pavement Crack Detection on 3D Asphalt Surfaces Using a Deep-Learning Network. Computer-Aided Civil and Infrastructure Engineering, 32, pp. 805–819.

APPENDIX: USER MANUAL OF THE SAFETY COST CALCULATOR

A.1 Installation and Preparation

The **Safety Cost Calculator** is developed and recommended to be run on the 32-bit version of the Microsoft Excel platform with macro content enabled. It is designed to run in Microsoft Excel 2000 or later versions. Besides, up-to-date service packs for Windows and Office 2000 (or Excel 2000) are essential to run the software.

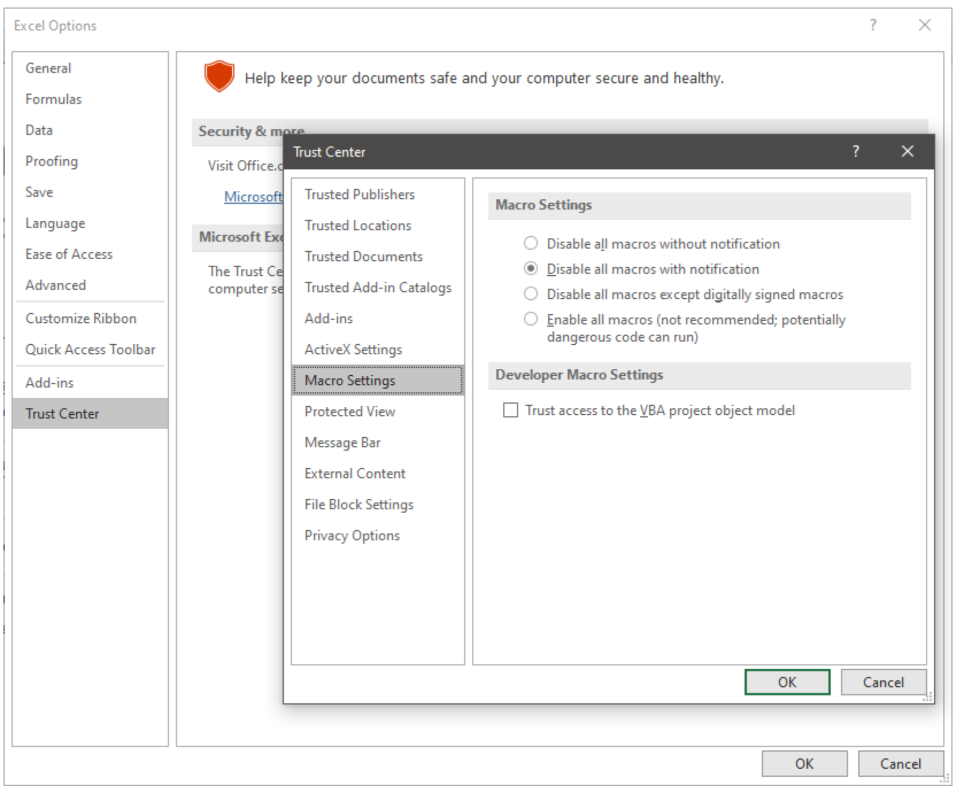

Figure A-1 Excel Macro Security Setting

Excel must be set to allow macros to run on the tool. As shown in Figure A-1, before starting the software, open Excel 2000, check the macro security settings, and ensure that macros are allowed. The security settings are accessed from the Excel 2000 menu bar.

After the Excel macro setting, an opening page would appear when the users open the tool, as shown in Figure A-2. Users need to "**Enable Content**" to display the **Main Menu** interface, which has seven buttons (Figure A-3). would appear when the users open the tool, as shown in Figure A-2. Users need to "**Enable Content**" to display the **Main Menu** interface, which has seven buttons (Figure A-3).

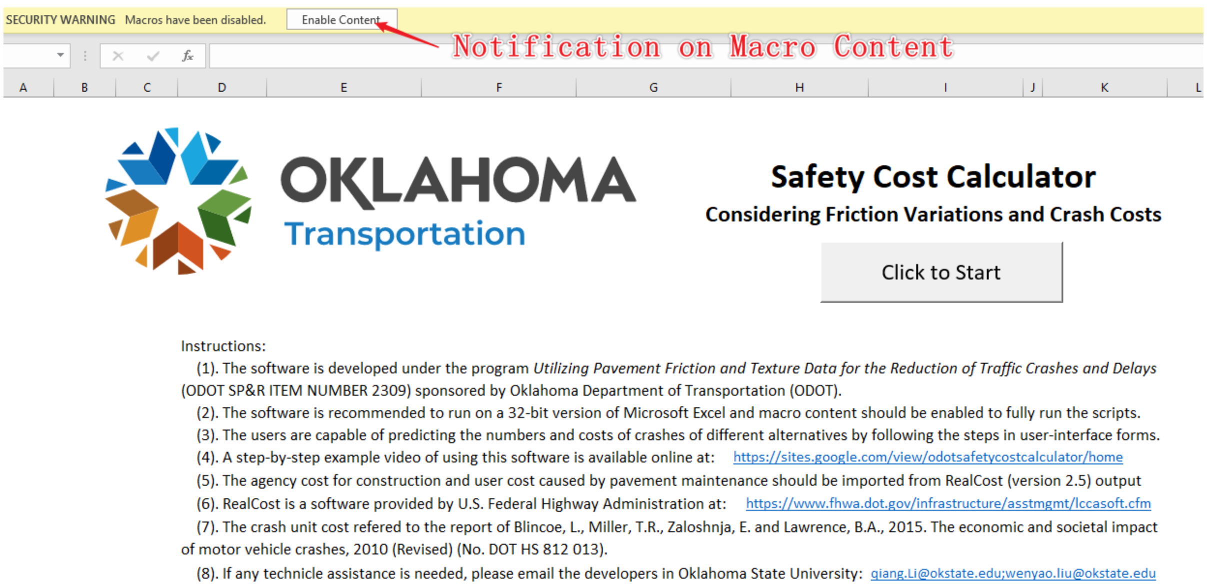

Figure A-2 Opening Page

If users only need to compare the crash costs of different maintenance strategies, it is sufficient to follow the first six modules (except the Total Cost module) shown in the main menu. If the user would like to compare all costs: agency, user, and crash costs, the RealCost (version 2.5) software should be downloaded the FHWA Life-Cycle Cost Analysis Software website and installed as well. The system requirement and configuration of RealCost are the same as those for the **Safety Cost Calculator**.

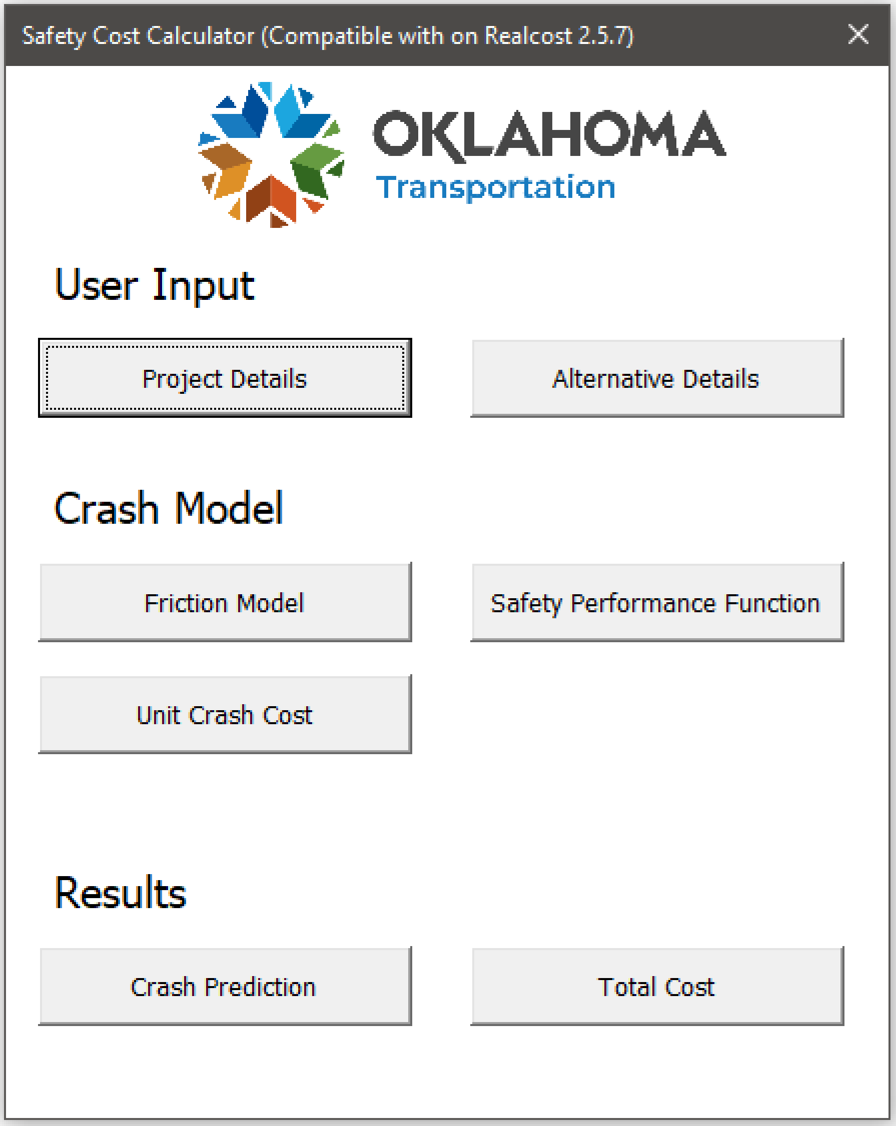

Figure A-3 Main Menu

A.2 User Input

In the user input section, users can input the project details, including project name, analysis period, beginning year, discount rate, project length, etc. Some of these items, such as the “**Presence of Shoulders or Median**” and “**Number of Alternatives**” can be chosen from the drop-down menu (Figure A-4). Except for the “**Project Name**”, the only number is allowed for other input items. Some items such as the “**Analysis Period**” and “**No. of Lanes**” only accept integers, while other items, such as “**Discount Rate**” and “**Average Longitudinal Grade**” allow decimals. After clicking the “**Confirm and Continue**” button, the program will automatically switch to the **Alternative Details** interface (Figure A-5). The number of columns will be dynamically assigned based on the number of alternatives used in the **Project Details** interface.

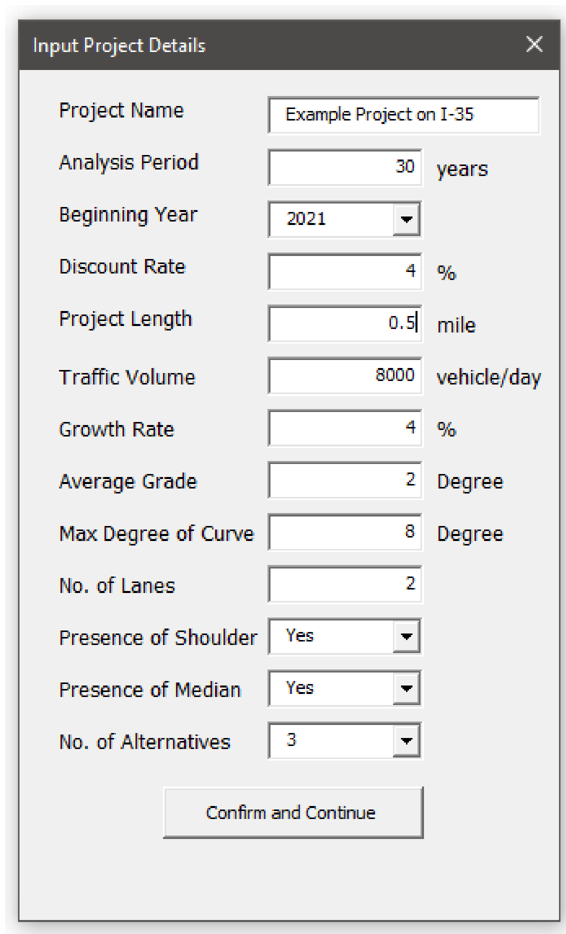

Figure A-4 Input Project Details

In the **Alternative Details** interface, the program will populate the treatment type and service life of the available preservation treatments. The user can choose the activity type and the corresponding service year in the drop-down menu for each alternative. Once one activity is specified, the following activities will be automatically updated using the present alternative settings for the entire life cycle period. Users can also modify the input values for each activity.

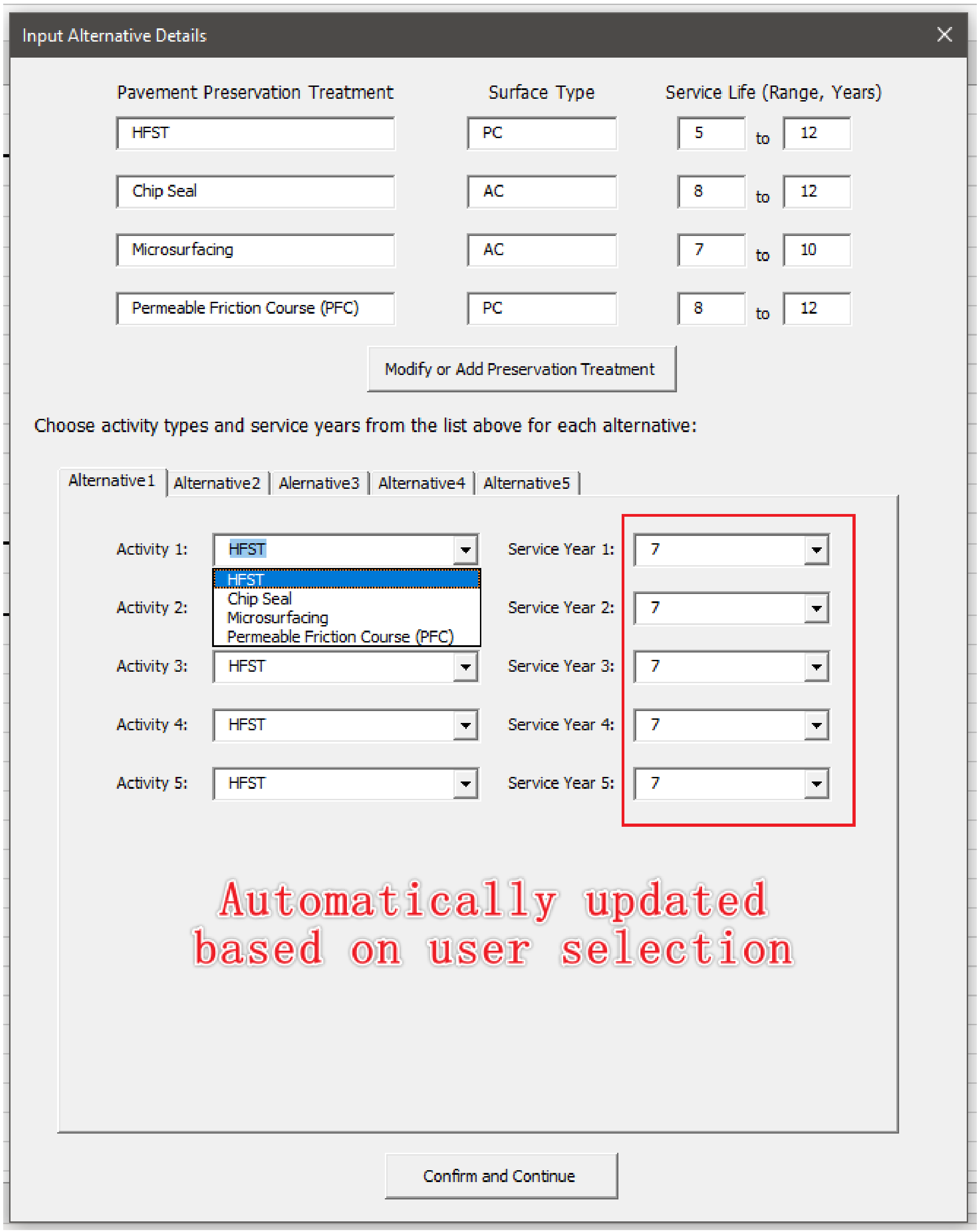

Figure A-5 Input Alternative Details

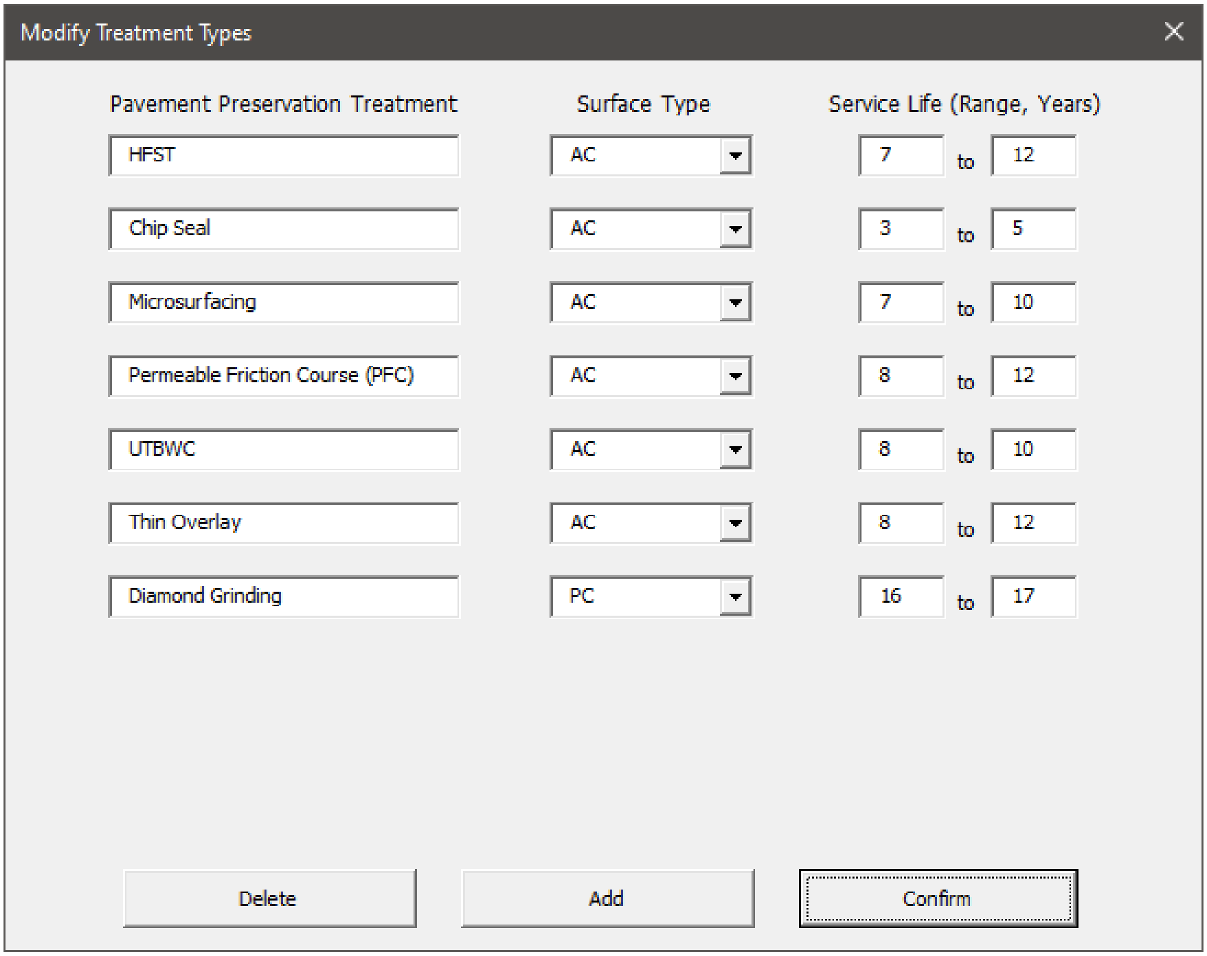

Figure A-6 Modify Treatment Types

The Software is capable of storing and listing data for up to ten types of preservation treatments. If a specific treatment type is not included, users can modify or add treatment types by clicking the "**Modify or Add Treatment**" button (Figure A-6). Users can also delete unnecessary treatment types (Figure A-7).

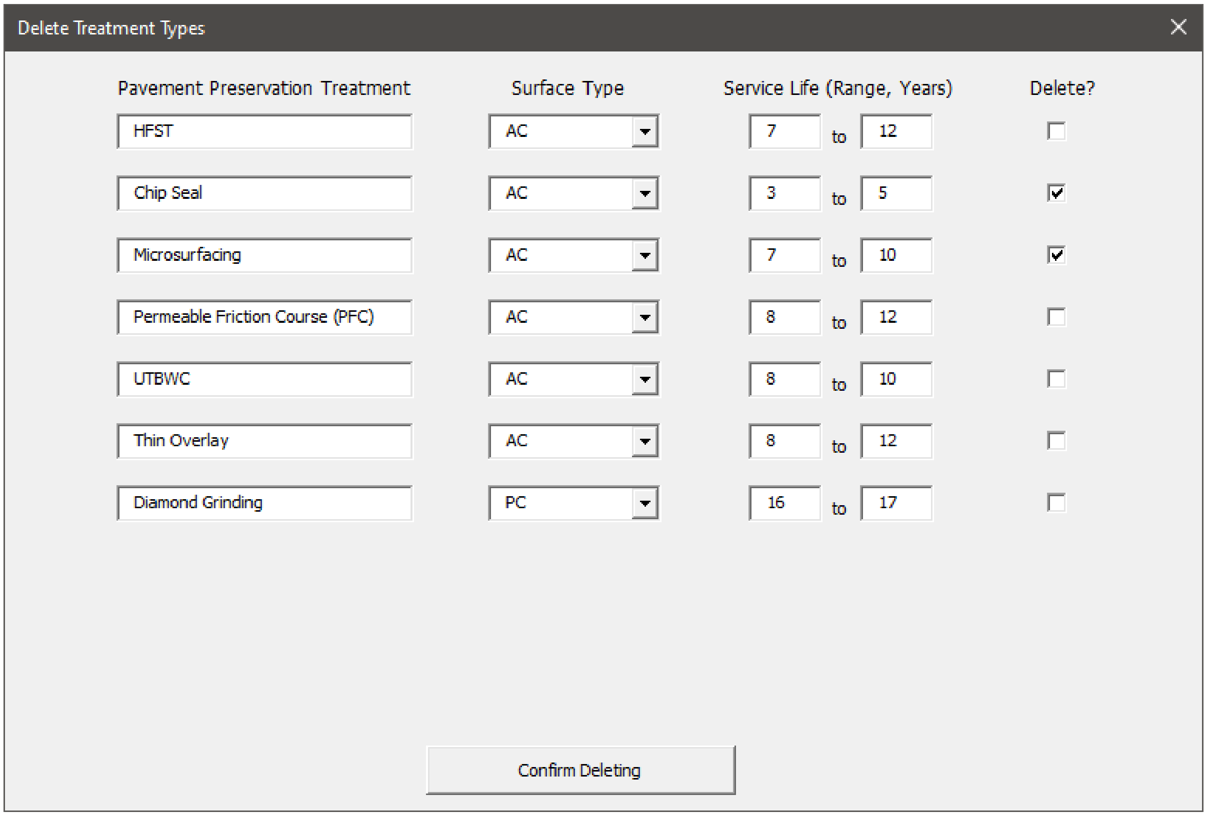

Figure A-7 Delete Treatment Types

Once the user has modified and confirmed the list of treatment types, the software will empty the alternative details and require user selection. When all alternatives have been updated, the user can click the "**Confirm and Continue**" (Figure A-5) and moves to the **Crash Model** section.

A.3 Crash Model

The **Crash Model** section specifies the parameters for the "**Friction Model**", "**Safety Performance Function**", and the "**Unit Crash Cos**t". The "**Friction Model**" enables the software to predict pavement friction numbers after each activity. The predicted friction numbers and inputted project details will be fed into the "**Safety**

Performance Function” to predict the numbers of crashes for each alternative. The intercept and deterioration rate for each treatment type can be automatically loaded with the parameters saved in the tool or modified with user inputs (Figure A-8). The “**Safety Performance Function**” interface displays the model coefficients developed in Chapter 4 and allows users to update them when a new model is more appropriate (Figure A-9). All the friction model and SPF prediction results are stored along with the project details in the **User Input** worksheet.

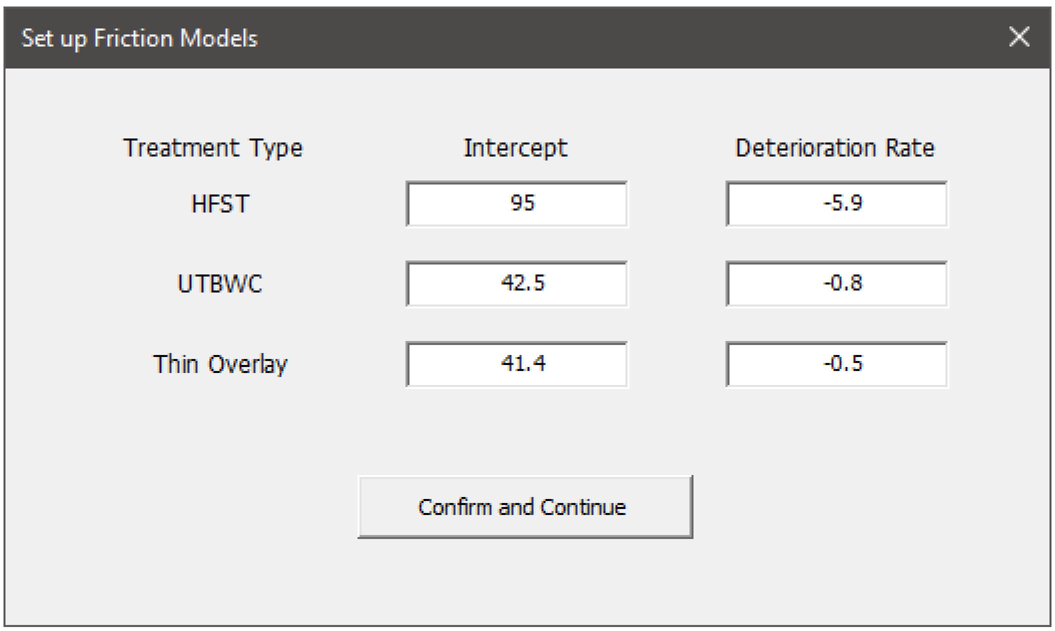

Figure A-8 Friction Models

After confirming the SPF coefficients, the software will shift to the Crash Unit Cost worksheet and its interface (Figure A-10). The unit crash cost data are adopted from the *Economic and Societal Impact of Motor Vehicle Crashes, 2010 (Revised*) (No. DOT HS 812 013) report (Blincoe, Lawrence, et al., 2015). The crashes are divided into different severity levels and the unit cost and probability of crashes at each level are estimated.

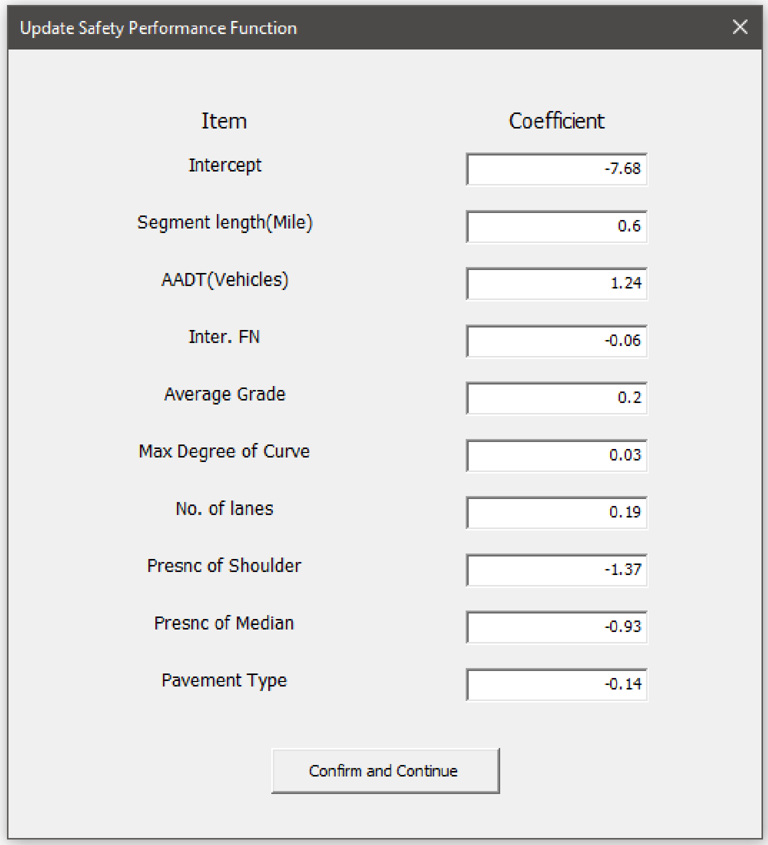

Figure A-9 Safety Performance Function

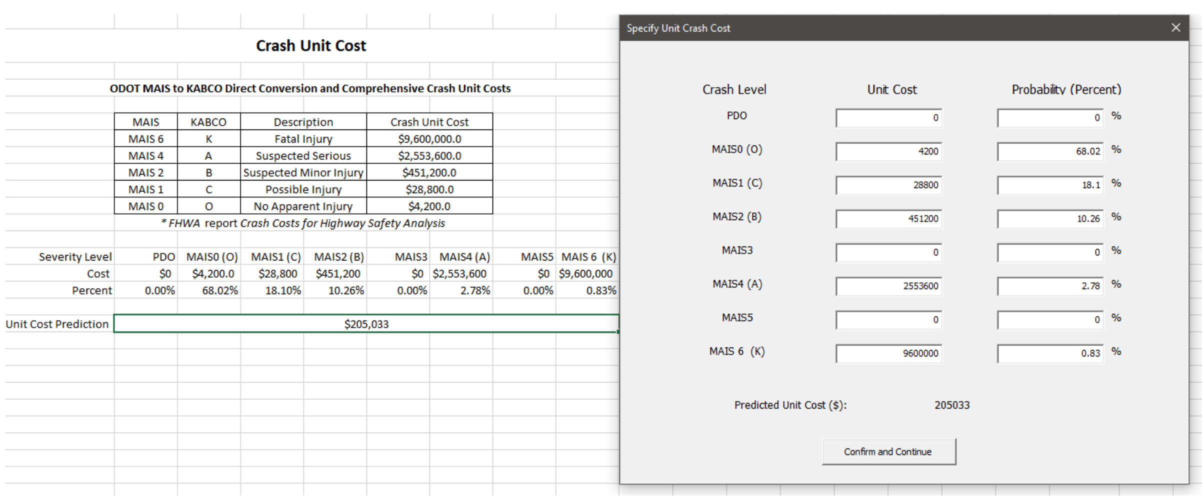

Figure A-10 Unit Crash Cost

A.4 Results

The **Results** section includes two buttons: "**Crash Prediction**" and "**Total Cost**". The **Crash Prediction** button initiates the software to calculate the predicted friction numbers, estimate expected crash frequency, and compute the crash cost of each alternative (Figure A-11). Users can click either of the three buttons to switch to the corresponding Excel worksheet. In each worksheet, the detailed data (friction number, crash number, or crash cost in $1000) are listed by year during the life cycle period, and the plots are also presented. Specifically, the investigatory and intervention levels established in Chapter 4 are also added to the friction plot (Figure A-12). These two friction demand levels are password protected and only the administrator can modify them. In case the friction variations of one alternative reach lower than the friction levels, users should reconsider the alternative and modify its inputs in the **Alternative Details** interface.

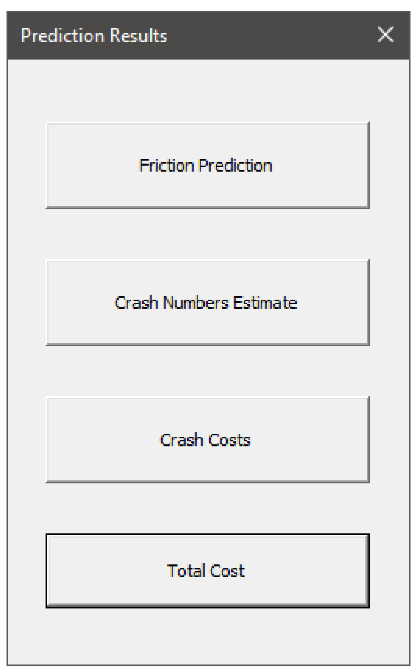

Figure A-11 Viewing Results

Friction Number Prediction

Year	HFST	UTBWC	Thin Overlay
2021	95.0	42.5	41.4
2022	89.1	41.7	40.9
2023	83.2	40.9	40.4
2024	77.3	40.1	39.9
2025	71.4	39.3	39.4
2026	65.5	38.5	38.9
2027	59.6	37.7	38.4
2028	53.7	36.9	37.9
2029	95.0	36.1	37.4
2030	89.1	42.5	36.9
2031	83.2	41.7	41.4
2032	77.3	40.9	40.9
2033	71.4	40.1	40.4
2034	65.5	39.3	39.9
2035	59.6	38.5	39.4
2036	53.7	37.7	38.9
2037	95.0	36.9	38.4
2038	89.1	36.1	37.9
2039	83.2	42.5	37.4
2040	77.3	41.7	36.9
2041	71.4	40.9	41.4
2042	65.5	40.1	40.9
2043	59.6	39.3	40.4
2044	53.7	38.5	39.9
2045	95.0	37.7	39.4
2046	89.1	36.9	38.9
2047	83.2	36.1	38.4
2048	77.3	42.5	37.9
2049	71.4	41.7	37.4
2050	65.5	40.9	36.9

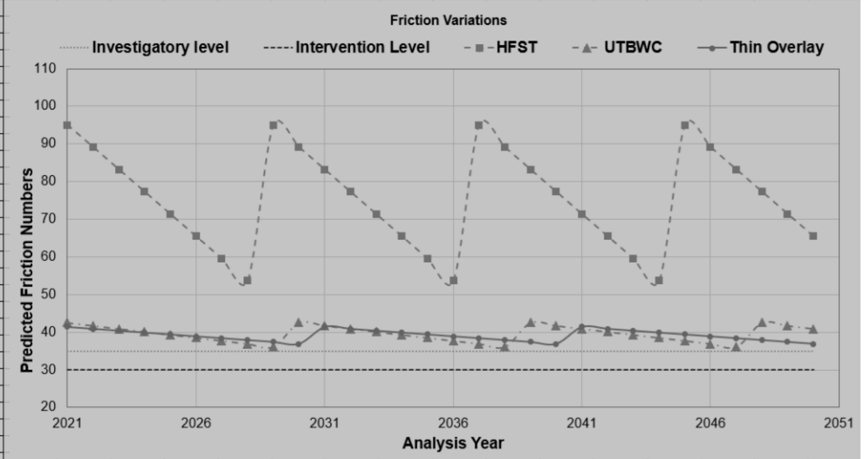

Figure A-12 Friction Prediction and Comparisons

The **Safety Cost Calculator** does not calculate the agency construction cost, or the user cost caused by construction, as these capabilities have already been integrated into several existing software such as LCCAExpress and RealCost. However, the **Safety Cost Calculator** offers the option to directly import the RealCost results so that the total cost of each alternative can be compared.

Users should follow the RealCost User Guide to calculate agency and user costs available at the [FHWA Life-Cycle Cost Analysis Software] website. Users should make consistent inputs in the RealCost software and the **Safety Cost Calculator**. Once the results were obtained in RealCost, save the RealCost excel file (Figure A-13) for direct import into the **Safety Cost Calculator** by clicking the "**Compare Total Cost**" button (Figure A-11) or the "**Total Cost**" button in the **Main Menu** (Figure A-14) and then clicking "**Import RealCost File**" (Figure A-15). The **Safety Cost Calculator** software will read the deterministic results of RealCost, combine them with the crash costs and plot the corresponding figures in the "**Total**

Cost Comparison” worksheet (Figure A-16). The users can click the “**View Cost Data**” to switch from the detailed numbers and the plots.

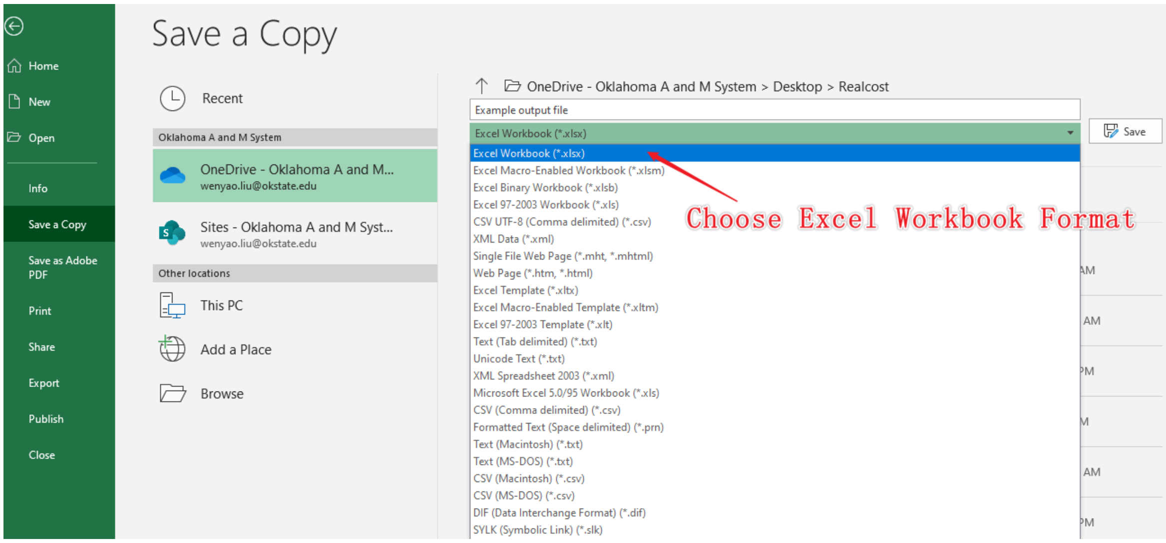

Figure A-13 Save RealCost Output File

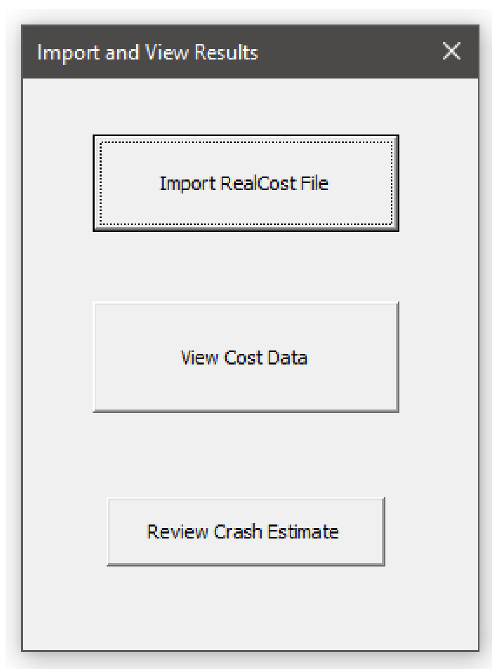

Figure A-14 Import and View Results

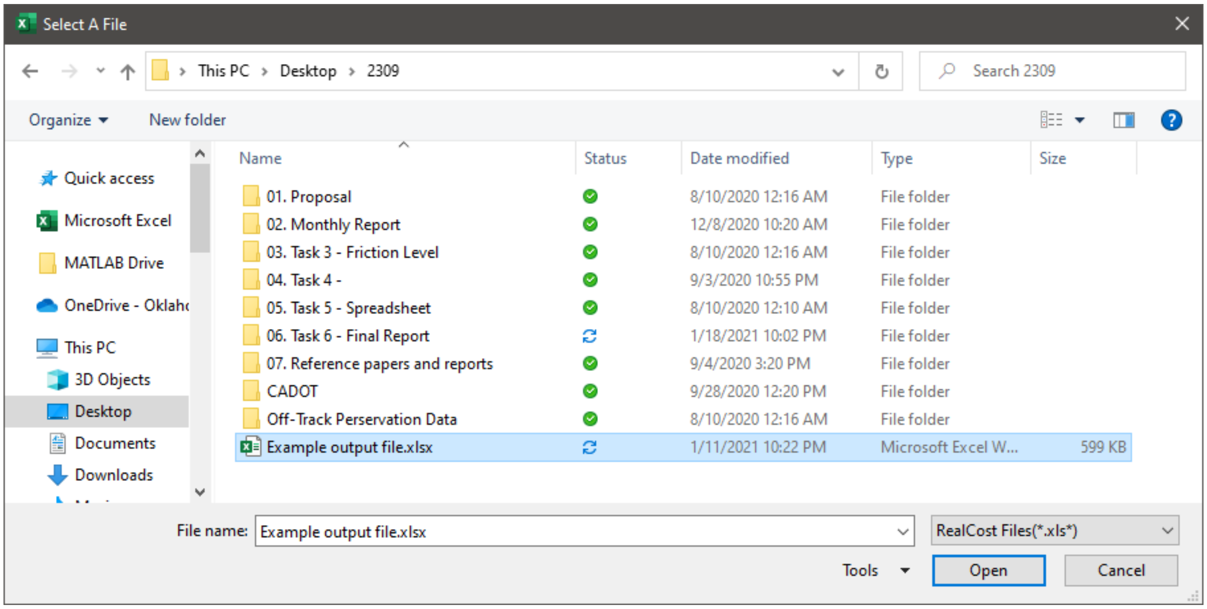

Figure A-15 Import RealCost Output File

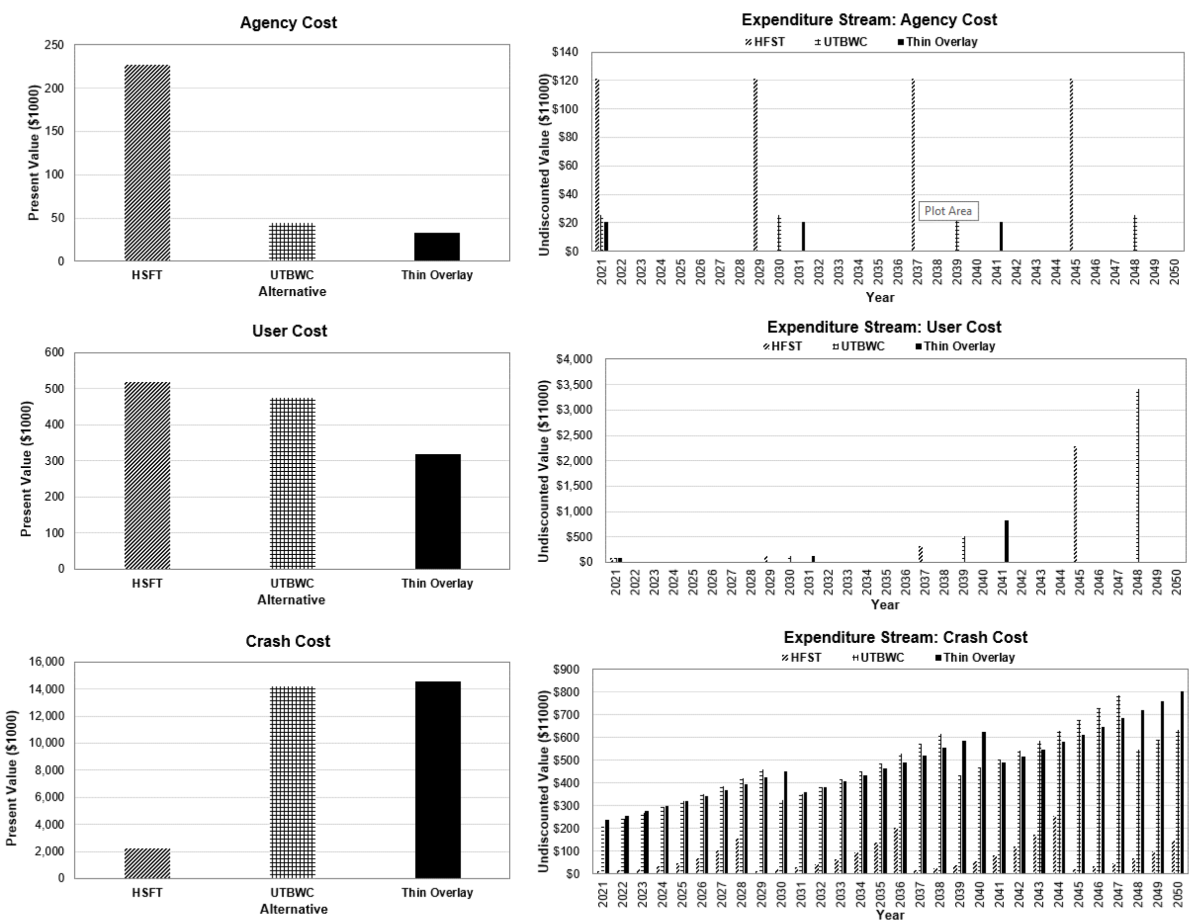

Figure A-16 Total Cost Comparison Results